# Identification of Genes Involved in Gliding Motility and Proteomic Analysis of Spore Inner Membrane Proteins in *Clostridium perfringens*

Hualan Liu

Dissertation submitted to the faculty of the Virginia Polytechnic Institute and State University in partial fulfillment of the requirements for the degree of

Doctor of Philosophy
In
Biological Sciences

Stephen B. Melville, Chair
Ann M. Stevens
David L. Popham
Richard F. Helm

May 7, 2014
Blacksburg, VA

Keywords: *Clostridium perfringens*, transposon, mutagenesis, spore, proteome

# Identification of Genes Involved in Gliding Motility and Proteomic Analysis of Spore Inner Membrane Proteins in *Clostridium perfringens*

Hualan Liu

## ABSTRACT

*Clostridium perfringens* is a Gram-positive anaerobic pathogen of humans and animals. While lacking flagella, *C. perfringens* cells can still migrate across surfaces using a type of gilding motility that involves the formation of filaments of bacteria lined up in an end to end conformation.

To discover the gene products that play a role in gliding, we developed a plasmid-based mariner transposon mutagenesis system that works effectively in *C. perfringens*. Twenty-four mutants with deficiency in gliding motility were identified and one gene, which encodes a homolog of the SagA cell wall-dependent endopeptidase, was further characterized.

We also isolated and characterized two hypermotile variants of strain SM101. Compared to wide type cells, the hypermotile cells are longer and video microscopy of their gliding motility suggests they form long, thin filaments that move rapidly away from a colony, analogous to swarmer cells in bacteria with flagella. Whole genome sequencing analysis showed that both mutants have mutations in cell division genes. Complementation of these mutations with wild-type copies of each gene restored the normal motility phenotype. A model is presented explaining the principles underlying the hypermotility phenotype.

Heat resistant spores are the major route for disease transmission for *C. perfringens*,

which cause food poisoning. To elucidate the molecular mechanisms involved in spore germination as well as to identify attractive targets for development of germination inhibitors to kill spores, we combined 1D-SDS-PAGE and MALDI-TOF-MS/MS to map the whole spore inner membrane proteome, both from dormant and germinated spores. As the first comprehensive spore inner membrane proteome study, we identified 494 proteins in total and 119 are predicted to be membrane-associated proteins. Among those membrane-associated proteins, 71 changed at least two-fold in abundance after germination. This study provides the first comprehensive list of the spore inner membrane proteins that may be involved in germination of the *C. perfringens* spore and their relative levels during germination.

# DEDICATION

This work is dedicated to my families. To my husband Yan, for being extremely patient all the time, and also for being a fun and cheerful friend. To my lovely sister, for taking care of our parents while I am so far away from home. Also to my parents, for unconditionally providing their love, support and guidance though my life.

# ACKNOWLEDGMENTS

I first want to thank my supervisor, Stephen Melville, for his consistent guidance over the years. He was extremely patient and approachable whenever I had trouble with my projects. He always encourages me to ask questions and discuss our own ideas, not to mention teaching me English at any time or any chance. I also want to thank him for all the conversations we had that helped me to fit my life into a completely different country in an enjoyable way.

I would like to thank my committee members David Popham, Ann Stevens, and Rich Helm, for all the useful ideas and constructive comments about my research. I can't forget how much editing Dr. Popham did for every piece of my writing; I can't forget all the words from Dr. Stevens about successfully managing graduate school life and life after; I also remember the moment when Dr. Helm told me to not just work hard, but also work smart at my first committee meeting. I really appreciate your care and mentoring.

My lab colleagues, Andrea Hartman, Will Hendrick and Sarah Nikraftar, were and are great people to work with. Andrea walked me through my first year in the lab and I couldn't disagree that her dedication, hard work and selfless sharing motivated and inspired me a lot. Will is the person that I am jealous of and admire the most. I wish I could steal or clone your amazingly exceptional memory. Sarah is the person that reminds me of all those flashbacks in graduate school, except that you are a much harder worker and I wish you the best of luck in your research.

I also want to thank those amazing undergraduates who worked with me in the lab, Katherine Lee, Meghan Rochford and Kristy McCord. I am grateful for all the great help and our friendship through the time we spent in the lab together.

I want to thank our microbiology group, not for just being great friends, but also for being brave bakery tasters. You won't be surprised if you see me bragging in front of my friends about how awesome this group is. Finally, I want to thank VT Rec Sports for offering such a wonderful group exercise program. It has been a great way for kicking away stress and keeping a positive attitude, both at work and in life.

# TABLE OF CONTENT

# LIST OF FIGURES

# LIST OF TABLES

# Chapter 1

# Introduction and Review of Literature

*Clostridium perfringens* is a Gram-positive, anaerobic, spore-forming rod, which can be found in the intestinal tract of humans and many animals, as well as in soils and sewage (1, 2). *C. perfringens* is a common pathogen of humans and domestic animals, and it produces at least 12 toxins which are responsible for the main symptoms of various diseases. Instead of producing all 12 toxins, a given isolate of *C. perfringens* can only produce a specific selection of these toxins. So, based on their toxigenicity, clinical isolations of *C. perfringens* are classified into 5 types, type A-E (3).

***C. perfringens* associated diseases in humans.** *C. perfringens* toxinotype A is responsible for several diseases in humans, from the mild, self-limiting food poisoning to life-threatening gas gangrene (1). Clostridial gas gangrene is a highly lethal necrotizing soft tissue infection. Since *C. perfringens* are anaerobes, the infection normally starts with a deep wound in muscle tissue. With a low oxygen tension, *C. perfringens* can multiply quickly and produce toxins. Among these toxins, the alpha-toxin, also named phospholipase C, is the most important virulence factor responsible for cytotoxicity, necrosis, and hemolysis (1). Food poisoning is caused by sporulating *C. perfringens* cells that produce an enterotoxin (CPE). Less than 5% of *C. perfringens* type A isolates have the *cpe* gene (1). Among these *cpe*-positive isolates, the isolates carrying a chromosomal *cpe* gene are more common in food poisoning outbreaks, while the isolates carrying a plasmid-borne *cpe* gene are more frequently involved in antibiotic-associated and sporadic diarrhea (4, 5).

**Transmission and epidemics of *C. perfringens*.** *C. perfringens* food poisoning results from eating food contaminated by *C. perfringens*, especially the heat-resistant spores. Even with appropriate cooking, the spores can survive in the food, grow and multiply when the food cools down. Once these bacteria are ingested, they produce large quantity of enterotoxin during sporulation in the small intestine.

*C. perfringens* is one of the leading causes of food poisoning in the United States (6). Based on a conservative estimate from the Centers for Disease Control and Prevention, about 250,000 people suffer from *C. perfringens* food poisoning annually (7). In the United States, from 1982 to 1997, *C. perfringens* was responsible for about 13% of documented foodborne outbreaks; while it was responsible for about 14% of foodborne disease outbreaks in Australia from 1995 to 2000 (6, 8). In May 2010, *C. perfringens* contaminated chicken salad caused 40 illnesses and 3 deaths at the Central State Hospital in Pineville, LA. Investigations indicate that improper holding of food after cooking contributes to about 84% of all *C. perfringens* food poisoning outbreaks (6).

***C. perfringens* gliding motility.** Bacteria possess various motility patterns when they colonize surfaces. Flagella- dependent swarming motility is adopted by many flagellated bacteria such as *E. coli*, *B. subtilis*, *Pseudomonas aeruginosa* and *Salmonella typhimurium* when grown on moist nutrient-rich surface, (9-11). Twitching motility is flagella-independent, but it requires type IV pili. This type of motility has been best studied in *Pseudomonas aeruginosa*, *Neisseria gonorrhoeae*, and *Myxococcus xanthus* (12, 13). Gliding motility is the movement of cells in the direction of the long axis of the cell without the requirement of flagella, and they usually form thin spreading colony edges (14). Gliding motility is widely observed among a diverse group of bacterial species (15), but the mechanism of gliding motility is much less well understood compared to swarming and twitching motility. It has been proposed that several different mechanisms are probably involved in gliding motility in different species (15).

*C. perfringens* is able to move away from the center of the original inoculation site and form a spreading colony on agar plates. This motility resembles the type IV pili-mediated social gliding motility in *M. xanthus*, but it is also different in some ways (16, 17). Compared

to *M. xanthus*, single *C .perfringens* cells can not move individually, also no reverse movement was observed in *C. perfringens* gliding motility. Type IV pili proteins were found to play a role in *C. perfringens* gliding motility and this movement can be repressed by glucose via carbon catabolite repression (16, 18, 19).

**Mutagenesis of *C. perfringens.*** The *C. perfringens* strain 13 genome sequence was published in 2002 (20). With completed genome sequences, mutation of specific genes is an important way to understand the genome information. However, due to the low efficiency of incorporation of recombinant DNA into the chromosome, genetic analysis in *C. perfringens* was limited in the past.

Several years ago, group II introns (TargeTron) have been adapted to generate insertion mutants in Cl*ostridium*. The mobile group II intron can propagate into a specific site via an RNA-mediated 'retrohoming' mechanism. Base pairing between the target site DNA and the excised intron lariat RNA results in target site recognition instead of homologous recognition (21). Though several mutants have been successfully made by these methods, insertion mutation sometimes makes it impossible to identify the roles of specific genes in operons due to the polarity effect. In 2011, the Okabe group developed a galactose-based counter-selection system in *C. perfringens* strain 13 with a disrupted *galKT* operon (22). This system is comprised of a *galKT* deletion strain and a suicide *galK* plasmid. The first homologous recombination is selected by gaining antibiotic resistance from the chloramphenicol acetyltransferase (*catP*) gene on the plasmid backbone, and the second homologous recombination is selected by gaining resistance to galactose and screening for sensitivity to chloramphenicol antibiotics. Mutants are verified by PCR-screening. This system enables the efficient generation of non-lethal targeted in-frame deletion mutants and largely speeds up the genetic study of *C. perfringens* at the molecular level (23-25). However, a random

mutagenesis system would be particularly useful to identify new genes responsible for a specific phenotype. Transposon mutation system has been considered to be a strategy to make random mutants in *Clostridium*. For *C. perfringens*, a Tn916 conjugative transposon system, a phage Mu transposon system, and an EZ-Tn5-based transposon have been described (21, 26, 27). Though transposon-based mutation systems do produce insertion mutants, these systems have some significant limitations. Some transposons have site-preferences, some transposons produce multiple copy insertions, and some isolates are unstable. In this study, we constructed a mariner transposon-based random mutagenesis system incorporating the CatP/GalK counter-selection strategy. It enables us to generate genome-wide random insertion mutants for specific phenotype study.

**Bacterial spore structure**. Bacterial spores are metabolically dormant cells, with several layers outside to protect their highly dehydrated and compacted cytoplasm. These external layers and dehydration of the inner core make the dormant spore highly resistant to normal chemical and physical antibacterial treatments (28). Figure 1 shows the basic structure of a dormant spore.

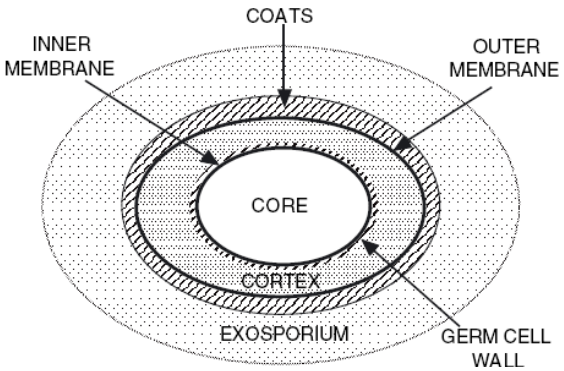


**Figure 1.1.** Spore structure. The spore structure is responsible for its resistance to normal antibacterial treatments and also their lasting stability in various harsh environments. From outside to inside, these layers are the exosporium, coat, outer membrane, cortex, germ cell wall, inner membrane and core (28). (Used with permission from RightsLink in 2014)

The exosporium is considered to be an extension of the spore coat, and its main components are proteins, including some glycoproteins. The spore coat is a complex structure composed of numerous proteins in several layers, and it gives the spore resistance to some kinds of chemicals and lytic enzymes. The cortex is a thick layer of peptidoglycan, which helps to hold the core in a highly dehydrated state. The germ cell wall is also a layer of peptidoglycan, but it is much thinner. The outer membrane is likely not an intact permeability barrier, while the inner membrane is considered to play a major role in maintaining core dehydration and dormancy. Extensive studies in *B. subtilis* have verified that the receptors which bind germinants to trigger germination are located in the inner membrane (28-30). The innermost part is the spore core, which contains the basic cellular structures such as DNA, RNA, ribosomes, nucleoprotein complexes and enzymes. The core is very low in free water and has a relatively high concentration of pyridine-2,6- dicarboxylic acid (dipicolinic acid, DPA) (28). There are also small, acid-soluble spore proteins (SASPs) located in the core, which play an important role in protecting DNA from UV damage (31).

**Spore germination**. Sporulation is a survival strategy for bacteria under starvation, but the metabolic dormancy does not mean that spores completely keep themselves isolated from the environment. In fact, dormant spores are very sensitive to the available nutrients. Once they sense favorable conditions, they will go through germination and outgrowth to become vegetative cells again. Germination is significant for *C. difficile* pathogenesis, because only when the spores germinate in the large intestine, can they secrete large amount of toxin A and toxin B to cause diseases (32).

Germination has been most intensively studied in *B. subtilis*. The initiation of germination is triggered by some nutrients, which are termed germinants (33). Commonly, these germinants can be single amino acids, sugars, and mixtures of some nutrients (34). This

early sensing of a germinant is required for following events, but how it works is still unclear. It has been shown that after being mixed together with germinants for a few seconds, spores will commit to germination and germination will continue even after removal of the germinants (34). Once germination starts, two stages follow. The first stage is the release of ions and calcium DPA from the spore core, and partial rehydration of the core (34). The second stage is the degradation of peptidoglycan of the spore cortex and partial degradation of the spore coat layers, which results in further rehydration of the core and expansion of the germ cell wall (33-35).

Cation transport was first identified playing an important role in germination in *B. megaterium* spores (36). A *grmA* insertion mutant was blocked at an early stage of germination. Sequence analysis found that GrmA is a Na/H+ antiporter homolog. It was proposed that cation transport is critical for spore germination (36, 37).

*gerN* is a homolog of *grmA* identified in *B. cereus*, and GerN has been verified as a $Na^+/H^+$-$K^+$ antiporter. *gerN* insertional mutant spores have a lower germination efficiency with inosine, but retain a normal germination rate with alanine (37). When the concentration of germinant was reduced to a suboptimal concentration, germination with inosine was blocked and the germination with alanine was reduced to 1/3 compared to wild-type spores (37). This evidence indicates that GerN may be involved in the interaction between inosine and inosine germinant receptors (37).

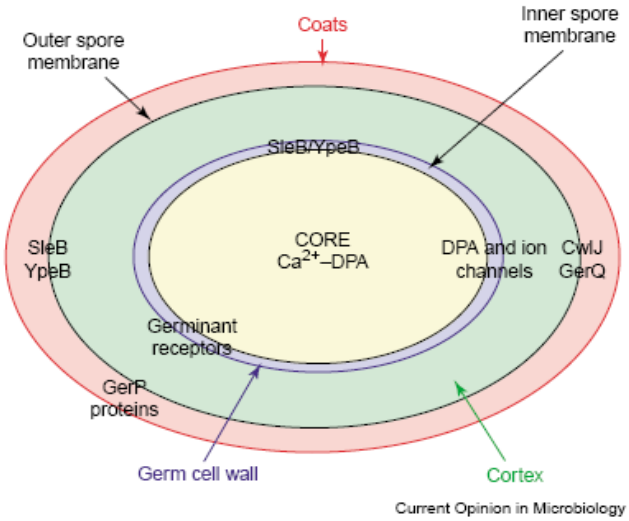


**Figure 1.2.** Components of spore germination apparatus (34). GerP proteins encoded by the *gerP* locus of B. cereus are considered to be involved in movement of small molecules during spore germination. (Used with permission from RightsLink in 2014)

The *gerP* insertional mutant was blocked at an early stage of germination, while coat extraction rescued this germination defect (34, 38). Mutation in a GerP homolog in *B. subtilis* also results in a germination defect, which can also be rescued by spore coat extraction (38). However, although some proteins involved in ion transport or membrane permeability change during spore germination, their specific role during this process is still unclear (34).

Dormant spores are highly dehydrated due to the spore cortex, which is composed of modified peptidoglycan (39). During germination, cortex hydrolysis is driven by germination-specific cortex lytic enzymes (GSLEs). GSLEs are divided into two groups based on their specific functions. One group named spore cortex lytic enzymes (SCLEs) are thought to depolymerize intact cortical peptidoglycan; the other group named cortical fragment lytic enzymes (CFLEs) are thought to further degrade partially hydrolyzed cortex fragments (40).

Several genes encoding cortex lytic enzymes involved in peptidoglycan hydrolysis have been identified in different spore-forming species. *cwlJ* and *sleB* are two crucial lytic enzyme

encoding genes in *B. subtilis*. Both CwlJ and SleB need a second protein to help them to localize in the dormant spores (33). Four GSLEs have been identified in *B. anthracis*. CwIJ1, CwIJ2 and SleB are considered to be SCLEs, while SleL is considered to be a CFLE (40). Evidence suggests that these enzymes are in their mature form in dormant spores, how they change from an inactive state to active state during germination is still unclear (33).

There are two identified lytic enzymes in *C. perfringens*, SleC and SleM. While mature SleM was thought to be held in an inactive state in the dormant spore, SleC exists in the dormant spore as a pro-SleC containing a N-terminal pro-sequence. During germination, the N-terminal pro-sequence is cleaved by a germination-specific protease (41).

**Spore germinants.** Germinant is defined as a specific molecule which can trigger spore germination alone, while a co-germinant is defined as a molecule which can enhance germination efficiency, but cannot trigger germination alone. Germinants are usually nutrients. Common nutrient germinants in *Bacillus* species are amino acids, sugars, and purine nucleosides. For *B. megaterium* spores, L-proline is a nutrient germinant. For *B. subtilis*, both L-alanine and L-valine alone can trigger germination as typical nutrient germinants. A mixture of D-glucose, D-fructose and $K^+$ termed GFK, works as a co-germinant when used with L-asparagine as a germinant (AGFK) for *B. subtilis* (42). For *C. difficile*, glycine and taurocholate act as co-germinants and are sufficient to induce germination (43). L-alanine and L-valine are also good nutrient germinants for *C. perfringens* carrying a plasmid-borne *cpe* gene. However, neither of them is a highly efficient germinant for *C. perfringens* carrying a chromosome-borne *cpe* gene (C-*cpe*). So, the specific nutrient germinants vary in a species- and strain-specific manner (42).

Besides nutrients, various non-nutrients, such as salts, $Ca^{2+}$-DPA, lysozyme and high

pressure, can also trigger spore germination. KCl is a good germinant for *C. perfringens* carrying a C-*cpe* gene, and KBr alone can trigger germination of *B. megaterium* spores (29, 34). Exogenous $Ca^{2+}$-DPA is a good germinant for *B. subtilis* (44). Lysozyme can also trigger the germination of *B. subtilis* spores once the spore coats are damaged.

**Germinant receptors in *Bacillus* species.** Germination triggered by nutrients starts with the interaction of nutrients and their specific germinant receptors. Identification of germinant receptors is based on genetic analysis. When a mutation is introduced into some specific gene, if the spores become non-responsive to some particular nutrient germinant, but still can germinate normally in the presence of other germinants, this gene is considered a germinant receptor for this particular nutrient (39). Characterization of mutants affecting germination include germination assays on plates, phase darkening, release of DPA and loss of hexosamine during germination (45).

The GerA proteins, GerAA, GerAB, GerAC, encoded by the *gerA* operon, have been intensively studied for their functions as germinant receptor of L-alanine and L-valine in *B. subtilis*. All the GerA proteins are predicted to be associated with the inner spore membrane. GerAA has a predicted domain containing at least 5 membrane-spanning segments; GerAB is predicted to be an integral membrane protein with 10 transmembrane helices, and it belongs to the single-component amino acid/polyamine/organocation transporter superfamily; GerAC is a lipoprotein (33, 39, 46). The *gerA* operon is expressed in the developing forespore in a sigma G-dependent manner, and western blot analysis suggests that all the GerA proteins are localized in the spore inner membrane.

Genetic analysis of the *gerA* operon indicates that a null mutation in any single gene in this operon will block spore germination if L-alanine or L-valine is the sole germinant, but

germinate normally with AGFK as germinant. This defect blocks the germination at the earliest stages, because the spores still have heat resistance. The particular tricistronic structure of all three *gerA* genes and the requirement for all three proteins for complete functions imply that the GerA proteins are likely to interact during spore germination, while there is as yet no biochemical evidence for physical interaction between the A, B, and C proteins (39, 45). All these data suggests a model for the early stage of spore germination. The nutrient germinant should cross the spore coat and cortex and interact with the inner membrane-associated specific receptor complex containing at least all three polypeptide subunits (33, 45).

Besides the *gerA* operon, other two *gerA* homologs named as *gerB* and *gerK* operons were also identified in *B. subtilis*. Both *gerB* and *gerK* operons have a cluster of three ORFs encoding three proteins: A and B have substantial hydrophobic regions, and C is a possible lipoprotein (47, 48). Spores of either GerB or GerK mutants are defective in the AGFK germination pathway, but germinate normally with L-alanine (45).

Though GerA, GerB and GerK respond to different germinants and co-germinants, further evidence suggest that there are cooperative interactions between different Ger proteins. The germination with L-alanine via GerA proteins is stimulated by glucose, and this stimulation likely requires cooperation with GerK (42). Germination of L-alanine or L-asparagine plus GFK needs both GerB and GerK proteins. Various mutagenesis analyses also indicate that the GerBC may interact with GerAA-GerAB (49).

Non-nutrient germination stimuli include lysozyme, salts, $Ca^{2+}$-DPA and high pressure (33, 34). These non-nutrient germinants can trigger germination without the presence of individual components of the nutrient germination pathway (34).

Lysozyme can trigger germination of de-coated spores, as has been shown in *B. subtilis* and *C. perfringens* (50, 51). This enzyme can bypass the whole germination receptor apparatus and degrade the cortex of most spores (34, 50).

$Ca^{2+}$-DPA is not only an important factor for spore resistance; it also plays an important role in spore germination. Exogenous $Ca^{2+}$-DPA triggers germination even without the presence of germination receptors in a CwlJ-dependent way. The *cwlJ* null mutant spores do not germinate with $Ca^{2+}$-DPA, but germinate normally in nutrient germinants. However, how $Ca^{2+}$-DPA interacts with CwlJ is still unclear (34).

Recently, the Dworkin research group found that muropeptides from partially digested peptidoglycan fragments generated by growing cells can serve as a germinant for *B. subtilis* dormant spores (52)**.** During cell growth, the mature peptidoglycan should be partially broken to insert new peptidoglycan monomers. During this process, growing cells of gram-positive bacteria release lots of muropeptides into the environment (52). A membrane protein, PrkC, is responsible for this germination pathway. PrkC is a eukaryotic-like Ser/Thr membrane kinase containing three potential peptidoglycan binding sequences called PASTA ("penicillin and Ser/Thr kinase associated"). Subcellular fractionation of spores expressing an epitope-tagged PrkC indicates that PrkC localizes to the spore inner membrane (56). Peptidoglycan binding assay showed that about 40% of the soluble extracellular PrkC containing three PASTA repeats went to the insoluble pellet after incubation with insoluble peptidoglycan fragments for 1 hour, this result is consistent with the hypothesis that PrkC triggers germination by binding to peptidoglycan fragments (52).

**Germinant receptors in *C. perfringens*.** Spore germination is not as well studied in *Clostridium* species. Compared to *B. subtilis*, not many nutrient germinants have been found

for *Clostridium* spore germination. For *C. difficile*, bile salts have been shown to be a germinant and glycine is a co-germinant for bile salts (43). For *C. perfringens*, a mixture of L-asparagine and KCl (AK) is a good germinant for both C-*cpe* and P-*cpe* isolates. KCl alone is a good germinant for a C-*cpe* isolate, while L-asparagine alone can also trigger germination but with a much lower efficiency (29). Neither KCl nor L-asparagine trigger efficient germination for a P-*cpe* isolate, but L-alanine or L-valine can induce significant spore germination for a P-*cpe* isolate (29).

*C. perfringens* genome sequence analysis found four ORFs (CPR0614, CPR0613, CPR0616, CPR1053) encoding proteins with high amino acid sequence similarity to *B. subtilis* Ger proteins (29). CPR1053 is predicted to encode a GerAA homologue with 53% amino acid sequence similarity to *B. subtilis* GerAA protein. CPR0614, CPR0613, CPR0616 are predicted to encode GerKB, GerKA and GerKC, which have 55%, 56%, and 41% amino acid sequence similarities compared to the relative GerK proteins in *B. subtilis* (29). The spores of a GerAA null mutant containing C-*cpe* have lower germination efficiency at suboptimal concentration of KCl or AK, but germinate similarly with optimal germinant concentrations compared with the wild type spores. Also, the mutant and the wild type showed similar germination efficiency with different concentrations of L-asparagine (29). Mutations in the *gerK* operon resulted in significantly lower germination efficiency for a C-*cpe* isolate, especially when L-asparagine is the germinant (29).

**Objectives of this work.** The first objective of this research was to identify and characterize new genes that are involved in *C. perfringens* gliding motility. To achieve this goal, an effective random mutagenesis strategy for a genome wide screening of genes responsible for this phenotype was developed. In Chapter 2, we combined the CatP/GalK counter-selection system and the mariner-transposon, and successfully generated the random

mutagenesis system by adopting the high mutation screening efficiency using galactose and the high degree of randomness of the mariner transposition.

To further illustrate the mechanism of *C. perfringens* gliding motility, we characterized two spontaneous laboratory mutants from *C. perfringens* food poisoning strain SM101, which possess significantly increased motility compared to the wild type. Chapter 3 summarizes the comprehensive study of those two mutants with whole genome sequencing and intensive microscopy analysis. The filamentous cell morphology led us to link the hypermotility to the single mutation in a cell division protein in each mutant, and this was confirmed by complementation experiments.

Chapter 4 details our research on the spore inner membrane proteome in *C. perfringens* SM101. Compared to the well-studied *Bacillus* species, *C. perfringens* spores do not germinate with traditional nutrient germinants. To characterize the germination apparatus in *C. perfringens*, we mapped the whole spore inner membrane proteins from both dormant and germinated spores, using SDS-PAGE gel-based protein separation and mass spectrometry-based protein identification.

# Chapter 2

## Use of a Mariner-based Transposon Mutagenesis System to Isolate *Clostridium perfringens* Mutants Deficient in Gliding Motility

Hualan Liu[e], Laurent Bouillaut[b], Abraham L. Sonenshein[b], and Stephen B. Melville[a]
Department of Biological Sciences, Virginia Tech, Blacksburg, Virginia, USA[a]; Department of Molecular Biology and Microbiology, Tufts University School of Medicine, Boston, Massachusetts, USA[b]

Journal of Bacteriology. 195(3):629-36

## CO-AUTHOR'S ATTRIBUTION:

Laurent Bouillaut, from the department of Molecular Biology and Microbiology, Tufts University School of Medicine, Boston, Massachusetts, constructed the plasmid pBL79, and helped the manuscript preparation.

Abraham L. Sonenshein from the department of Molecular Biology and Microbiology, Tufts University School of Medicine, Boston, Massachusetts, helped the experiment design and manuscript preparation.

Stephen B. Melville, from the department of Biological Sciences, Virginia Tech, Blacksburg, Virginia, was the principle investigator and helped manuscript preparation.

## ABSTRACT

*Clostridium perfringens* is an anaerobic Gram positive pathogen that causes many human and animal diseases, including food poisoning and gas gangrene. *C. perfringens* lacks flagella but possesses type IV pili (TFP). We have previously shown that *C. perfringens* can glide across an agar surface in long filaments composed of individual bacteria attached end-to-end and that two TFP-associated proteins, PilT and PilC, are needed for this. To discover additional gene products that play a role in gliding, we developed a plasmid-based mariner transposon mutagenesis system that works effectively in *C. perfringens*. More than 10,000 clones were screened for mutants that lacked the ability to move away from the edge of a colony. Twenty four mutants (0.24%) were identified that fit the criteria. The genes containing insertions that affected gliding motility fell into nine different categories. One gene, *CPE0278*, which encodes a homolog of the SagA cell wall-dependent endopeptidase, acquired distinct transposon insertions in two independent mutants. *sagA* mutants were unable to form filaments due to a complete lack of end-to-end connections essential for gliding motility. Complementation of the *sagA* mutants with a wild-type copy of the gene restored gliding motility. We constructed an in-frame deletion mutation in the *sagA* gene and found this mutant had a similar phenotype to the transposon mutants. We hypothesize that the *sagA* mutant strains are unable to form the molecular complexes which are needed to keep the cells in an end-to-end orientation, leading to separation of daughter cells and the inability to carry out gliding motility.

## INTRODUCTION

*Clostridium perfringens* is a Gram-positive anaerobic bacteria that causes a wide variety of diseases in humans and animals, including acute food poisoning and gas gangrene (53). We have discovered that *C. perfringens* and the other Clostridia have the ability to produce type IV pili (TFP), a feature that was previously thought to be confined to Gram-negative bacteria (16). *C. perfringens* lacks flagella and flagella-mediated swimming but can move across an agar medium with a unique type of gliding motility, in which curvilinear flares of densely packed cells move away from a colony (16). The flares are themselves composed of filaments of individual bacteria lined up in an end-to-end orientation. This orientation is essential for gliding motility; cells that are randomly oriented do not form the filaments and flares seen in motile cells ((16) and Video S1). The bacteria within a filament can clearly be seen growing and dividing as the filament extends, suggesting that growth and division of individual bacteria provide at least some of the force necessary for movement across the surface of the agar (16) and Video S1. We also noted that the curvilinear flares move away from the colony in the direction of the long axis of the cells lined up within the filaments but eventually, due to their curvilinear nature, collide, leaving a region surrounded by *C. perfringens* cells. This empty space is then quickly filled in by growing bacteria. Thus, gliding motility has the effect of engulfing a local area, leading to consumption of the nutrients available within the engulfed area. We observed that plasmid insertion mutations in the *pilT* and *pilC* genes, which encode a retraction ATPase and an integral membrane protein, respectively, cause a significant defect in gliding motility (16). Therefore, we surmised that TFP appear to play a role in gliding motility (16), although the exact nature of this function is still unknown.

There are three separate loci that include TFP-associated genes in *C. perfringens* strain

13: (i) a monocistronic *pilT* gene; (ii) a putative operon comprised of four genes, *pilB-pilC-CPE1842-CPE1841*; and (iii) a multigene locus extending from *CPE2288-CPE2277*, which likely includes more than one operon (data not shown). To determine if any of these gene products, or any other gene products, were needed for gliding motility on agar plates, we sought a random mutagenesis procedure that would function in *C. perfringens* and yield mutations that were easily mappable. So far, three different methods, all using transposons, have been described for carrying out random mutagenesis in this bacterium. The first method utilizes a Tn916-based vector system (54-56), but has significant disadvantages; it frequently results in multiple insertions in the same chromosome, has several "hot spots" where the majority of the insertions are located and results in deletions at the site of insertion (54, 55). The second utilizes a derivative of Mu phage for insertion, and while this resulted in single transposon insertions, ~43% were in ribosomal RNA operons and 12% in intergenic regions (57). The phage Mu transposition system was also inefficient, giving just 239 transformants/µg DNA in strain JIR325, a derivative of strain 13 (57). A more efficient EZ-Tn5-based random mutagenesis system showed a lower but significant frequency of insertion into rRNA genes (18%) in comparison to the phage Mu-based system (27). Another major limitation of the EZ-Tn5 and phage Mu systems is that both require that the recipient strain to be highly transformable by electroporation (27, 57).

Given the lack of a truly random mutagenesis procedure that shows no preference for rRNA genes, does not require expensive reagents and is flexible in how it is used, we sought to develop a mariner transposon-based system for mutagenesis of *C. perfringens*. Mariner transposon mutagenesis systems have been developed for use in many Gram-negative and Gram-positive bacteria, including *Clostridium difficile* (26). The advantage of the mariner system is that its preferred target is a TA dinucleotide. Given the low G+C content of *C.*

*perfringens* strains, 27-29% (20, 58), a mariner-based transposon would be ideal for mutagenesis due to the preponderance of TA sequences found in the genome. In this report we describe the construction of a plasmid-based mariner transposon system that has three unique features not found in other *C. perfringens* systems: (i) It is carried on a replicating plasmid, so every cell is subject to transposition; (ii) the transposase is under the control of an inducible promoter; and, (iii) a negative selection system has been incorporated into the plasmid for efficient elimination of the replicating plasmid once transposition has occurred. This system was used to identify gene products required for *C. perfringens* gliding motility on agar plates, providing valuable insights into the mechanism used for moving across surfaces.

## MATERIALS AND METHODS

**Bacterial strains, growth conditions and DNA manipulations.** Bacterial strains, plasmids, and primers used in this study are listed in Table 1. *E. coli* was grown in Luria-Bertani (LB) medium supplemented with antibiotics as needed: 400 µg/ml erythromycin, 100 µg/ml ampicillin, or 20 µg/ml chloramphenicol. *C. perfringens* was grown in a Coy anaerobic chamber at 37°C. Two different media were used for *C. perfringens*, brain heart infusion (BHI) medium (Difco), and TY medium (3% tryptone, 2% yeast extract, 0.1% sodium thioglycolate), with the appropriate antibiotics as indicated: 30 µg/ml erythromycin or 20 µg/ml chloramphenicol. Galactose (3%) was used as a supplement in TY medium when needed; this medium is referred to as TYGal.

DNA manipulation was performed using standard protocols. Transformation of *E. coli* and *C. perfringens* was performed by electroporation as described before (59). All constructs were verified by DNA sequencing.

**Construction of plasmids**. We created pBL79, a plasmid for delivery of the mariner transposon, in several steps from the following components: (a) A promoterless version of the hyperactive *Himar1* C9 transposase gene (1045 bp) from pBADC9 (60); (b) a 519-bp fragment containing the *tcdA* promoter region amplified from *C. difficile* strain JIR8094 with primers OLB94/OLB95; (c) a 1,264-bp mariner transposable element obtained by cloning the 1,087-bp *ermBP* gene of pJIR1457 (amplified using primers OLB97 and OLB98) between the two internal terminal repeats of pMMOrf (60); (d) the 5,172-bp *Eco*RI-*Hind*III backbone fragment of pMTL82151 (61). Note that during the construction the *Hima*r1C9 gene was PCR modified using primers OLB92 and OLB93 to convert an internal *Nco*I site to *Nde*I and an *Nde*I site of pMTL82151 was destroyed. We designed primers, OHL15 and OHL16, to

amplify the lactose inducible promoter *PbgaL* from pKRAH1 (59). A consensus ribosome binding site and *XbaI* site were included in primer OHL15, while a *NdeI* site was included in OHL16. The PCR product was ligated to pGEM-T Easy to create plasmid pHLL7. pBL79 and pHLL7 were digested with *XbaI* and *NdeI*, the *tcdA* promoter was replaced with the *PbgaL* fragment after ligation, which gave plasmid pHLL9. The *galK* gene with its ferredoxin promoter was amplified from pCM-GALK (22) by PCR using primers OHL41 and OHL42 and ligated to pGEM-T Easy to give plasmid pHLL23. pHLL9 and pHLL23 were digested with *KpnI* and *SacII*, and the *galK* gene and its promoter were ligated to pHLL23 and to give plasmid pHLL24.

**Mariner transposon mutagenesis.** pHLL24 was introduced into *C. perfringens* strain HN13 (22) by electroporation and transformants were plated on BHI plus erythromycin and chloramphenicol. Cells resistant to both antibiotics were used to inoculate liquid BHI containing erythromycin and chloramphenicol and grown to mid-log phase. The culture was then washed twice with Dulbecco's modified phosphate buffered saline (DPBS), resuspended in the original culture volume of BHI plus 1 mM lactose and incubated for two hours. The cell culture was then washed three times with DPBS and diluted 100-fold in liquid BHI and incubated for 4 hours at 37C. The culture was again diluted 100-fold into liquid TY medium containing 3% galactose and erythromycin, and incubated for four hours. In principle, only those bacteria in which transposition had occurred and the plasmid had been lost would be able to grow. Cells were then plated on TYGal plates plus erythromycin after which all the colonies were harvested and stored at -80°C to generate a transposon mutant pool.

To check for the randomness of insertion, Southern blot analysis was done with the *ermBP* gene as probe on 17 randomly chosen mutants from the pool. Chromosomal DNA was extracted using the Quick extract Chromosomal DNA Extraction Kit (Epicentre

Biotechnologies), digested overnight with *EcoRI* and a Southern blot was performed as previously described (62).

**Screen for motility mutants.** The *C. perfringens* HN13 mariner transposon mutant library was plated from a frozen stock culture onto BHI plates plus 30 µg/ml erythromycin and incubated overnight at 37 °C. Since colonies of the parent strain HN13 have an irregular border due to migration on agar plates, mutagenized bacteria that formed colonies with smooth edges were picked and saved as potential motility mutants.

**Sequencing analysis to locate the insertion sites of mutants.** The chromosomal DNA of motility mutants was extracted using the Quick extract Chromosomal DNA Extraction Kit (Epicentre Biotechnologies), digested overnight with *HindIII* and then ligated to *HindIII* digested pBSII KS+. The ligation products were introduced into *E. coli* strain DH10B by electroporation and plated on LB agar plus ampicillin and erythromycin. Purified recombinant plasmids were sequenced using primers OHL21 and OHL22, which anneal inside the *ermBP* gene but are directed towards the DNA flanking the *ermBP* and transposon sequences. To identify the genomic location of transposon insertions, sequence data were analyzed using BLAST and compared to the genome sequence of *C. perfringens* strain 13, the parent of strain HN13 (http://www.xbase.ac.uk/genome/clostridium-perfringens-str-13).

**Complementation of the CPE0278 mutations in strain HN13.** The coding sequence of *CPE0278* was amplified with primers OHL75 and OHL76, using HN13 chromosomal DNA as template, and cloned in pKRAH1 at the unique *SalI* and *BamHI* sites (59). This placed the *CPE0278* gene under control of the lactose-inducible promoter ($P_{bgaL}$) in pKRAH1 (59). This plasmid, pHLL42, was introduced into the *CPE0278* mutant strains HLL9 and HLL28 by electroporation.

**Construction of a CPE0278 in-frame deletion mutant.** An in-frame deletion mutant of the *CPE0278* gene was constructed as previously described (22). The 5' (1,003 bp) and 3' (991 bp) flanking regions of gene *CPE0278* were amplified using *C. perfringens* HN13 chromosomal DNA as template, with primers OHL105 and OHL106 (N-terminal), OHL107 and OHL108 (C-terminal), respectively. A second round of over-lapping PCR was performed using the flanking region PCR products as template and OHL105 and OHL108 as primers. This PCR product was ligated into pGEM-T Easy and then sub-cloned into pCM-GALK (22) using *SalI* and *BamHI* as restriction sites. This plasmid, pHLL49, was transformed into *C. perfringens* HN13 by electroporation. Mutants were screened (22) and confirmed by PCR using primers OHL109 and OHL110. The mutant retained, in frame, the first two and last twelve codons of the *CPE0278* gene (data not shown).

**Expression of *CPE0278* in *C. perfringens* HN13**. pHLL42, which has the CPE0278 gene under control of the lactose-inducible promoter $P_{bgaL}$, was transformed into *C. perfringens* HN13 by electroporation. Expression was induced for 2 hours by adding lactose to a final concentration of 10 mM in liquid BHI medium to a culture in mid-log phase.

**Microscopy and video imaging.** Between 194 and 587 individual bacteria from each sample were used to measure cell length and width using MicrobeTracker software (63) linked to a MATLAB (Mathworks) platform. Frozen stocks of cells were streaked on BHI agar plates with 0.5 mM lactose and incubated in the anaerobic chamber for 6 hours. Cells were scraped from the plate, suspended in PBS and examined in an Olympus IX81 upright microscope linked to a Hamamatsu Model C4742 CCD camera. Slidebook 5.1 Intelligent Imaging Innovations imaging software was used to compile motility videos. Images of colonies were obtained using a Bio-Rad Gel Doc XR Imager with Applied One 4.6.5 version software. Colony areas were measured using ImageJ software (http://rsbweb.nih.gov/ij/).

## RESULTS

**Construction of a mariner transposon system for *C. perfringens*.** Our goal was to design a self-replicating plasmid that would deliver the mariner transposon to the *C. perfringens* chromosome under the control of an inducible promoter. As the backbone for the vector, we used pMTL82151, a plasmid developed by Heap et al. (61) that contains a Gram-positive origin of replication from pBP1 and a chloramphenicol resistance gene. The *C. difficile tcdA* promoter was initially used to drive expression of the *Himar* transposase. While the constructed plasmid, pBL79, could replicate in *C. perfringens*, it did not provide efficient delivery of the mariner transposon to the chromosome (data not shown). To provide regulated, higher-level expression of the transposase, we substituted the *C. perfringens bgaL* promoter for the *tcdA* promoter. We have shown previously that the *bgaL* promoter is inducible in *C. perfringens* by the addtion of lactose and mediates high levels of expression of genes under its control (59). The modified plasmid, pHLL9, was able to deliver the transposon to the chromosome of *C. perfringens* strain 13, as indicated by the presence of clones that were erythromycin- and chloramphenicol-resistant. However, even after 24 h of growth in non-selective medium, 80-90% of all clones were still chloramphenicol-resistant, indicating the plasmid was still present. Therefore, we added a counterselectable marker originally used by Nariya et al (22). We added the *galK* gene from pCM-GALK (22) to pHLL9 to create pHLL24 (Fig. 1A) and showed that the introduction of pHLL24 into strain HN13, a derivative of *C. perfringens* strain 13, in which the *galK* and *galT* genes have been deleted (22), causes the cells to be unable to grow in the presence of a high concentration of galactose (see Fig. S1 in the Supplemental Material). The presumed mechanism of lethality is that expression of *galK* in the absence of *galT* leads to accumulation of toxic levels of galactose-1-phosphate. In addition, after induction of the transposase by lactose followed by

24 h of growth in galactose-containing medium, ~90% of the clones were erythromycin-resistant and chloramphenicol-sensitive (data not shown), indicating that *galK*-mediated negative selection was effective at removing the pHLL24 plasmid backbone after transposition had occurred.

To see if the mariner transposon had hopped randomly, chromosomal DNA was isolated from 17 mutants, digested with the restriction enzyme *EcoRI*, and analyzed by Southern blotting using an *ermBP* gene-specific probe. The banding pattern indicated each of the mutants had an insertion in a different location and only 2 (~12%) of the clones had multiple insertions (data not shown). This is a higher rate of multiple insertions reported for the Mu transposition system (0 out of 30 tested (57)) or the EZ-Tn*5*-based system (0 out of 8 tested (27)) but this rate may be lowered by changing the level of induction of the transposase gene. The chromosomal DNA flanking the site of insertion in ten of these clones was sequenced (see Materials and Methods); the sites of insertion were randomly distributed around the chromosome and none of the insertions were in rRNA operons (Table S1). The point of insertion of each mutant corresponded to a TA dinucleotide, which was duplicated, as is typical for mariner transposition.

**Identification of mutants lacking gliding motility on agar plates.** We had observed that cells of strain HN13, similar to strain 13, exhibit a distinctive ability to migrate away from the colony when grown on agar plates containing a low glucose medium such as BHI (see Fig. 2C for example). Since we have shown in previous work that migration across agar surfaces is dependent on type IV pili-related functions (16), we screened a transposon-mutagenized culture for mutants lacking the ability to migrate on BHI plates. Colonies that showed a smooth, round appearance were chosen and streaked on plates containing either chloramphenicol and erythromycin or erythromycin alone to identify

mutants with transposon insertions but lacking the pHLL24 plasmid backbone.

Of more than 10,000 mutant colonies screened, 24 transposon mutants (0.24%) were identified that fit the criteria described above. The site of insertion in each mutant was determined by sequencing the flanking chromosomal DNA. The genes with transposon insertions that affected gliding motility are listed in Table 2. A schematic diagram showing the location of the affected genes on a map of the *C. perfringens* chromosome is shown in Fig. 1B. Two features of the transposon insertion sites are apparent: (i) They appear at many locations around the chromosome; and, (ii) there are specific clusters of genes in operons that were affected. Three different genes, *CPE0278, CPE1820,* and *CPE2070* each had two transposon insertions but at different locations in the same gene, indicating they are not siblings but rather independent mutants. Given the small percentage of transposon mutants that were lacking gliding motility and clustering of insertions in the same gene or genes in the same operon (see below), it appeared that a small but specific subset of gene products is required for gliding motility.

**Characterization of gliding motility mutants.** Gliding motility on agar plates gives colonies an irregular pattern, with multiple flares coming out of the edge of a colony. To determine the extent of the deficiency in gliding motility of the transposon mutants listed in Table 2, four replicates of a 15 µl suspension of cells of each mutant at an $OD_{600}$ of 10 was placed on a BHI plate, giving a zone of ~1 cm of dense growth (see Fig. 2C for an example). Movement away from this zone (i.e., gliding motility) was estimated by measuring the area covered by the entire colony and then subtracting the central zone where bacteria were plated using ImageJ software. The results are shown in Fig. 1C. In the original screen, in which several hundred colonies each with a ~2 mm diameter were on each plate, all of non-motile colonies had smooth edges. For a few of the mutants, HLL29 and HLL30 for example, in

the quantitative migration assay (where the inoculation zone was ~1 cm), a few flares spread out rapidly from the edge of the colony and covered an area similar to that seen with the parent strain, HN13. We hypothesize these flares are due to reversion of the original mutation or secondary compensating mutations that permit the bacteria to glide on the plates. Because a single bacterium, if it can glide, will quickly multiply and move across the plate, these flares show up as visually obvious features, despite the frequency of reversion being quite low within the large population at the center of the colony.

The genes found to have transposon insertions that affected gliding motility fell into the following extremely diverse categories: (i) Cell wall biosynthesis/maintenance (*CPE0278*, *CPE1634*); (ii) chromosomal DNA replication/segregation (*CPE1702*, *CPE1716*, *CPE1815*); (iii) transport across the cytoplasmic membrane (*CPE0527*, *CPE1408*, *CPE1421*); (iv) carbohydrate metabolism (*CPE0296*, *CPE0614-CPE0617*, *CPE1634*, *CPE2071*); (v) Vitamin biosynthesis (*CPE0566*); (vi) lipid metabolism (*CPE1820*); (vii) enzymes that modify tRNA (*CPE0014*, *CPE2070*); and, (viii) type IV pili functions (*CPE1767*). These assignments were made with the caveat that the effects on gliding motility may be due to polar effects on downstream genes in the same operon and not to inactivation of the gene.

**Characterization and complementation of mutant strains HLL9 and HLL28.** We chose the transposon mutants HLL9 and HLL28 for further characterization and complementation of the motility phenotype. Both strains have insertions in the gene *CPE0278*; the insertion in HLL9 is at the 5' end of the gene, while the insertion in HLL28 is at the 3' end of the gene (Fig. 2B). CPE0278 encodes a homolog of the SagA (secreted antigen) protein family that has been found in many Gram-positive species. Therefore, we designate the *sagA* allele in HLL9 and HLL28 as *sagA2* and *sagA3*, respectively. In other Gram-positive bacteria, the SagA protein has been shown to function as a peptidoglycan

endopeptidase that plays a role in septum formation and maintaining cell shape (64-67). It cleaves the bond between D-Glu and meso-diaminopimelic acid in the peptide crosslink between the polysaccharide chains (Fig. 2A). The *sagA* gene in *C. perfringens* is predicted to be monocistronic by the operon prediction software available in Microbesonline (http://www.microbesonline.org/cgi-bin/fetchLocus.cgi?locus=184876&disp=1). A rho-independent transcription terminator is predicted to lie in the 174-bp intergenic region between *sagA* and *CPE0279* (Fig. 2B) using the ARNold software (http://rna.igmors.u-psud.fr/toolbox/arnold/index.php).

Since it was possible that failure to migrate could be a consequence of a slower growth rate, we cultured strains HN13, HLL9 (*sagA2*), HLL28 (*sagA3*) in liquid BHI medium and observed no difference in growth rate under these conditions (Fig. S2).

Since the SagA protein is likely a peptidoglycan-specific endopeptidase it could be toxic or have significant phenotypic effects if expressed at high levels on a multicopy plasmid under control of its own promoter. Therefore, to complement the *sagA* mutants the wild type *sagA* gene was cloned in the vector pKRAH1, a plasmid we developed for regulating gene expression in *C. perfringens* using the lactose-inducible promoter $P_{bglA}$ (59), creating pHLL42. After 43 h of growth on BHI with 0.5 mM lactose, strain HN13 exhibited the dense flare-like pattern of migration away from the initial site of inoculation, while the *sagA2* and *sagA3* mutant strains failed to migrate to any significant extent (Fig. 2C). Both strains, when carrying the complementing plasmid pHLL42, showed similar and significant levels of migration, although somewhat less than that seen with the parental strain HN13 (Fig. 2B), suggesting that the mutations play a significant role in the mutant phenotypes. The failure of the complementing plasmid to provide complete restoration of gliding motility is likely due to the *sagA* gene being expressed at a somewhat lower level than that of the wild-type strain.

The addition of higher lactose levels leads to increased expression of the *sagA* gene when under control of $P_{bgaL}$, but high levels of lactose also inhibit gliding motility in *C. perfringens* strains (16, 18), which is the phenotype we are studying here.

We next examined the morphology of individual cells of the *sagA2* and *sagA3* mutants by phase contrast microscopy. In comparison to strain HN13, cells of the *sagA2* mutant were 32% and the *sagA3* mutant 22% shorter in length (5.24 +/- 1.45 versus 3.95 +/- 0.75 and 4.28 +/- 0.83 µm, respectively; $P< 0.001$ for both). In contrast the cells of strain HLL28 were 15% wider than those of strain HN13 (1.2 +/- 0.068 versus 1.01 +/- 0.081 µm ($P< 0.001$)). The complemented mutant strains exhibited cell lengths and widths closer to those seen in strain HN13 than the mutants, but normal cell dimensions were not fully restored (Fig. 3). Since the mutants did exhibit changes in cell morphology, we placed pHLL42, which has the *sagA* gene under control of the lactose-inducible promoter $P_{bgaL}$, into wild type strain HN13 and induced its expression by adding 10 mM lactose to cells in the mid-log phase of growth. Two hours after induction the cells were examined by light microscopy for changes in morphology but no significant differences were detected.

Using mutants lacking the type IV pilus-related proteins PilT and PilC we have demonstrated that gliding motility seen at the colony level is related to the ability of *C. perfringens* strains to form long chains with end-to-end connections between individual cells (16). We made time lapse videos of strain HN13 and the *sagA2* and *sagA3* mutants on BHI agar to see if the mutants were defective in any aspect of gliding motility at the microscopic level. Similar to what we had observed with strain 13 (16), strain HN13 forms extensive and stable long chains of cells (i.e., filaments) that migrate over the agar surface (Video S1). In contrast, the *sagA2* and *sagA3* mutant strains failed to form stable end-to-end connections, did not form chains of any length and had no organized migration pattern detectable in the

videos (see Videos S2 and S3, respectively). The complemented mutant strains carrying pHLL42 showed an intermediate phenotype between the wild type and mutant strains; they formed end-to-end connections between the cells and had filaments but the filaments were not as long or as stable as the filaments seen with strain HN13 (see Videos S4 and S5 for HLL9 (*sagA2*) and HLL28 (*sagA3*), respectively).

To confirm that the mutations in the *sagA* gene were solely responsible for the phenotypes we observed, we constructed an in-frame deletion mutation in the *sagA* gene using a homologous recombination/negative selection method reported by Nariya et al (22). This mutant allele, called *sagA*1, retained, in-frame, only the first 2 and last 12 codons of the *sagA* gene (see Materials and Methods). The migration pattern on BHI agar plates was similar to the *sagA*2 and *sagA*3 mutants (Fig. 2C) and the extent of migration (228 +/- 26 $mm^2$) lay between that seen with the other *sagA* mutant strains, HLL9 and HLL28 ( compare to Fig. 1C). The cell dimensions of the *sagA*1 mutant were 3.10 +/- 0.58 µm long and 1.21 +/- 0.08 µm wide. While similar in length to the wild type strain in length, the *sagA*1 mutant was 33% wider than the wild type strain (Fig. 3). Video microscopy of the *sagA*1 mutant showed the same lack of end-to-end connections seen in the other *sagA* mutants (compare Video S6 to Videos S2 and S3). Complementation of the *sagA*1 mutant using pHLL42 partially restored gliding motility on agar plates (Fig. 2C) and the end-to-end connections seen in video microscopy on BHI agar plates (Video S7). Therefore, the inframe deletion mutation, *sagA*1, gave very similar phenotypes to the transposon-generated mutants in all the assays we tested, suggesting the *sagA* gene product is responsible for the effects we observed.

## DISCUSSION

We constructed a random mutagenesis system for *C. perfringens* using a mariner transposon carried on a multicopy plasmid. We showed that the transposon hops in a random fashion and shows no detectable hot spots in rRNA operons or other locations. Because the transposon was delivered on a replicating plasmid in *C. perfringens*, it was possible to create and screen very large mutant libraries quickly and at low cost with no detectable bias towards insertions in rRNA genes. This construct seems to provide a versatile and useful mutagenesis system for use in *C. perfringens*. One potential limitation is the need to use as the host a strain lacking the *galK* and *galT* genes in order to make the selection against plasmid retention efficient. Since strain HN13 is a derivative of strain 13 and appears to harbor all of the known secreted virulence factors found in strain 13 (22), for most experiments this would not be a significant issue. To broaden the usefulness of this method, we have constructed a *galK galT* mutant of strain SM101 (data not shown), which is used as a model for sporulation and enterotoxin synthesis and regulation in *C. perfringens* (68). A similar approach can be used in any strain that is transformable enough to allow integration of a non-replicating (suicide) plasmid into the chromosome, as demonstrated by Nariya et al (22).

The mariner transposon mutagenesis scheme reported here allowed us to generate novel mutants defective in gliding motility on agar plates. Of the 24 gliding motility-defective mutants isolated, only one had a mutation in a type IV-pili-associated gene (*pilT*) that had been identified previously as being involved in gliding motility. This may be due to fact that the number of clones that we screened, ~10,000, did not reach that required for saturation mutagenesis (>30,000 (69)).

We chose to characterize the two mutations in the *CPE0278* gene in more detail because

this gene is likely monocistronic and its presumed product, SagA, has known biological activities. In *S. mutans* the homologous protein is secreted in vivo to such an extent that it induces a significant antibody response in human patients (65). In *Enterococcus faecium*, the SagA protein binds to host extracellular matrix proteins and is essential for growth but does not have cell wall hydrolase activity (67). The *C. perfringens* SagA protein has a signal sequence compatible for secretion via the Sec pathway (not shown). The SagA homolog in *C. perfringens* strain ATCC 13124 was identified as the most abundant secreted protein, even more so than alpha toxin and collagenase, two well-studied secreted toxins (70). This is consistent with our observation that even maximum expression from the PbgaL promoter on a multicopy plasmid The *C. perfringens* SagA protein displayed three different isoforms in two-dimensional gel electrophoresis, which suggests post-translational modification of the protein (70).

The FUGUE structural prediction software (tardis.nibio.go.jp/fugue/prfsearch.html) found that the closest structural homolog available is the C-terminal domain of the rv1477 protein (also designated as RipA) from *Mycobacterium tuberculosis* (64). Originally identified as a gene product necessary for invasion and intracellular replication (66), rv1477 was later found to be a cell wall hydrolase similar in function to SagA homologs in the *Firmicutes* (71). This is consistent with the *CPE0278* gene product playing a role in maintaining cell shape, which supports its assignment as a SagA homolog. The homology to rv1477 extends over the C-terminal half of the *C. perfringens* 432-residue SagA protein from Arg247 to the Ser427 (Fig. S3). This region contains the NLP/P60 cell wall hydrolase domain which catalyzes cleavage of the peptide bond between meso-DAP and D-glutamate in the peptide cross-link between glycan strands (64). In *Mycobacterium smegmatis*, a *ripA* mutant forms long chains and branches (71). In *C. perfringens*, the three *sagA* mutants showed some

defects in cell length and/or width and failed to form end-to-end connections important for gliding motility (Fig. 3). These different phenotypes suggest that the SagA homologs in these species have different effects on maintenance of shape and morphology mediated by the cell wall.

Since our screening procedure identified only mutants that can grow on agar plates but not spread, it is clear that gliding motility requires more than ability to grow. The videos in the Supplemental Material show that end-to-end connections are essential for gliding motility. We theorize that most of our mutants, for one reason or another, have a defect in placing the cell organelle responsible for cell-cell adherence on the surface of the bacteria, where it is needed. The nature of the structures responsible for the end-to-end connections has not yet been identified, but is a major focus of our current research.

The wide variety of gene categories that emerged from the screen indicated that gliding motility depends upon multiple factors. The *CPE0614-0617* gene cluster had four individual insertions in four adjacent genes (Table 2). The dTDP-L-rhamnose biosynthesis pathway I, which converts glucose-1 phosphate and TTP to dTDP-L-rhamnose requires, in consecutive order, the activity of the RfbABCD enzymes. In *C. perfringens* strain 13, the *rfbABCD* genes are distributed in two separate operons, *CPE0613-rfbP-rfbN-rfbA* and *rfbC-rfbD-rfbB* (http://www.microbesonline.org/cgi-bin/fetchLocus.cgi?locus=185212&disp=1). The function of CPE0613 is unknown but it contains a haloacid dehydrogenase (HAD) hydrolase domain (COG0561) which is often associated with hydrolysis of sugar phosphates (http://www.ncbi.nlm.nih.gov/COG/grace/wiew.cgi?COG561). RfbP and RfbN are associated with transport of rhamnose across the cytoplasmic membrane and transfer of rhamnose to a growing polysaccharide, respectively. These gene functions and their association with gliding motility suggest that they are involved in synthesis of a polysaccharide that is exposed on the

surface of *C. perfringens*. Since there are no reports in the literature regarding the nature of surface polymers such as teichoic or lipoteichoic acid in *C. perfringens*, the role these genes play in gliding motility remains an open question.

## ACKNOWLEDGEMENTS

We thank Elizabeth Pickering (Aerospace Engineering, Virginia Tech) and Sean Mury (Biological Sciences, Virginia Tech) for help with imaging software. This work was supported by National Institutes of Health grants R21 AI088298 (to S.B.M.), R21 AI101536 (to A.L.S.) and R01 AI057637 (to A.L.S.) and by NSF grant 1057871 to (S. B. M.)

## Table 2.1. Bacterial strains, plasmids and primers used in the study

| Strain/ plasmid/ primer | Relevant characteristics or sequence | Source or reference |
|---|---|---|
| **Strains** | | |
| *E. coli* DH10B | F$^-$ *mcrA*Δ *mrr-hsdRMS mcrBC* ϕ80d*lacZ*ΔM15 *lacX74 deoR recA1 araD139*Δ *ara, leu7697 galU galK*Δ*rpsL endA1 nupG* | Gibco/BRL |
| *C. perfingens* HN13 | Strain 13, Δ*galKT* | (22) |
| HLL50 | HN13, Δ*CPE0278* (*sagA*) | |
| *C. difficile* JIR8094 | | |
| **Plasmids** | | |
| pGEM-T Easy | PCR cloning vector, ampicillin resistance | Promega |
| pBADC9 | | (60) |
| pJIR1457 | | (60) |
| pMTL82151 | | (61) |
| pKRAHI | Contains *bgaR*-$P_{bgaL}$, chloramphenicol resistance | (59) |
| pCM-GALK | Contains a *C. beijerinckii galK* gene under control of a ferredoxin promoter from *C. perfringens* | (22) |
| pBSII KS+ | Ampicillin resistance | Fermentas |
| pBL79 | Contains a *Himar1* C9 transposase under a *tcdA* promoter, erythromycin and chloramphenicol resistance | This study |
| pHLL7 | Contains $P_{bgaL}$ in pGEM-T Easy | This study |
| pHLL9 | Replaced *tcdA* promoter with $P_{bgaL}$ in pBL79 | This study |
| pHLL23 | *galK* with its ferredoxin promoter in pGEM-T Easy | This study |
| pHLL24 | Contains a *Himar1* C9 transposase under $P_{bgaL}$ and the *galK* gene from pCM-GALK, erythromycin and chloramphenicol resistance | This study |
| pHLL42 | The *cpe0278* gene under control of the lactose-inducible promoter in pKRAH1 | This study |
| pHLL49 | Contains the 5' and 3' flanking regions of *CPE0278*(*sagA*) | This study |
| **Primers** | **Sequence 5' to 3'** | **Restriction sites** |
| OLB92 | GGAGGAATTCCATATGGAAAAAAAGGAATTTCGTGTTTTGATAAAATACTG | EcoRI/NdeI |
| OLB93 | AAGCTTGCATGC**CTGCAG**ATTCCGGTCTAACAAAG | PstI/SphI/Hind III |
| OLB94 | GGAATTCCATATGAACCTCCTAGTATTATTATTTTTGATAATAAATCC | NdeI |
| OLB95 | CCCGAATTCTAGAGCATGGTCAGTTGGTAAAATCTATTAAGC | EcoRI/XbaI |
| OLB96 | GCAACTCTCTACTGTTTCTCCATACCCG | |
| OLB97 | TCCCCCGGGACATGTAGCTCACTCATTAGGCACCCCAGG | SmaI |
| OLB98 | TCCCCCGGGCTCTTCCAGGGTTATGCAGCGGAAAAGATCCGTCGA | SmaI |
| OHL15 | GCTTCTAGATTCTACCTCCTAACCTATAAAATTAGCC | XbaI |
| OHL16 | CATATGACCCTCCTCCTTCATTTAAAATAATTATGTATTCATGAAACATGATTG | NdeI |
| OHL21 | GCAATGAAACACGCCAAAGTAAACAATTTAAGTACCG | |
| OHL22 | GTTTTATTATTTGGTTGAGTACTTTTTCACTCG | |
| OHL41 | GGTACCTAGGCTAAATATGCTTAAAAGAG | KpnI |
| OHL42 | CCGCGGCTAGTTTATTTTTTTAGCACCATC | SacII |
| OHL75 | GTCGACATGAAGAAAAAAATAATTTCAACAGTTC | SalI |
| OHL76 | GGATCCTTATAATATTCTTCTTGCTGATGAG | BamHI |
| OHL105 | GTCGACGGATGTTTTATATGGCTTTATTTACTGC | SalI |
| OHL106 | CTTCTTGCTGATGAGAAATTATATATAGGCTTCATATCTACTTGCTCCCATTTAATG | |
| OHL107 | CATTAAATGGGAGCAAGTAGATATGAAGCCTATATATAATTTCTCATCAGCAAGAAG | |
| OHL108 | GGATCCCTCATTTTTATTTACTCTCCCTTCC | BamHI |
| OHL109 | GAGTTATACTTTTTATTCATAATAAATCCTCC | |
| OHL110 | CTTGTATCCTCAGCAGCTATTAAATCAACAC | |

a: Underlining indicates the locations of restriction sites used for subsequent cloning. Bold type and italics are used to separate the sites from each other when there are multiple sites in the same primer.

**Table 2.2. Mariner transposon mutants with altered gliding motility**

| Gene | s tag (if designated), description | Strain |
|---|---|---|
| None | Parent strain, wild type | HN13 |
| *CPE0013-CPE0014* | Intergenic between CPE0013 and SerS seryl-tRNA synthetase, *serS* | HLL38 |
| *CPE0278* | SagA homolog | HLL28 |
| *CPE0278* | SagA homolog | HLL9 |
| *CPE0296* | *tktN*, transketolase | HLL20 |
| *CPE0527* | ABC transporter | HLL37 |
| *CPE0566* | *ribB*, riboflavin biosynthesis protein | HLL19 |
| *CPE0614* | *rfbP*, undecaprenyl phosphate galactosephosphotransferase | HLL40 |
| *CPE0615* | *rfbN,* rhamnosyl transferase | HLL26 |
| *CPE0616* | *rfbA,* glucose-1-phosphate thymidylyltransferase | HLL22 |
| *CPE0617* | *rfbC* dTDP-4-dehydrorhamnose 3,5-epimerase | HLL36 |
| *CPE1408* | Chloride channel protein | HLL39 |
| *CPE1421* | Putative membrane protein | HLL11 |
| *CPE1634* | *tagO*, undecaprenyl-phosphate N-acetylglucosaminyltransferase | HLL10 |
| *CPE1702* | *topA*, DNA topoisomerase I | HLL6 |
| *CPE1716* | *smc*, chromosome partition protein SMC | HLL1 |
| *CPE1767* | *pilT*, twitching motility protein | HLL29 |
| *CPE1815* | *recN*, DNA repair protein | HLL27 |
| *CPE1820* | Geranyltranstransferase | HLL23 |
| *CPE1820* | Geranyltranstransferase | HLL30 |
| *CPE2070* | tRNA 2-selenouridine synthase | HLL25 |
| *CPE2070* | tRNA 2-selenouridine synthase | HLL21 |
| *CPE2071* | Glycosyl transferase | HLL8 |
| *CPE2357* | Phosphoenolpyruvate-protein phosphotransferase | HLL12 |
| *CPE2425* | *thyX*, FAD-dependent thymidylate synthase | HLL14 |

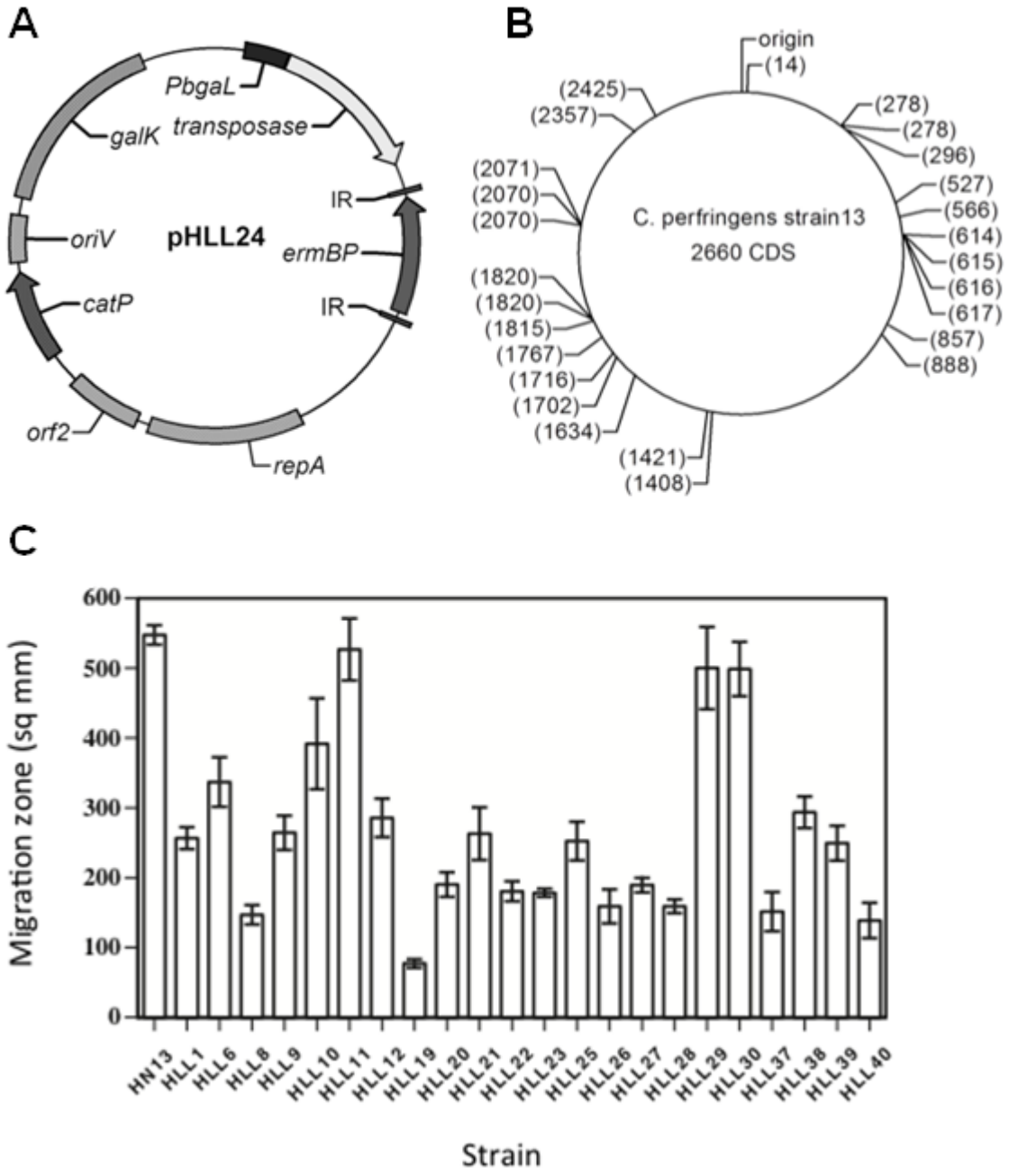


**Figure 2.1. (A)** Schematic diagram of plasmid pHLL42, showing important genetic elements. **(B)** Chromosoaml location of mariner transposon insertions that disrupted gliding motility in strain *C. perfringens* HN13. Numbers in parentheses indicate gene assignments. **(C)** The area covered by migration of bacteria away from the initial site of inoculation on BHI agar plates. Values show the mean and SD of quadruplicate samples.

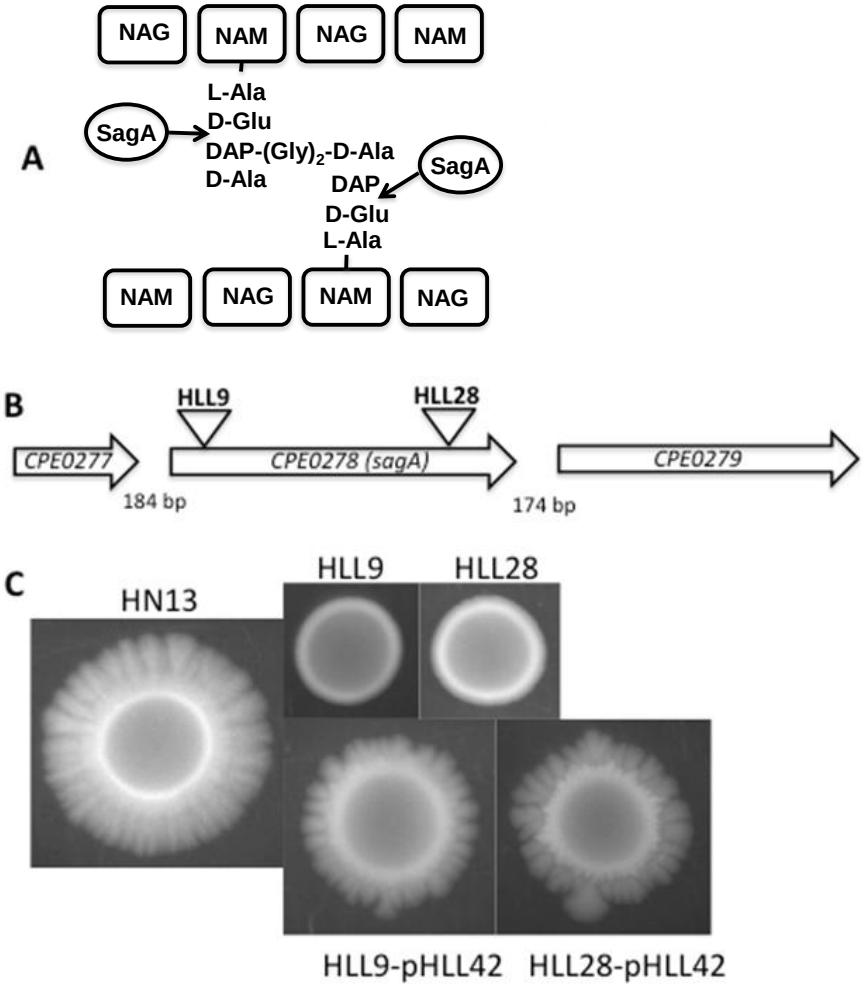


**Figure 2.2. (A)** Schematic diagram showing the structure of peptidoglycan in *C. perfringens* and the sites of activity of the SagA endopeptidase. NAG, N-acetyl glucosamine; NAM, N-acetyl muramic acid; DAP, meso-diaminopimelic acid. **(B)** Diagram of the genetic locus containing the *CPE0278* (*sagA*) gene in strain HN13. Triangles indicate the position of mariner transposon insertions in mutant strains HLL9 and HLL28. The lengths of the intergenic regions are shown below the arrows representing each gene. **(C)** Colony morphology of wild type and mutant strains as indicated above and below each image. All images are set to the same scale.

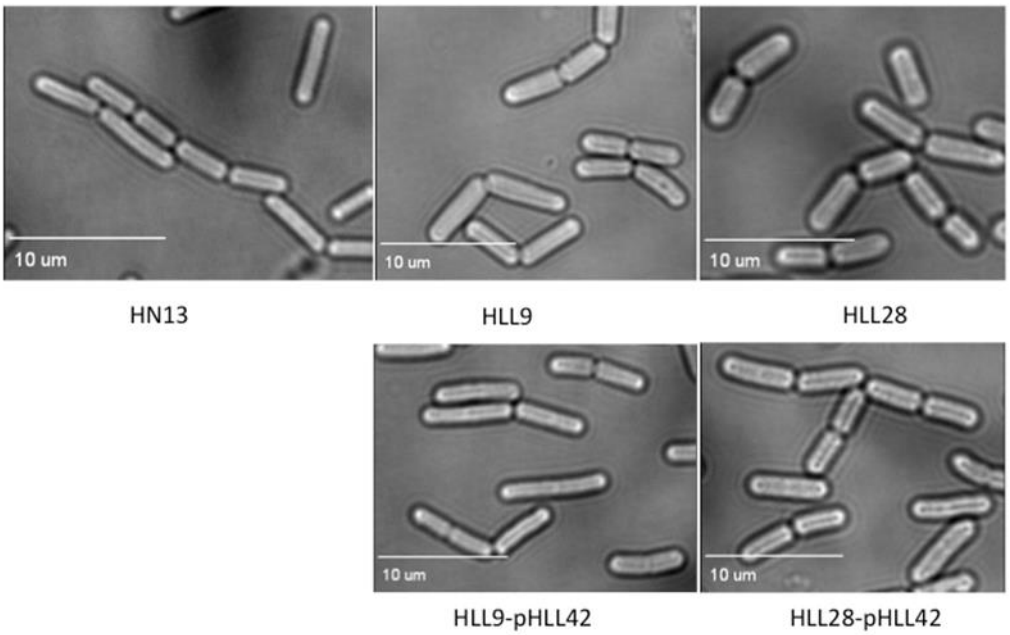


**Figure 2.3.** Representative images of wild type and *sagA* mutants *C. perfringens*.

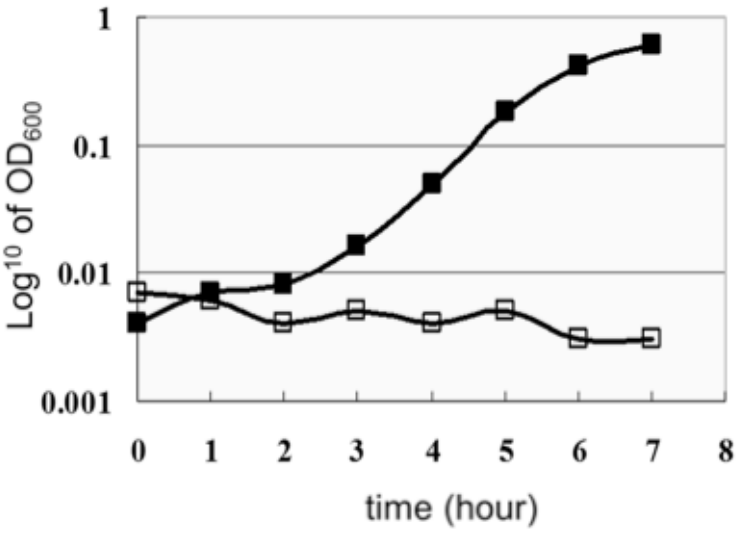


**Figure S2.1.** Growth of strain HN13 in PY with 3% galactose. Solid squares, HN13 alone; open squares HN13 carrying pHLL24.

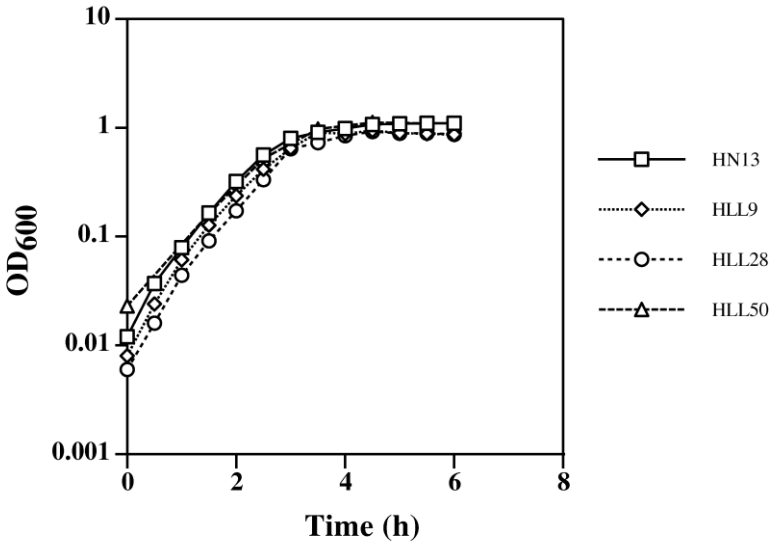


**Figure S2.2.** Growth curves of *C. perfringens* strains. HN13 and HLL50 were grown in BHI; HLL9 and HLL28, were grown in BHI plus 30 µg/ml erythromycin.

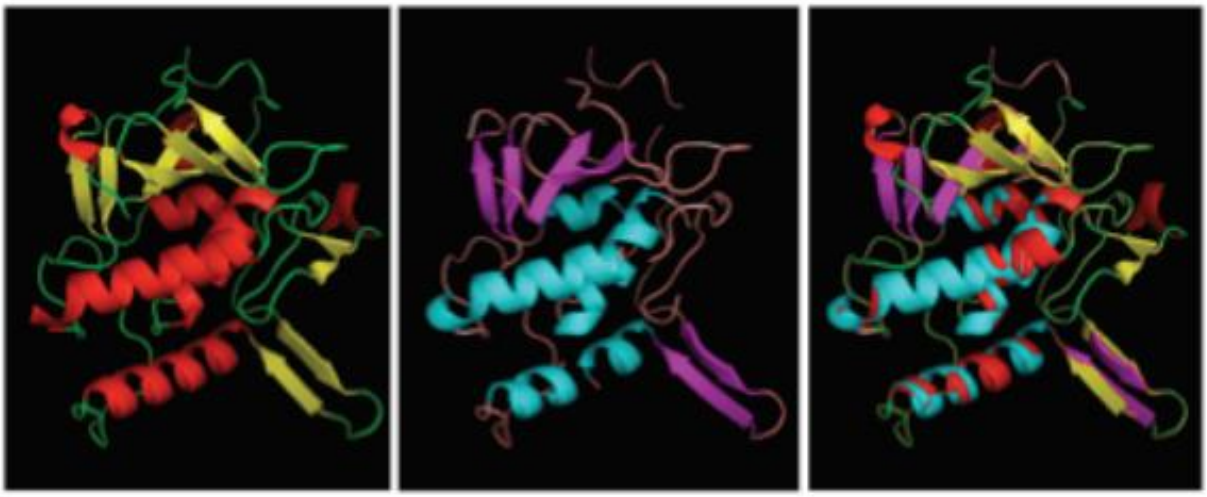

Known structures of the C-terminal half of rv1477 from *M. tuberculosis.*

Molecular model of the C-terminushalf of SagA from *C. perfringens.*

Combined models showing overlap of structural features.

**Figure S2.3.** Molecular structures of rv1447 from *M. tuberculosis* and the model for *C. perfringens* SagA, separately (left and middle panels) and combined (right panel).

Other supplemental videos and movies can be found at:
http://jb.asm.org/content/195/3/629/suppl/DCSupplemental

# Chapter 3

## Hypermotility in *Clostridium perfringens* Strain SM101 is Due to Spontaneous Mutations in Genes Linked to Cell Division

Hualan Liu[a], Kristin D. McCord[a], Jonathon Howarth[b], David L. Popham[a], Roderick V. Jensen[a], and Stephen B. Melville[a]

Departments of Biological Sciences[a] and Biochemistry[b], Virginia Tech, Blacksburg, VA

Published online ahead of print on 18 April 2014 by Journal of Bacteriology.

## CO-AUTHOR'S ATTRIBUTION:

Kristin D. McCord, from the department of Biological Sciences, Virginia Tech, helped with the plasmid construction and osmotic stress sensitivity expe preparation. Jonathon Howarth, from the department of Biochemistry, Virginia Tech, helped with the genome sequence analysis and manuscript preparation. David L. Popham, from the department of Biological Sciences, Virginia Tech, did the peptidoglycan measurement, and helped with experiment design and manuscript preparation. Roderick V. Jensen, from the department of Biological Sciences, Virginia Tech, helped the genome sequence analysis and manuscript preparation. Stephen B. Melville was the principle investigator and helped manuscript.

## ABSTRACT

*Clostridium perfringens* is a Gram-positive anaerobic pathogen of humans and animals. While lacking flagella, *C. perfringens* bacteria can still migrate across surfaces using a type of gliding motility that involves the formation of filaments of bacteria lined up in an end to end conformation. In strain SM101, hypermotile variants are often found arising from the edges of colonies on agar plates. Hypermotile cells are longer than wild type cells and video microscopy of their gliding motility suggests they form long, thin filaments that move rapidly away from a colony, analogous to swarmer cells in bacteria with flagella. To identify the cause(s) of the hypermotility phenotype, the genome sequences of normal strains and their direct hypermotile derivatives were determined and compared. Strains SM124 and SM127, hypermotile derivatives of strains SM101 and SM102, respectively, contained 10 and 6 single nucleotide polymorphisms (SNPs) compared to their parent strains. While SNPs were located in different genes in the two sets of strains, one feature in common were mutations in cell division genes, an *ftsI* homolog in strain SM124 (*CPR_1831*) and a *minE* homolog in strain SM127 (*CPR_2104*). Complementation of these mutations with wild-type copies of each gene restored the normal motility phenotype. A model is presented explaining the principles underlying the hypermotility phenotype.

## INTRODUCTION

*Clostridium perfringens* is a Gram-positive, spore-forming, anaerobic bacterium that is capable of causing numerous diseases in humans and animals, including intestinal and invasive tissue infections (53). *C. perfringens* genome sequencing indicates that the species lacks flagella and any recognizable chemotaxis system (20, 58). However, we had previously reported that *C. perfringens* and other *Clostridium* species possess type IV pili (TFP) and exhibit a unique type of social gliding motility on agar plates (16). *C. perfringens* motile cells align themselves in an end to end configuration along their long axis to form filaments that move across the surface of an agar plate (16, 19). Most filaments have other filaments attached to them to form thicker elements we refer to as flares. If one end of a flare is attached to a colony, its extension in that direction is blocked and the filament moves in a direction pointing away from the colony. This motility is dependent on the products of the *pilT* and *pilC1* genes (16), although the precise role that TFP play in this motility is still not understood.

The key factors that seem to support motility are formation of the end to end connections and growth and division of individual cells within the filament. Evidence in support of these factors comes from our study in which a pool of mariner transposon insertion mutants in strain 13 was screened for mutations which prevented gliding motility on brain heart infusion (BHI) agar plates. Several different categories of genes were found to be deficient in motility but the most common were those encoding proteins likely to be associated with the cell envelope (72). One of these genes encoded an endopeptidase, SagA, predicted to be involved in modifying peptidoglycan (72). This mutant lacked end to end connections between the bacteria and was unable to form the motile filaments but the mutant phenotype was reversed by complementation with a wild-type copy of the gene (72).

However, the composition of the material that forms the end to end connections is still unknown.

Multiple factors appear to play a role in the initiation of filament formation and gliding motility. In liquid cultures composed of the same nutrients as those found in agar plates (e.g., BHI), the cells do not form the end to end connections and so do not form filaments (16). This implies the bacteria can sense when they are in contact with a surface and modify their surface appendages, a feature shared by *Pseudomonas aeruginosa*, which produces more TFP on agar surfaces than in liquid media (73). Carbohydrates in the form of readily metabolizable hexoses act to suppress motility on agar plates, and this is mediated via the carbohydrate catabolite regulatory protein, CcpA, in *C. perfringens* strain 13 (18). Interestingly, CcpA was also required for maximum motility in strain 13 in the absence of added sugar (18). We detected similar phenotypes in a wild-type and *ccpA* mutant of strain SM101 (74).

If a concentrated bacterial suspension of *C. perfringens* strains 13, SM101 and ATCC 13124 is inoculated onto plates containing BHI with 1% agar, growth of the bacteria at the site of inoculation leads to a slight increase in the diameter of the colony (16, 18). After a period of 12-24 hours, thick flares can be seen migrating away from the original inoculation site (16, 18) and the cells within the flares are usually aligned in the end to end conformation (16). However, of these 3 strains, only strain SM101 exhibited a third form visible on plates: a rapidly migrating thin film of bacteria that can be seen emerging from the edge of a colony (Fig. 1). After cells in the hypermotile flares were moved to new plates they maintained the hypermotile phenotype, suggesting there was a genetic basis for this phenotype. To identify the mechanism, we sequenced the genomes of two hypermotile derivatives and their parental strains, one from SM101 and the other from a closely related strain, SM102. The hypermotile

strains had multiple single nucleotide polymorphisms (SNPs) in different genes. However, two genes that encoded proteins involved in cell division and led to the production of longer cells were solely responsible for the hypermotile phenotype. These results suggest there is a link between the length of individual cells and the macroscopic appearance of gliding motility in *C. perfringens*.

## MATERIALS AND METHODS

**Bacterial strains and growth conditions.** Bacterial strains, plasmids, and primers used in this study are listed in Table 1. *E. coli* was grown in Luria-Bertani (LB) medium supplemented with antibiotics as needed (100 µg/ml ampicillin, 20 µg/ml chloramphenicol) and 1% agar for plates. Three different media were used for *C. perfringens*: BHI (Difco), fluid thioglycollate (FTG) (Difco), and Duncan-Strong sporulation medium with 0.4% raffinose (DSSM) (75). BHI was supplemented with 20 µg/ml chloramphenicol and 0.5 mM lactose for the following four *C. perfringens* strains, SM124(pKRAH1), SM124(pHLL59), SM127(pKRAH1) and SM127(pHLL61). All *C. perfringens* cultures were incubated in a Coy anaerobic chamber at 37°C in an atmosphere of 85% $N_2$, 10% $CO_2$, and 5% $H_2$.

To measure growth rates and yields of *C. perfringens* strains SM101, SM124, SM124(pKRAH1) and SM124(pHLL59), 5 ml of an overnight liquid culture of each strain was adjusted to $OD_{600} \approx 1$ and then inoculated into 45 ml of BHI liquid medium. Because cells of strain SM127 tended to lyse after several hours in stationary phase (data not shown), for strains SM102, SM127, SM127(pKRAH1) and SM127(pHLL61), 5 ml of mid-log phase liquid culture of each strain was inoculated into BHI liquid medium at the start of the experiment. One ml of culture was removed every hour and $OD_{600}$ value was measured in 1 cm cuvettes in a Genesys 10S spectrophotometer (Thermo Scientific) until the culture reached stationary phase. Since the complementing plasmids have the gene of interest behind a lactose-inducible promoter (Table 1), lactose was added every two hours to bring the final concentration to 0.5 mM. One of two duplicate curves is shown in Fig. S1.

The cell mass produced by individual colonies was measured by inoculating

duplicate BHI agar plates in four spots with 10 µl of log-phase cells from a liquid BHI culture. The plates were incubated at 37°C in the anaerobic chamber for 40 hours. The cells were scraped off the plate with a plastic loop and remaining cells were recovered by washing the plate with 3 ml of Dulbecco's phosphate buffered saline (DPBS). The cell suspension was pelleted by centrifugation, resuspended in 8 ml of DPBS, and the $OD_{600}$ was measured.

**Genome sequencing.** Chromosomal DNA was isolated from non-motile and hypermotile strains using a modified version the method of Pospiech et al. (76). For *C. perfringens* strains, instead of a single chloroform extraction, the cell lysates were extracted once with phenol, twice with phenol:chloroform:isoamyl alcohol (25:24:1), and once with chloroform. The sequence library was prepared as follows: genomic DNA was sheared to 500 bp using a Covaris M220 focused ultrasonicater (Covaris, Woburn, Massachusetts). Sonication was done at peak incident power of 50 W, duty factor of 20%, cycles per burst of 100 for 50 s. DNA-Seq libraries were constructed using Illumina's TruSeq DNA PCR-Free Sample Preparation Kit V2-Set A/B (part number FC-121-3001). A 650 bp library was selected by a double SPRI Ampure XP protocol. Each library was individually barcoded to enable multiplexing on a single MiSeq sequencing run. Each library was quantitated using Quant-iT dsDNA HS Kit (Invitrogen) and the library size validated on a BioAnalyzer 2200. The libraries were further quantitated using qPCR to generate optimal sequencing densities. For MiSeq sequencing, individual libraries were pooled in equimolar amounts, denatured and loaded onto MiSeq at 10 pM. The pooled library was sequenced to 2 x 250 paired ends (PE) on the MiSeq using the MiSeq Reagent Kit Ve, 500 cycles (part number MS-102-2003).

**Sequence analysis.** The fastq files containing between 4,000,000 and 15,000,000, 250 bp PE reads for each sample were aligned to the reference *C. perfringens* SM101 genome (NC_008262.1) using the Geneious Software Version 6.1.2 (Biomatters,

http://www.geneious.com). Variants consisting of single base substitutions and insertions and deletions were called if they occurred in >90% of the aligned reads with between 40% and 60% representation in forward and reverse orientations and >100x coverage. Thirty one variants from the reference were found in every sample (Table S1, Supplemental Material). These were presumed to be either variants in the current parent laboratory strains or errors in the original reference assembly. Therefore, the analysis of genotypic variants associated with phenotypic changes focused on the remaining base substitutions or indels that were unique to individual samples. The positions of all variants are reported relative to the SM101 reference genome.

**Plasmid construction**. DNA manipulation was performed using standard protocols (77). Two plasmids, pHLL59 and pHLL61, were constructed to complement mutations in *CPR_1831* and *CPR_2104*, respectively. Primers OHL141 and OHL142 were used to amplify the coding sequence of *CPR_1831* and its own ribosome binding site. A *Sal*I site was included in primer OHL141, while a *Bam*HI site was included in OHL142. The PCR product was ligated to pGEM-T Easy (Promega) to create plasmid pHLL58 and the gene was then cloned into pKRAH1 (59) to create plasmid pHLL59. The *CPR_2104* complementing plasmid pHLL61 was constructed in the same manner using primers OKM13 and OKM14. Transformation of *E. coli* and *C. perfringens* was performed by electroporation as previously described (59). All constructs were verified by DNA sequencing.

**Colony and cell morphology and video microscopy.** Five µl of log phase liquid culture was spotted onto BHI plates (supplemented with chloramphenicol and lactose if needed) and incubated in the anaerobic chamber for 40 h. Images of colonies were obtained using a Bio-Rad Gel Doc XR imager with Applied One 4.6.5 version software. For video microscopy, bacteria grown overnight on a BHI agar plate were inoculated into a tissue culture flask

coated with a thin layer of BHI agar medium (16) and incubated for 30 minutes in an anaerobic chamber. The cap on the flask was then closed, and the flask removed from the chamber and imaged in an Olympus IX81 upright microscope linked to a Hamamatsu model C4742 CCD camera. Slidebook 5.1 Intelligent Imaging Innovations software was used to compile time-lapse videos and measure the cell length of cephalexin-treated cells. For all other conditions and strains, cell length measurements were obtained using phase contrast images obtained from an Olympus IX81 upright microscope linked to DeltaVision imaging software package (Applied Precision). MicrobeTracker software (63) linked to a MATLAB (Mathworks) platform was used to measure cell length and width of ~1,000 to ~6,000 individual bacteria, depending on the strain, in the phase contrast images.

**Sporulation assay.** To determine if the *CPR_1831* gene plays a role in sporulation, we performed sporulation assays with *C. perfringens* SM101 and SM124 as previously described (78). Briefly, cells were inoculated into 4 ml BHI liquid medium and incubated for 7 hours, then 40 µl of the BHI culture was transferred to 4 ml of FTG medium and incubated for 18 hours. In triplicate, 40 µl of the FTG culture was transferred into 4 ml of DSSM and incubated for 24 hours. Cultures were divided in half; one half was incubated at 75 °C for 10 min to kill vegetative cells and one half was untreated; both were then serially diluted in DPBS and plated on 0.5X strength BHI agar plates and the number of CFU was determined.

**Measurements of N-acetyl-muramic acid (NAM) levels as an indicator of peptidoglycan (PG).** *C. perfringens* cell suspensions were made in triplicate by scraping bacteria from the edges of colonies grown overnight on BHI plates, suspending them in DPBS and washing once with 1 mM $MgCl_2$. Cells at a known $OD_{600}$ were lyophilized, acid hydrolyzed, and subjected to amino sugar analysis as previously described (79, 80). Hydrolysis and analysis of known NAM standards allowed determination of the amount of

muramic acid per $OD_{600}$ unit. This amount was then used to calculate the amount of PG in units of nmol NAM/$\mu m^2$ of cell surface. This was done by first measuring the number of cells per ml, using a hemocytometer, in a suspension of bacteria at a known $OD_{600}$ value to calculate the number of bacteria/$OD_{600}$ unit (Table S2). This number was then multiplied by the surface area of an average bacteria (Fig. 2B and Table S2), assuming bacteria were cylindrical in shape and the formula for the surface area of a cylinder, $A = 2\pi r^2 + 2\pi rl$, where l is the length of an average cell, applies. This product gave the total surface area of all the bacteria in the suspension in units of $\mu m^2$ of cell surface/ml. After correcting for the actual $OD_{600}$ reading of the sample, the number of nmol NAM/ml was then divided by the $\mu m^2$ of cell surface/ml to give nmol NAM/$\mu m^2$ of cell surface.

**Cell volume produced by colonies of each strain.** The cell volume produced by individual colonies was measured by inoculating duplicate BHI agar plates in four spots with 10 µl of log-phase cells from a liquid BHI culture. The plates were incubated at 37°C in the anaerobic chamber for 40 hours. The cells were scraped off the plate with a plastic loop and remaining cells were recovered by washing the plate with 3 ml of Dulbecco's phosphate buffered saline (DPBS). The cell suspension was pelleted by centrifugation, resuspended in 8 ml of DPBS, and the $OD_{600}$ was measured. This value was then used to calculate the total volume using the formula for the volume of a cylinder and the length of an average cell from each strain.

**Cephalexin-induced filamentous growth.** *C. perfringens* SM101 and SM102 cells were struck out on BHI plates supplemented with increasing concentrations of cephalexin and incubated overnight at 37°C. Light microscopy images indicated all of the cephalexin concentrations induced filamentous growth, but only the cells from the plate with the lowest concentration of cephalexin (0.1 µg/ml) did not exhibit significant autolysis. To determine

whether cephalexin-induced filamentous growth can cause the spreading colony phenotype in wild type strains SM101 and SM102, 5µl of liquid culture in log phase was spotted on BHI plates supplemented with 0.1 µg/ml cephalexin. The culture was incubated for 40 h at 37°C and images of colonies were obtained in the same manner as described above.

## RESULTS

**Spontaneous hypermotile variants arise in *C. perfringens* strains SM101 and SM102.** Strains SM101 and SM102 are highly electroporation competent derivatives of the acute food poisoning strain, NCTC 8798 (68). When cultured on BHI with 1% agar, strains SM101 and SM102 exhibit normal gliding motility, which can be seen as the 1-2 mm spreading zone beyond the site of inoculation (Fig. 1 B-C). At random points, rapidly migrating zones of bacteria moving away from the initial zone of inoculation can be seen (arrows in Fig. 1 B-C). The parent strain of SM101 and SM102, NCTC 8798, also showed these hypermotile derivatives (Fig. 1A), suggesting SM101 and SM102 were not different in that respect. When a suspension of hypermotile derivatives, strains SM124 and SM127 from strains SM101 and SM102, respectively, were spotted onto plates, they maintained their rapidly migrating phenotype (Fig. 1 D and G). Closer examination showed the SM124 and SM127 colonies, while rapidly spreading, were thinner than the mucoid appearance of the thick flares on the outer edge of the slower moving parental strains (compare the centers of Fig. 1 B-C to Fig. 1 D and G). This suggested there was a genetic, and not physiological, basis for the dramatic change in motility.

Examination of cells scraped off BHI agar plates indicated strains SM124 and SM127 were significantly longer than their respective parent strains, SM101 and SM102 (Fig. 2A). Measurements of cell lengths using phase contrast images of cells and the MicrobeTracker software indicated SM124 cells were 1.75 times longer than SM101 cells while SM127 cells were 2.4 times longer than SM102 cells (Fig. 2B), but there were no differences in bacterial widths (data not shown).

Video microscopy of cells taken from the edge of a colony on a plate and spread on

BHI with 1% agar in tissue culture flasks indicated that strains SM124 and SM127 made long, thin filaments of cells attached end to end and each individual cell was longer, on average, than those seen with strains SM101 and SM102 (compare the cells in Video S1 to Video S3 and Video S2 to Video S4 in Supplemental Materials). The long thin filaments in strains SM124 and SM127 also appear to move in a straighter, less curvilinear fashion than those of strains SM101 and SM102, leading to greater extension away from the source colony (see Videos S1-S4). Taken together, these microscopic details are consistent with the macroscopic appearance of the colonies on agar plates (Fig. 1).

**Identification of genetic differences between the parent and hypermotile strains.**

Because the hypermotile strains appeared to have undergone a gain of function phenotypic change that was genetically stable, we wanted to determine if this was due to changes in the sequence of the genome such as SNPs, inversions or deletions. Therefore, we isolated chromosomal DNA from each parental strain and its hypermotile derivative and used next generation sequencing methods to identify changes. The sequence for strain SM101 has been previously determined using the Sanger method on chromosomal DNA isolated in our laboratory (58). Comparison of the DNA sequences for strain SM101 from this report to the previously published sequence showed there were 31 SNPs and short sequence differences present (Table S1). These could be due to actual changes in the genomes or sequencing errors but it is difficult to differentiate between these two scenarios. Ten SNPs were identified between strains SM101 and SM124 and 6 between strains SM102 and SM127 (Table 2). The two plasmids and the episomal phage chromosome found in strain SM101 (58) were present in all strains but none contained SNPs (28, 58). Also, none of the SNPs were located in or adjacent to, the same gene in each pair of strains (Table 2), suggesting there were different genetic changes involved in producing the hypermotile phenotype in SM124 and

SM127. Interestingly, 12/16 of the SNPs involved GC to AT mutations, despite the fact that strain SM101 is only ~28% GC (58). Although a small sample size, this suggests an increased mutation rate bias in the replication of GC bases, a phenomenon seen in many organisms (81).

The one common denominator we could identify was that both lists included genes associated with cell division: an *ftsI* homolog (*CPR_1831*) in the SM101-SM124 pair and a *minE* homolog (*CPR_2104*) in the SM102-SM127 pair (Table 2). Since we noted that cells from the hypermotile strains were longer than those of their parents (Fig. 2), we investigated whether these mutations were the cause of the hypermotility.

**Complementation of cell division mutations.** The genes encoding the FtsI and MinE homologs were cloned into a plasmid vector, pKRAH1, which contains a lactose-inducible promoter for regulated gene expression (59). These plasmids, pHLL59 (FtsI) and pHLL61 (MinE), were transformed into strains SM124 and SM127, respectively. In the presence of BHI with 0.5 mM lactose, the colony morphology of strains SM124 (pHLL59) and SM127 (pHLL61) were restored to that exhibited by their respective parental strains, SM101 and SM102 (Fig. 1 E and H). The control strains containing the empty vector pKRAH1 did not show reversion back to the parental colony morphology (Fig. 1F and I). Addition of 0.5 mM lactose to BHI plates did not affect the colony morphology of strains SM101, SM102, SM124, or SM127 (data not shown). Complementation of each mutation also led to a reduction in the average cell length comparable to the parental strains while the empty vector controls did not (Fig. 2). Video microscopy of moving filaments in the complemented strains (Videos S5 and S6) showed the cells were shorter than the hypermotile strains and the filaments were not as consistently long and straight (a low density of cells were filmed in these videos to highlight individual cell lengths and filament structure more clearly).

**Other phenotypic changes conferred by the mutations in genes encoding the FtsI and MinE homologs.** The growth rate and growth yield of each parent, mutant, and complemented mutant strains were compared (Fig. S2 in Supplemental Materials). There was a longer lag time for strains carrying plasmids but no differences in growth rate or yield for each strain except SM127(pKRAH1), which had a somewhat slower growth rate (Fig. S2). Using light microscopy, we did note that strain SM127, containing the point mutation in the *CPR_2104* gene (the only *minE* homolog in strain SM101), exhibited a higher level of cell lysis after it reached stationary phase than did any of the other strains, including SM127 (pHLL61), but this was not sufficient to affect the growth yield to any great extent (Fig. S2).

As a test to determine if hypermotility leads to higher cell reproduction efficiency on surfaces, we wanted to determine the total volume of cells produced by colonies of the hypermotile and parent strains. To do this, we measured the $OD_{600}$ of all the cells in quadruplicate colonies on duplicate plates, multiplied this by the number of bacteria/$OD_{600}$ unit of 1.0 and used the formula for the volume of a cylinder with the length of an average bacteria from each strain (Table S2). The hypermotile variant SM124 produced 10% greater cell volume than its parental strain, SM101, but strain SM127 produced only 66% as much cell volume as its parental strain, SM102 (Table S2).

*C. perfringens* SM101 contains 6 genes encoding FtsI homologues (Microbesonline, http://www.microbesonline.org/), including *CPR_1831*. A C to A transversion led to a nonsense mutation (Glu to a stop codon) at residue 63 out of 739 and truncation of the open reading frame at that site (Table 2). *CPR_1831* is predicted to be the third gene in an 11 gene operon (Fig. 3A). The other annotated genes in the operon (*murE*, *murF* etc.) appear to code for proteins involved in cell wall biosynthesis (Fig. 3A). Also, since the *minE* mutant strain SM127 produced significantly longer cells than its parent strain (Fig. 2B), it was

possible that PG levels would be altered in this strain. To determine if this was the case, we measured the amount of PG (using NAM as indicator) present in the cells of the hypermotile, parent, and complemented hypermotile strains. We found there were similar levels of PG in cells from strain SM101 than SM124 (Fig. S2), suggesting the *CPR_1831* gene product is not involved in PG synthesis for the entire cell. In contrast, strain SM127 had twice as much PG per unit of cell surface area as its parent strain, but this level was reduced to that of the parent strain when the *minE* mutation was complemented (Fig. S2).

Like the other *ftsI* homologs in *C. perfringens*, the product of *CPR_1831* is annotated as being in the Stage V sporulation protein D (SpoVD) subfamily of PBPs (also called PBP-2B). Since *CPR_1831* may encode a SpoVD homolog, we tested the effect of the mutation on sporulation. Strains SM101 and SM124 were grown in DSSM sporulation media and the percent sporulation measured, but there was no significant difference seen between the two strains (SM101, 101 +/- 53.5%; SM124, 55.1 +/- 38.1%; $P = 0.293$, two-tailed student's t-test). These results suggest CPR_1831 does not function as a sporulation-associated SpoVD protein in *C. perfringens* strain SM101.

Since the *CPR_1831* and *minE* mutations leading to increased cell length likely have effects on division septum formation and perhaps other cell wall-related functions, we tested the parental and hypermotile strains to determine if they were more sensitive to osmotic stress, defined in this case by incubation in distilled water for 30 min. However, neither of the hypermotile strains was more sensitive to this treatment than the parental strains (data not shown).

**The antibiotic cephalexin increases cell length but does not lead to hypermotility.** One feature that the *CPR_1831* and *minE* mutants had in common was increased cell length

(Fig. 2). Since it was possible that increased cell length alone was sufficient to induce hypermotility, we looked for a method to induce long cell formation artificially. The antibiotic cephalexin has been shown to inhibit FtsI function (82) and, at sublethal doses, inhibit the completion of septum formation and produce *C. perfringens* cells of increased length (data not shown). To determine if cephalexin-induced production of longer cells can also cause the hypermotility phenotype in the wild type strains of *C. perfringens*, we spotted 5 µl of cells on BHI plates supplemented with 0.1 µg/ml cephalexin, a concentration that induced the formation of long cells (13.9 µm +/- 1.1 for SM101; 13.4 µm +/- 1.6 for SM102 (mean +/- SEM)) but not extensive lysis (Fig. S3A-B in Supplemental Materials). However, colonies exposed to this concentration did not show the characteristic hypermotility movement on agar plates (Fig. S3C-D). This suggests that increased cell length due to cephalexin exposure was not sufficient for hypermotility.

## DISCUSSION

While experimenting with *C. perfringens* strain SM101, we noticed that rapidly migrating offshoots of cells arose from the edge of a colony at seemingly random times and locations. Neither of the other two strains of *C. perfringens* with complete genome sequences, strains 13 and ATCC 13124, appear to do this although all 3 strains did exhibit the typical thicker flares that move away from a colony, as previously described (16, 72). Why SM101 is unique among these strains in producing this phenotype is unknown but one possible explanation is that strain SM101 has significantly stronger cell to cell connections that allow long filaments of cells to remain attached without breaking apart as they experience shear forces moving through a viscous medium like that found on an agar surface (83).

We identified two mutations that were responsible for the hypermotility phenotype, one in *CPR_1831*, encoding an FtsI homolog and the other encoding a MinE homolog. This was accomplished by successfully restoring the wild-type motility and cells size by complementation of the genes with mutations. However, since there are several other SNPs in each strain, it is possible that some of these SNPs, even though they are not directly responsible for the hypermotile phenotype, enable the mutant strains to survive with the defects that cause hypermotility. Since it is unlikely that complementation of each SNP would show an obvious phenotypic difference, we did not carry out these experiments.

The exact function of the FtsI-like *CPR_1831* gene product is unknown, but it seems likely to be involved in non-sporulation-associated PG biogenesis, based on the mutant's increased cell length, motility phenotype, predicted function, and genetic location (see Results). Given that there are 6 separate FtsI-like proteins in strain SM101, there is probably some redundancy or overlap in their functions, so that the mutation leading to loss of

CPR_1831 gives a significant phenotype (i.e., hypermotility) but is not lethal to the cell.

In *C. perfringens*, the *minE* gene appears to be in an operon with *minC* and *minD* (Fig. 3B). The MinCDE system has been well characterized in several species of Gram-negative bacteria. In *E. coli*, MinE has been shown to oscillate from one end of the cell to the other and act as a topological specificity factor for the MinC/D complex, which inhibits cell division by disrupting FtsZ ring formation (84). *Bacillus subtilis*, a Gram-positive bacterium, lacks a MinE homolog and instead uses another protein, DivIVA, to localize the MinC/D complex (85). Interestingly, *C. perfringens* and other *Clostridium* species such as *C. botulinum* and *C. difficile* have homologs of both MinE and DivIVA (CPR_1819 in *C. perfringens* strain SM101). Which (or both) of these proteins is used to specify the location of the MinCD complex in *C. perfringens* is unknown but it does suggest differences between the Clostridia and both the *Bacillus* and Gram-negative mechanisms for divisome formation. Considering the large number of important human and animal pathogens present in the Clostridia and the number of antibiotics that affect cell division, this subject appears to need more research devoted to it.

The mutation in the strain SM127 *minE* gene resulted in a Gly71 to Trp71 substitution. The first ~30 residues of MinE are thought to function in the inhibition of the MinCD complex, while the rest of the protein is reported to provide the topological specificity in the MinE oscillation (86). The structural prediction program FUGUE (87) was used to construct a model of the *C. perfringens* MinE protein based on the crystal structure of the *Helicobacter pylori* MinE (29% sequence identity). The *H. pylori* MinE structure is disordered between residues L60 and S65. The model, derived from the FUGUE server (http://tardis.nibio.go.jp/fugue/prfsearch.html) with 99% confidence, suggests the mutation at Gly71 occurs in an analogous region of the *C. perfringens* MinE protein (data not shown).

Given the location of the mutation, it seems more likely that the topological specificity function of MinE was more affected than MinCD inhibition, although there is no direct evidence yet to support this.

Strain SM127 does contain twice the amount of PG per $\mu m^2$ of surface area as does its parental strain, SM102 (Fig. S2). We are not certain about the reasons of this, but it is interesting that one $OD_{600}$ unit of these cells contains just half the volume as its parent (Table S2), suggesting there may be a correlation between PG levels and the optical properties of a cell suspension.

A biomechanical model for why the hypermotility phenotype appears is shown in Fig. 4, with strains SM101 and SM124 used as examples. The contours of the migration zones arising from SM101 and SM124 colonies are different, with a shorter, thicker zone for SM101 and thinner more dispersed zone for SM124 (Fig. 4, top images). Although the growth rate and yield for each strain is similar in liquid BHI cultures (Fig. S1), there are lower amounts of total cell volume made by the hypermotile strains under plate growth conditions (Table S2). This suggests that even though the strains that spread more rapidly can move away from a zone of nutrient depletion, allowing them access to more nutrients from the growth medium, they do not produce more cells in a given amount of time (triangular gradients in Fig. 4, top). The thicker flares seen with SM101 are significantly more curvilinear than those seen with the hypermotile strain SM124 (Fig. 4, middle images) which means that they bend back towards the colony before they migrate as great a distance. What accounts for the more linear migration pattern seen in the hypermotile strains? One feature is that, being longer, there are fewer cell junctions per unit length in the hypermotile strains. Since the cells are rigid in comparison to the cell-cell juncture points, this allows for less deflection from linearity of the filament over the same length and a more linear path of

motion (Fig. 4, bottom images).

Mendez et al (18) published images of *C. perfringens* strains besides SM101 that appear to have the hypermotile phenotype in the absence of glucose. However, it is difficult to determine if the published images represent the originally isolated form of the strain or hypermotile variants that were selected in the laboratory. Therefore, in terms of studying motility in *C. perfringens* strains, it is important to maintain separate laboratory stocks of both the normal and hypermotile variants if they arise naturally.

We have attempted to find revertants of the hypermotile strains back to normal motility but, because of their rapid spreading, hypermotile bacteria tend to grow over and cover up any slower moving variants that arise in their midst. To overcome this problem, we looked for revertants on plates using single cells to form colonies but did not see any after examining several thousand colonies (data not shown).

We selected for mutants that converted to the hypermotile phenotype simply by picking cells that were contained in the fast-moving flares. There were $>10^9$ bacteria in the inoculation zone from which the hypermotile cells arose and only a few flares arose from each zone (Fig. 1A-C). If the hypermotile strains arise as a consequence of a single mutation, then the frequency with which these occur is low. In strain SM124 complemented using a multicopy plasmid carrying the wild-type *CPR_1831* gene, a hypermotile variant can be seen at the edge of the inoculum site (Fig. 1E). Since it is unlikely every copy of the complementing gene is mutated or that the cell lost all copies of the complementation plasmid in the presence of antibiotic selection, this is likely due to a mutation in a second gene that leads to hypermotility, possibly *minE*. In addition, while the antibiotic cephalexin was able to produce elongated cells of *C. perfringens*, it did not duplicate the hypermotile

phenotype (Fig. S3). Added together, these observations support a model in which specific, but relatively rare, spontaneous mutations lead to the hypermotility phenotype. An important question then is: Do hypermotile variants arise in natural settings outside of the laboratory such as the soil or the intestinal tracts of animals and humans? The two hypermotile strains isolated in this study were not deficient in growth in rich media, and were not overly sensitive to the environmental conditions we tested, such as osmotic stress and sporulation conditions for the FtsI mutant (see Results section). Therefore, it is conceivable that hypermotile variants do arise naturally, confer a temporary selective advantage on their progeny, and then revert back to the normal motility phenotype. This could be tested by immediately identifying fresh clinical and soil isolates that have the hypermotile phenotype and sequencing the genomes. Any strains with mutations in cell division genes could be complemented with the wild-type copy to restore the normal motility phenotype, as we have done in this report. Such studies are planned in our laboratory.

## ACKNOWLEDGEMENTS

We thank the Virginia Bioinformatics Institute (VBI) Genomics Research Laboratory for the genome sequencing results reported here and Timofey Arapov for assistance with the MicrobeTracker software. This work was supported by the VBI and The Fralin Life Sciences Institute as well as National Institutes of Health grant R21 AI088298 and NSF grant 1057871 to S. B. M.

**Table 3.1. Strains, plasmids and primers used in this study**

| Strains/ plasmids/primers | Relevant characteristics | Source or reference |
|---|---|---|
| **Strains** | | |
| ***E. coli*** | | |
| DH10B | F$^-$ *mcrA*Δ (*mrr-hsdRMS mcrBC*) ϕ80d*lacZ*ΔM15 *lacX74 deoR recA1 araD139*Δ (*ara, leu*)*7697 galU galK*Δr*psL endA1 nupG* | Gibco/BRL |
| ***C. perfringens*** | | |
| NCTC 8798 | Acute food poisoning strain | R. Labbe |
| SM101 | Electroporation efficient derivative of strain NCTC 8798 | (68) |
| SM102 | Electroporation efficient derivative of strain NCTC 8798 | (68) |
| SM124 | SM101, mutation in gene *CPR_1831* | This study |
| SM127 | SM102, mutation in gene *CPR_2104* | This study |
| **Plasmids** | | |
| pGEMT-Easy | Cloning vector | Promega |
| pKRAH1 | Contains *bgaR*-$P_{bgaL}$ and polylinker; chloramphenicol resistance | (59) |
| pHLL58 | Contains the *CPR_1831* coding sequence in pGEM-T Easy | This study |
| pHLL59 | Contains the *CPR_1831* coding sequence in pKRAH1 | This study |
| pHLL60 | Contains the *CPR_2104* coding sequence in pGEM-T Easy | This study |
| pHLL61 | Contains the *CPR_2104* coding sequence in pKRAH1 | This study |
| **Primers** | **5' to 3' sequence** | |
| OHL141 | GTCGACGAACTCATTTTATTTAACTTACTACGGAGGG | This study |
| OHL142 | GGATCCCACAAAATACTAGCATGTGAAATTACTC | This study |
| OKM13 | GTCGACTCTATATTAAAGTTGTTTAGAAGAGGG | This study |
| OKM14 | GGATCCTTATCTAGCTTTACCCTTTATATTTTTTATTG | This study |

**Table 3.2. Location of SNPs between each parent strain and its hypermotile derivative strain**

| Gene | Annotated protein function | Location[1] | Base change | Codon change[2] | Mutation type |
|---|---|---|---|---|---|
| **Differences between SM101 and SM124** | | | | | |
| CPR_0055 | DNA polymerase III subunits gamma and tau subunits | 61,664 | T to G | AAT to AAG, Asn to Lys | Substitution |
| CPR_0185-CPR_0186 | Between cobalt transporter subunit and hypothetical protein | 227,182 | C to T | | |
| CPR_0458 | N-acetylmannosaminyl transferase | 544,247 | C to A | GCT to GAT, Ala to Asp | Substitution |
| CPR_0547-CPR_0548 | Between ISCpe2 transposase and phosphate transport regulator CPR_0548 | 648,489 | G to T | | |
| CPR_0911 | lipoprotein, putative CDS | 1,043,513 | T to G | AAT to AAG, Asn to Lys | Substitution |
| CPR_1135 | Transcriptional regulator of fatty acid biosynthesis FabT | 1,281,879 | G to T | GTT to TTT, Val to Phe | Substitution |
| CPR_1215 | Activator of (R)-2-hydroxyglutaryl-CoA dehydratase | 1,365,085 | C to A | GAG to GAT, Glu to Asp | Substitution |
| CPR_1831 | Cell division protein Ftsl (Peptidoglycan synthetase) | 2,023,347 | C to A | GAA to TAA, Glu to stop codon | Truncation |
| CPR_2039 | Topoisomerase IV subunit A | 2,253,090 | T to G | AAA to CAA, Lys to Gln | Substitution |
| CPR_2578 | Hypothetical protein | 2,808,164 | C to A | TAC to TAA, Tyr to stop codon | Truncation |
| **Differences between SM102 and SM127** | | | | | |
| CPR_0456 | UDP-glucose dehydrogenase | 542,746 | G to T | GAG to TAG, Glu to stop codon | Truncation |
| CPR_0742-CPR_0743 | Between two proton/glutamate symporters and HAD hydrolase | 868,274 | A to C | | |
| CPR_0456 | putative membrane protein CDS | 1,450,256 | G to T | GAC to GAA, Asp to Glu | Substitution |
| CPR_1884 | Voltage-gated chloride channel family protein | 2,078,621 | G to T | GCT to GAT, Ala to Asp | Substitution |
| *CPR_2104* | Cell division topological specificity factor MinE | 2,331,046 | C to A | GGG to TGG, Gly to Trp | Substitution |
| CPR_2491-CPR_2492 | Between a foldase protein PrsA precursor and SpoVT, AbrB family transcriptional regulator | 2,705,576 | G to T | | |

1. Location in published sequence of strain SM101 (58).

2. May differ from base change if coding sequence on reverse strand.

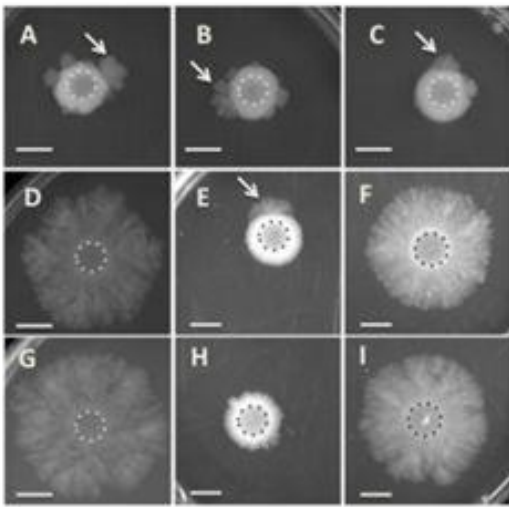


**Figure 3.1.** Representative images showing migration of different strains of *C. perfringens* on BHI plates (1% agar). A suspension of cells was spotted on plates at the beginning of the experiment; the extent of the original inocula are shown as dotted lines in each image. **(A)**, NCTC 8798; **(B)**, SM101; **(C)**, SM102; **(D)**, SM124; **(E)**, SM124(pHLL59); **(F)**, SM124(pKRAH1); **(G)**, SM127; **(H)**, SM127(pHLL61); **(I)**, SM127(pKRAH1). For panels E, F, H, and I, 0.5 mM lactose and 20 μg/ml chloramphenicol were added to the medium. Arrows point to migration flares moving away from the site of inoculation. Scale bars = 1 cm.

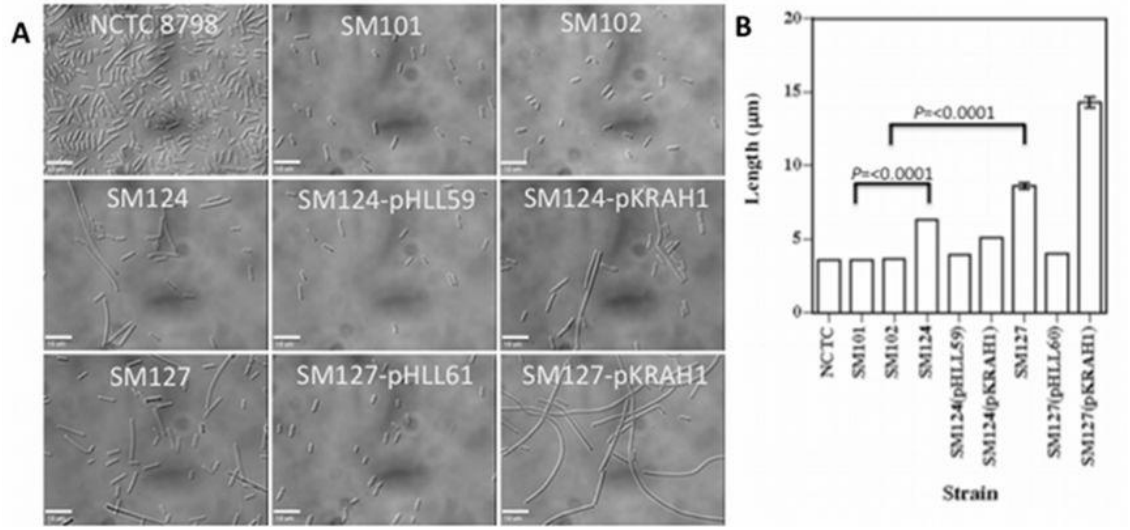


**Figure 3.2. (A).** Representative images showing cells scraped off plates of the strains listed for each panel. For the panels with bacteria from strains SM124(pHLL59), SM124(pKRAH1), SM127(pHLL61), and SM127(pKRAH1), 0.5 mM lactose and 20 μg/ml chloramphenicol were added to the medium. Scale bars = 10 μm. **(B)**. Length of bacteria isolated from plates grown under the same conditions listed in panel A. The values shown are the mean and SEM. The brackets show *P* values, obtained using the student's double tailed t-test, in length differences between the indicated strains.

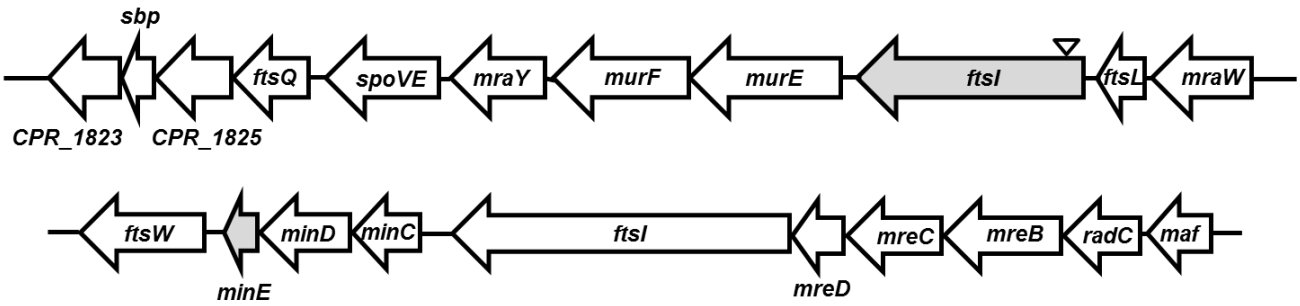


**Figure 3.3.** Location of genes (gray shading) associated with hypermotility in *C. perfringens* strain SM101 and SM102. The annotated putative gene function is shown; if the function is unknown the gene is given its genome assignment name. **(A).** *CPR_1831*; the inverted triangle indicates the location of the nonsense mutation. **(B).** *minE*; the gene appears to be the third gene in a *minCDE* operon, based on criteria used in the web site Microbesonline (http://www.microbesonline.org/).

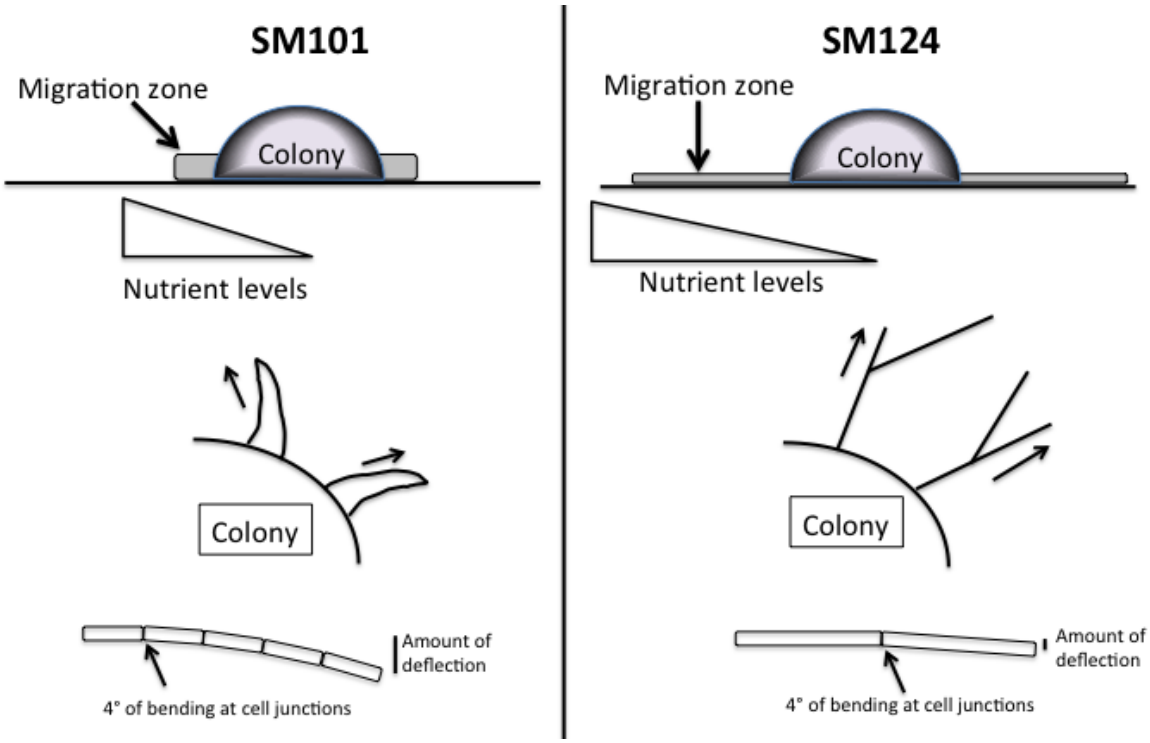


**Figure 3.4.** Model illustrating features of the hypermotility phenotype (strain SM124) in comparison to normal motility (strain SM101). Although not shown, similar features can be found in the comparison of strain SM127 to strain SM102. See the Discussion for a full description of the elements shown in the figure.

Other supplemental videos and movies can be found at:
http://jb.msubmit.net/jb_files/2014/04/11/00070822/01/70822_1_supp_1199682_n3vszv_convrt.pdf

# Chapter 4

# Proteomic Analysis of Spore Inner Membrane in *Clostridium perfringens* SM101

Hualan Liu[1], W. Keith Ray[2], Richard F. Helm[2], David L. Popham[1], and Stephen B. Melville[1]

Departments of Biological Sciences[1] and Biochemistry[2], Virginia Tech, Blacksburg, VA

This Chapter is to be submitted for publication in the Journal of Bacteriology.

# CO-AUTHOR'S ATTRIBUTION

W. Keith. Ray, from the department of Biochemistry, Virginia Tech, helped and supervised sample preparation and analysis, generated the raw Scaffold data and also helped with the manuscript preparation. Richard F. Helm, from the department of Biochemistry, Virginia Tech, helped design the research, analyze the data and edit the text. David L. Popham, from the department of Biological Sciences, Virginia Tech, helped design the research, analyze the data and edit the text. Stephen B. Melville, from the department of Biological Sciences, Virginia Tech, was the principle investigator and revised the manuscript.

## ABSTRACT

*Clostridium perfringens* endospores play an important role in *C. perfringens*-associated foodborne illness. As a survival strategy under harsh conditions, *C. perfringens* undergo sporulation to produce highly resistant spores. Once the environmental conditions become favorable, mainly when nutrients are available, the spores will germinate and resume vegetative growth. It has been established that germination starts with the activation of germinant receptors, which are located in the spore inner membrane. In this work, we did comparative spore inner membrane proteome analysis of *C. perfringens* dormant and germinated spores, using gel-based protein separation and liquid chromatography coupled with MALDI-TOF/TOF mass spectrometry. A total of 494 proteins were identified, and 117 of them were predicted to be integral membrane or membrane-associated proteins. Among those membrane proteins, 16 and 26 were found only in dormant and germinated spores, respectively. The rest were found in both dormant and germinated spore samples, with 28 of them changed at least 2-fold in abundance. The results indicated that proteins involved in ion transport, protein translocation, protein turnover, cell division, cell wall and membrane biogenesis were detected at two fold higher levels from the membranes of germinated spores than from the dormant spores. Fewer proteins showed at least a 2-fold decrease in abundance, including proteins involved in energy production, DNA replication, transcription, and germinant receptors. This study provides a list of the spore inner membrane proteins in *C. perfringens* that can be used to reveal insights into our understanding of this important cell developmental process.

## INTRODUCTION

*C. perfringens* is a Gram-positive, anaerobic, spore-forming, pathogenic bacterium. Strain SM101 is able to cause self-limiting food poisoning. Due to their general resistance properties (88), spores are the major means for the transmission of this pathogen. However, once the spore germination occurs, the organism loses its resistance quickly, becoming much more vulnerable to heat, disinfectants, and other antimicrobial treatments (45).

Spore germination has been intensively studied in *Bacillus* species. Based on the current model, the spore germination cascade is triggered by the interaction between germinant and germinant receptors, and those germinant receptors are located in the spore inner membrane (34). It is believed that the interaction between germinants and germinant receptors change the permeability of the spore inner membrane, which causes a resultant ion flux (89). However, the signal transduction involved in this process is poorly understood. During ion flux, monovalent cations such as $K^+$, $Na^+$ and $H^+$ are released from the spore core to the environment, along with a large amount of calcium dipicolinic acid (Ca-DPA) (39, 89, 90). Several ion channel proteins and transporters have been found to play a role in this stage, which include the spore inner membrane SpoVA proteins, and the putative spore outer-membrane Na+/H+-K+ antiporters (90, 91). Later events in spore germination include the degradation of spore cortex by germination-specific cortex-lytic enzymes and the degradation of core proteins by proteases, followed by full rehydration of the spore core and resumption of metabolism (34).

The spore germination process in *C. perfringens* is not as well studied as those in *Bacillus subtilis*. Current research also revealed some significant differences between the germination processes in these two species. First, *C. perfringens* SM101 spores do not

germinate efficiently with nutrient germinants such as amino acids or sugars. Instead, the cation potassium triggers germination quite well (29). Second, whole genome sequence analysis found that *C. perfringens* SM101 contains only one classical germinant receptor complex GerKABC, which contains three proteins that are homologues of the *B. subtilis* GerK proteins. However, the three GerK proteins in *C. perfringens* are not encoded by a tricistronic operon. Instead, *gerKB* is transcribed in the opposite direction of the bicistronic operon *gerKAC* (29). There is another GerA protein homologue, GerAA, encoded by a monocistronic locus. However, the deletion of *gerAA* does not result in significant germination deficiency when tested with various known germinants (29).

To better understand the initiation of germination in *C. perfringens*, we used a mass spectrometry approach was used to analyze the spore inner membrane proteome in both dormant and germinated spores. Over 100 membrane proteins were identified and their relative abundances were measured. Further studies of several membrane associated proteins are planned to illustrate their potential roles during spore germination.

## MATERIALS AND METHODS

**Bacterial strains, media and culture conditions.** *C. perfringens* SM101 is the sporulating strain used for this study. Three different media were used: brain heart infusion (BHI) medium (Difco), fluid thioglycollate (FTG) medium, and Duncan-Strong sporulation medium in the presence of 0.4% raffinose (DSSM). *C. perfringens* was grown in a Coy anaerobic chamber at 37°C.

**Sporulation.** The freezer stock of *C. perfringens* SM101 was streaked out on a freshly made BHI agar (1%) plate and incubated anaerobically at 37°C overnight. The next day, a single colony was picked and inoculated into liquid BHI medium and incubated until the culture entered exponential phase, about 8 hours after initial inoculation. Then it was subcultured into liquid FTG medium (1:100 dilution). The overnight FTG culture was then subcultured into liquid DSSM sporulation medium and incubated for 7 days.

**Dormant spore purification.** Three liters of sporulating culture was harvested by centrifugation at 5,000 x g for 10 minutes at 4°C, washed with cold deionized water 3 times, resuspended in cold deionized water, and kept on a shaker for 3 days at 4°C with a daily wash. After the last wash, the spores were resuspended in 20% sodium diatrizoate (Sigma) at an optical density of 600 nm ($OD_{600}$) = 10. Aliquots of the spore suspension (4 ml) were layered on top of a 50% sodium diatrizoate solution in 50-ml polypropylene conical tubes (BD Falcon), and then centrifuged for 45 min at maximum speed (6871 g) at 25°C with the acceleration set to slow and the brake turned off (Beckman Counter JS5.3 rotor). Due to their higher density, only the dormant spores will pellet at the bottom, while germinated spores and cell debris will float above the 50% layer. Dormant spores were harvested and washed with cold deionized water 5 times immediately after density gradient centrifugation. The $OD_{600}$ of

the spore suspension was measured again, and then a portion (2 $OD_{600}$ units) was reserved for germination assays, with the remaining spores aliquoted into two 1.7 ml centrifuge tubes. Liquid nitrogen was used to quick freeze the spore pellet which was then dried under vacuum using a refrigerated Vacufuge Concentrator (Savant). One tube of spores was used as the dormant spore sample; the other one was used for preparing the germinated spore sample. A total of 3 independent batches of spores were prepared and assayed separately.

**Germination assay.** Clean dormant spores were resuspended in cold deionized water with a final concentration of $OD_{600}$ equals 1. The spores were heat activated at 80°C for 10 minutes and then quenched on ice for 5 minutes. Then 200 µl of the spore suspension and 700 µl of deionized water (pre-warmed at 37°C water bath) were mixed together and 100 µl of 1 M KCl was added to initiate the germination assay. Germination was carried out in a 37°C water bath with frequent gentle shaking to avoid spore sedimentation. The $OD_{600}$ was measured every two minutes for 20 minutes. For the negative control, one hundred microliter of deionized water was used instead of 1 M KCl.

**Germinated spore preparation.** Dormant spores were heat activated and germinated with 100 mM KCl for 20 minutes as described previously (29). Germination was quenched by putting the spores on ice for 5 minutes, harvested by centrifugation at 5,000 x g for 10 minutes at 4°C, and washed with cold deionized water 5 times. The germinated spore sample was freeze-dried as described above.

**Spore inner membrane extraction.** Dry spores were broken with 0.4 g glass beads (0.1 mm diameter) for 35 cycles at 4,600 rpm with 30 seconds cooling on ice and 30 seconds shaking (Crescent Wig-L-Bug MSD Amalgamator). The disrupted spores were checked under a microscope to insure that greater than 80% of the spores were broken. The spore inner

membrane was isolated by differential centrifugation (92). A small portion of the membrane preparation was subjected to amino acid analysis to determine the protein concentration, and the rest was freeze-dried as described above.

**Gradient SDS-PAGE and gel slice preparation.** The spore inner membrane protein was resuspended in loading buffer (Bio-Rad's Laemmli sample buffer with 355 mM 2-mercaptoethanol) for a final protein concentration of 2 µg/µl. The sample was then heated in a boiling water bath for 10 minutes and cooled on ice for 10 minutes. Twenty six µg of protein from each sample was loaded and separated by SDS-PAGE in a 10.5-14% gradient polyacrylamide gel (Bio-Rad Criterion$^{TM}$). The gel was then visualized by Coomassie brilliant blue R-250 (Bio-Rad, Bio-Safe), and destained with deionized water. Each lane was hand cutted into 12 slices. Some gel slices only contain one or two high-abundance protein bands, other gel slices may contain several low-abundance bands. In this way, the high-abundance proteins won't mask detection of those from low-abundance. Each gel piece was homogenized with a pellet pestle and destained (25 mM ammonium bicarbonate to acetonitrile (ACN) in a 1:1 ratio). Destained gel pieces were then dehydrated with acetonitrile (ACN) and dried in a vacuum centrifuge.

**In-gel enzymatic digestion.** Dry gel plugs were rehydrated in trypsin solution (10 µg/ml trypsin and 25 mM ammonium bicarbonate) and digested at 37°C for 16 hours. Peptides were then extracted by adding 500 µl of 0.1% trifluoroacetic acid (TFA) 50% ACN and 15 minutes of sonication, dried under vacuum and resuspended in 40 µl 0.1% TFA in 2% ACN.

**2D-LC separation and fractionation of the tryptic peptides.** Fifteen µl of each peptide sample was injected into an injector sample loop that was in line with an Eksigent NanoLC-2D HPLC system and an Eksigent Ekspot MALDI plate spotting robot. Peptides

were eluted at a flow rate of 700 nL per minute through a trap cartridge (Magic $C_{18}$ AQ, 200Å, 3µm, Bruker) and a self-packed IntegraFrit 50 x 0.1 mm column (New Objective). The mobile phase was LC/MS grade water with 0.1% TFA (solvent A) and LC/MS grade ACN in LC/MS grade water (solvent B) in the gradient mode: 10 min, 90-10% B; 10—100 min, 10% to 36% B (linear increase over the time course); 100—101min, 36% to 75% B (rapid increase in one minute); 101—150 min, 75% B. The column eluate from between 53 - 149 minutes was spotted onto 384 spots at 15 seconds per spot.

**MALDI-TOF/TOF-MS analysis.** Freshly made matrix solution (4 mg of ACN-washed alpha-cyano-4-hydroxycinnamic acid, 50% ACN, 10 mM $NH_4Cl$, 0.1% TFA) was spotted on the plate and air dried right before analysis by MALDI-TOF/TOF (AB Sciex 4800 MALDI-TOF/TOF). The instrument was operated in 1 kV positive ion reflector mode and calibrated with internal calibrant. MS spectra were acquired across the m/z rang of 800–4000 from 1,000 laser shots. The 15 most abundant precursor ions with a minimum signal to noise ratio above 50 were selected for subsequent MS/MS analysis. The MS/MS spectra each acquired using 3000 laser shots were further processed.

**Data analysis and protein identification.** MS/MS spectra were interrogated using ProteinPilot 4.0 (AB Sciex) for searching against the *C. perfringens* Uniprot database (downloaded in October 2013) appended with the reverse decoy and contaminants databases. The following parameters were used for ProteinPilot analysis: Unused Score must be no less than 1, the Number of detected peptides of high quality (with at least 95% Confidence) must be no less than 1, and the protein must be identified at least twice in a total of three independent replicates.

**Relative abundance analysis of membrane proteins**. We used the on-line search

engine MASCOT (Matrix Science) to match tandem mass spectra with peptide sequences from the *C. perfringens* Uniprot database. The triplicates from each sample group were pooled together and the resulting data was further evaluated by Scaffold 3.0 software (Proteome Software) using spectral counting for quantification. The relative abundance of those membrane proteins (predicted by PSPRTb 3.0) that were detected in both dormant and germinated spore samples using ProteinPilot software was analyzed. Only those changed at least 2-fold in abundance were considered significantly changed during spore germination.

## RESULTS

**The response of *C. perfringens* spores to various germinants.** Several germinants of *C. perfringens* spores have been reported (29), with potassium ($K^+$) considered a very efficient germinant for *C. perfringens* SM101 spores (29). Germination assays with different germinants confirmed that 100 mM KCl efficiently triggered germination of >95% of the spores within 20 minutes, with a combination of potassium and L-asparagine producing a slightly higher efficiency (Figure 4.1). Sodium phosphate buffer can also slowly trigger germination (Figure.4.1). For germinated spore membrane preparation, water was used instead of sodium phosphate buffer and 100 mM KCl was used at the sole germinant.

**Differential spore inner membrane proteomics analysis using MALDI-TOF/MS MS.** The recovered spore inner membrane proteins were quantified using amino acid analyses, and 26 µg of protein from each sample was loaded onto a gradient polyacrylamide gel. Each lane was cut into 12 pieces for protein identification (Figure 4.2).

The gel slices containing membrane proteins from both dormant and germinated spores were ground and treated with trypsin. Peptides were extracted and analyzed by MALDI-TOF/MS MS. This search strategy resulted in the identification of 479 proteins. There were 393 and 402 proteins from dormant spore samples and germinated spore samples, respectively, with 316 proteins are detected in both. The complete listings can be found in Supplemental Tables S4.1 and S4.2, which can be found at the end of this Chapter.

A total of 117 predicted membrane proteins were found using PSORTb 3.0 software (93), while 75 of them were detected in both samples, there were 16 detected only in dormant spore samples, and 26 detected only in germinated spore samples (Table 4.1). We also used PSORTb 3.0 to identify the transmembrane helices (TMHs) of those 117 membrane proteins

(Figure 4.3). Among those 26 proteins containing no TMH, twenty five of them were predicted to be lipoproteins by both PRED-LIPO and LipoP 1.0 (94, 95). The MurG protein (CPR_2034) does not contain any TMH, but its homologue in *E.coli* has been shown to be a membrane-associated protein (96). Another 22 proteins contained just 1 TMH, and 6 of them were predicted to be lipoproteins. The remaining 69 proteins contain more than 1 TMH, and these proteins plus the 16 proteins containing just 1 TMH were considered either integral membrane proteins (IMPs) or membrane-associated. In this paper, membrane protein was used as a general term to include all lipoproteins, membrane-associated proteins and IMPs that were identified.

**Relative abundance analysis of membrane proteins**. The determination of relative abundances utilized the MASCOT search engine and the Scaffold proteomic data processing package. Among the 75 membrane proteins that were identified in both dormant and germinated spore samples by Protein Pilot, only 71 of them were detected in both dormant and germinated spore samples using the MASCOT software. The other 4 proteins were only detected in germinated spore samples using MASCOT software, and we consider them decreased in abundance during germination. Among those 71 membrane proteins found in both by MASCOT, 24 of them changed at least 2-fold (Table 4.1).

## DISCUSSION

Membrane proteins are involved in diverse biological processes. To provide further insight into those spore membrane proteins that changed at least 2-fold in abundance, their functional categories were examined using the database of Clusters of Orthologous Groups of proteins (COGs) and literature references (97). Those 70 membrane proteins fell into 9 major functional groups (Table 4.2). Details about functional categorization are shown in Table 4.3.

**Transport Processes**. The largest portion of the membrane proteins that changed significantly during spore germination are proteins involved in transport processes (Table 4.3). This includes classical ABC transporter complexes, ion transporters, permease proteins, the phosphotransferase system (PTS), transporters for other metabolites and putative transporters. It is not surprising to see several ion transporters increased in germinated spore samples considering the observation of a large efflux of cations during the early stages of germination in *Bacillus* species (98). Mutagenesis studies of several ion transporters have also shown that ion transport plays an important role in spore germination (37, 90). It is very possible that several of the identified transporters, such as the cation efflux superfamily protein CPR_0983, the cation-transporting ATPase CPR_2026, and the ion compound ABC transporter CPR_1115, serve as channels or gates for cation efflux during spore germination, especially the protein coded by CPR_2026 which shares 47% identity with the calcium pump ATPase YloB from *B. subtilis*. It was reported that deletion of YloB resulted in partial loss of spore resistance and also a slower germination rate (99). This might be due to the inefficient uptake of calcium at the sporulation stage to form high concentrations of Ca-DPA in the spore core, and the inefficient release of $Ca^{2+}$ at the germination step. The protein CPR_2026 is similar to YloB in that it contains 9 out of the 10 conserved residues in the eukaryotic $Ca^{2+}$ transporters (99), which are involved in the coordination of the two calcium ions that bind in the

transmembrane domain. There were several other ABC transporters (CPR_0363, CPR_0478, CPR_1550, and CPR_2340) with unknown specific endogenous substrates. However, considering the wide diversity of substrate specificity of ABC transporters (100) and the major events that occur in the early stages of germination, it is probable that some of them may be involved in ion exchange at the early germination stage, and/or signal transduction processes, if the translocated solute serves as a signaling molecule.

The glycerol uptake facilitator protein GlpE (encoded by gene CPR_1001) was present in higher levels in germinated spore samples. This protein belongs to the Major Intrinsic Protein (MIP) family of channel proteins, which are widely found in both eukaryotes and prokaryotes (101-103). Structurally these proteins contain 6 transmembrane helices and function as diffusion-controlled channels for water and small solutes like glycerol and urea (104). MIP proteins are classified into three groups based on their substrate specificity: aquaporins, glycerol facilitators and glyceroaquaporins. So far only the glyceroaquaporins are found to be able to transport both water and glycerol (105). The aquaporin protein AqpX from the Gram-negative bacterium *Brucella abortus* is a functional water channel and it's not able to uptake glycerol (105). The *C. perfringens* MIP family protein, GlpE, shares 55% sequence identity with the *B. subtilis* glycerol uptake facilitator protein, GlpF. Whole genome sequence analysis indicates that neither *B. subtilis* or *C. perfringens* contain aquaporin homologues (106). This leaves open the question of whether the GlpF protein from *B. subtilis* and *C. perfringens* also functions as a water channel during spore germination (34).

The PTS system, which is the major carbohydrate active-transport system, decreased in germinated spores. This trend was also observed during the *C. difficile* strain 630 spore germination at the transcriptional level (107). Since we incubated the dormant spores with only KCl for 20 minutes, there was no outgrowth following germination. The higher

abundance of those sugar transporters (CPR) in dormant spores may be carried over from mother cells during sporulation.

**Cell division, cell wall and membrane biogenesis**. Among the 7 proteins involvied in cell division, cell wall and membrane biogenesis, 6 of them were present in higher levels in germinated spore samples and one was present in lower levels (Table 4.3). During the early stage of spore germination, the spore cortex is hydrolyzed by spore-cortex-lytic enzymes, but both the germ cell wall and inner membrane remain intact and serve as the initial vegetative cell structure following spore germination (45, 108). However, both the germ cell wall and inner membrane have to expand due to the rehydration and expansion of the spore core (34). This brings up the question about how the spores maintain the integrity of the expanding inner membrane and germ cell wall without detectable synthesis (109). It's reasonable to postulate that those proteins may play a role during this expansion. Besides several penicillin-binding domain containing proteins (PBP), which are involved in the final stages of the synthesis of peptidoglycan (110), we also detected 3 lipoproteins that are homologues of cell wall biogenesis proteins. It was reported that interactions between several lipoproteins and PBPs are essential to form an active complex for peptidoglycan biogenesis in *E. coli* (111). It is possible that those lipoproteins participate in spore inner membrane dynamics by association with PBP during spore germination.

**Protein secretion, translocation and turnover**. Proteins involved in protein secretion and turnover in germinated spores were also detected (Table 4.3). This includes two components from the general secretory pathway (Sec), SecD, SecY and its accessory protein FtsY (112, 113). The signal peptidase class 1 protein (CPR_0564) is a serine protease that cleaves the signal peptide from proteins that are translocated across the membrane (114). The ATP-dependent zinc metalloprotease FtsH is a member of the AAA protease family, and it

plays an important role in membrane protein quality control by degrading misassembled membrane proteins and short-lived proteins (115, 116). The PPIase proteins are folding catalysts found in various organisms (117, 118) with peptidylprolyl cis/trans isomerase activity. In *E. coli*, the PPIC-type PPIase, SurA, was important for outer membrane protein composition and maturation (119). The cold-shock protein (Csp) family is involved in various environment stress responses. In *E. coli*, the CspC protein is able to regulate the expression of the global stress response regulator RpoS (120). We only detected one Sec component, a SecG homologue (CPR_1293), from the dormant spore samples, but with a very low abundance. The up-regulation of the Sec system was observed in *C. difficile* strain 630 at the transcriptional level during spore germination (107). The specific downstream effectors during spore germination from those proteins are unknown yet, mainly due to their general function and broad effector-specificity. Considering all the vast physiological changes within the spore structure in such a short period of time, it's reasonable to expect a massive amount of protein translocation, processing, turnover and post-translational modification, to readjust the protein location and composition in the spore (121), and possible signal transduction for completion of germination (122).

**Proteins decreased in germinated spores.** There were relatively few membrane proteins that were found in lower abundance in germinated spores relative to dormant spores (Table 4.3). This list includes two ATP synthase subunits, AtpF and AtpB, the elongation factor 4 (LepA), and the transcription termination factor Rho. It was found that in *Bacillus thuringiensis*, the translation of most ATP synthase subunits was up-regulated during late sporulation to meet energy demands (17). We believe that the ATP synthase subunits were present in high levels during sporulation from being carried over from mother cells to the spores. The elongation factor LepA is a highly conserved fidelity factor involved in accurate

protein synthesis (123). It was found that *E. coli* LepA is a membrane-bound GTPase, and it is released into the cytoplasm upon conditions of high ionic strength or low temperature (124). The results support a scenario where both Rho and LepA were present in high amounts during sporulation due to storage in the dormant spore.

**Known germination-associated membrane proteins**. *C. perfringens* contains four known germinant receptor homologues, GerAA, GerKA, GerKB and GerKC. GerKC is presently considered a lipoprotein associated with the spore inner membrane (46, 125), whereas GerAA, GerKA and GerKC are integral membrane proteins containing several transmembrane segments (29). All four germinant receptor proteins were detected, with only GerKB exhibiting a significant change in levels, with an almost 10 fold decrease in germinated spores. It is widely accepted that the germination commitment is irreversible once germinant receptors receive the signal from their germinants, and this commitment cannot be aborted by removing the germinants or by blocking the germinant receptors (126). It appears unlikely that those germinant receptors were still stored in the spore inner membrane since they are not required for vegetative growth and were only expressed under control of the sporulation sigma factor G (127-129). Considering the higher abundance of the AAA protease FtsH in germinated spores, we hypothesized that the germinant receptors were degraded as part of the commitment to germination.

The SpoVA operon in *B. subtilis* contains six proteins, all of which have several predicted membrane-spanning domains (109). The SpoVA proteins in *B. subtilis* play important roles in DPA uptake into the forespore during sporulation and DPA release during germination (91, 109). *C. perfringens* contains three SpoVA proteins, all containing several transmembrane segments. These proteins in *C. perfringens* are important for DNA uptake into forespores, but are thought to have no significant impact on DPA release during germination (130). We

detected all 3 (Table S4.1 and Table S4.2) in relatively high abundance, but none of them changed over 2-fold during germination.

It is reported that mutation of a putative $Na^+/H^+$-$K^+$ antiporter, GerO (CPR_0227), containing 10 potential membrane-spanning domains, negatively affected spore germination and outgrowth (90). However, the translation of GerO was only observed in the mother cell compartment, but not in the forespores (90). In our proteomic study, this protein was not detected at all either in dormant or in germinated spore samples. This result supports the hypothesis that GerO is very possibly not located in the spore inner membrane, or probably not in the spore compartment at all, and this germination deficiency might be due to some unknown spore structure deficiency when GerO was deleted (90).

## FINAL SUMMARY

The availability of whole genome-sequences, especially those of pathogenic bacteria, has provided us the ability to perform proteomic studies on those organisms. Extensive proteome studies have been done in *Bacillus* to identify total spore proteins, coat proteins, or germination-specific proteins (131-134). Those studies established the basic map of spore proteins, with the majority of them being cytoplasmic proteins. There are also several comprehensive transcriptional studies of temporal gene expression during spore germination, both in *Bacillus* and *Clostridium* species (107, 135). However, there are still gaps with respect to the molecular mechanism of spore germination, especially in the early stages, and the spore inner membrane proteins are intensively associated with those early events (126). In this study, we characterized the whole spore inner membrane proteins in the enterotoxin-producing food poisoning bacterium *C. perfringens* SM101, in both dormant and germinated spores. This is the first comprehensive proteomic study specifically focusing on the spore inner membrane in a *Clostridium* species. By coupling SDS-PAGE and LC-MALDI-TOF-MS/MS, a list of the spore inner membrane proteins was developed, and a comparison of their relative abundance before and after germination further revealed the proteins that may be actively involved in spore germination processes.

## ACKNOWLEDGEMENTS

We thank Katherine Lee for assistance with the spore preparation, and Yan Chen for help with the spore inner membrane fraction preparation. This work was supported by National Institutes of Health grant 1R21AI088298-01 to S. B. M. The mass spectrometry resources are maintained by the Virginia Tech Mass Spectrometry Incubator, a facility operated in part through funding by the Fralin Life Science Institute at Virginia Tech and by the Agricultural Experiment Station Hatch Program at Virginia Tech (CRIS Project Number: VA-135981).

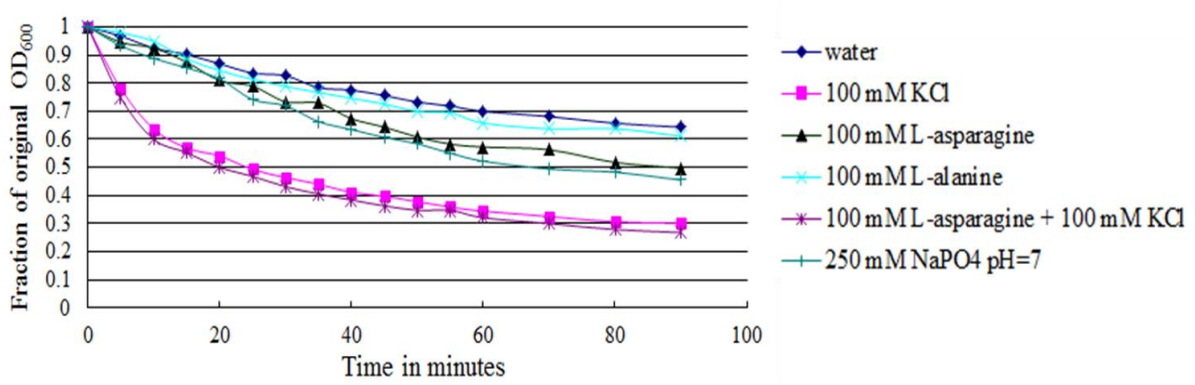


**Figure 4.1.** Response of *C. perfringens* spores to various germinants. Dormant spores were heat activated at 80°C for 10 minutes prior to germinant addition, and changes in $OD_{600}$ were monitored at every 5 minutes for the first one hour and then every ten minutes for another half an hour.

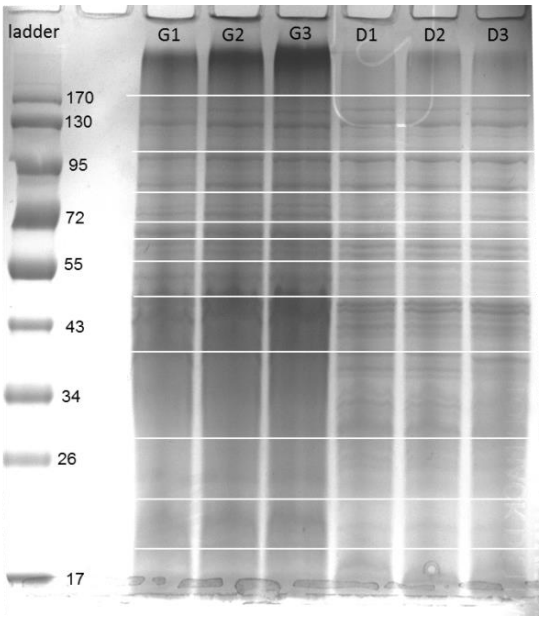


**Figure 4.2.** SDS-PAGE analysis of *C. perfringens* spore membrane protein preparation. Triplicate samples of dormant and germinated spore inner membrane proteins were separated by SDS-PAGE, and 11 gel slices from each sample were excised for proteome analysis. G: germinated spore inner membrane protein; D: dormant spore inner membrane protein.

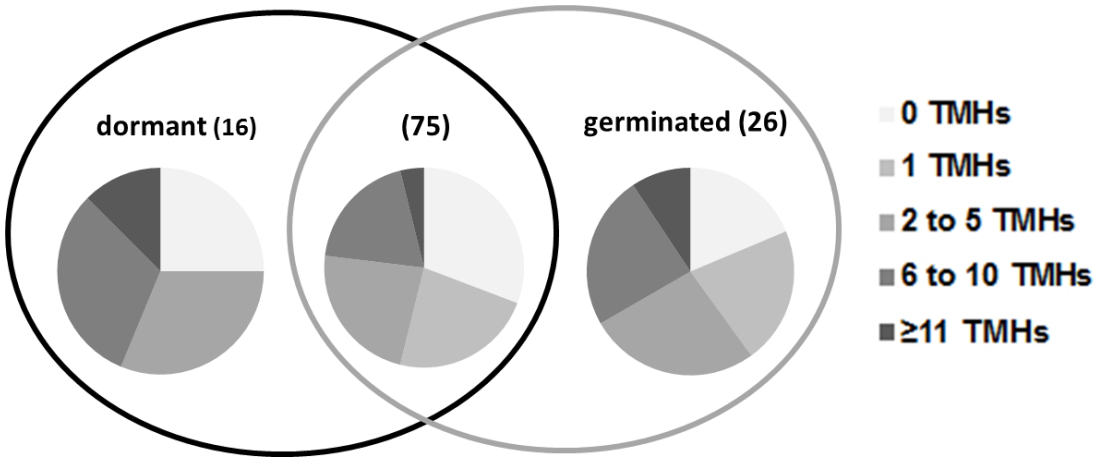


**Figure 4.3.** Venn diagram of membrane protein identification. The diagram shows TMH distribution of all membrane proteins identified from both dormant and germinated spore samples, according to the PSORTb 3.0 algorithm.

**Table 4.2. Differentially detected Membrane Protein Function Categorization Summary**

| Functional group[a] (Germinated /Dormant, with ≥ 2-fold change) | Increased[b] | Decreased[c] |
|---|---|---|
| ABC transporter, general transport system | 23 | 9 |
| Protein secretion, translocation, degradation, chaperones | 7 | 1 |
| Cell division, Cell wall and membrane biogenesis | 6 | 1 |
| Energy production and conversion | 2 | 2 |
| DNA replication, repair, transcription, translation | 0 | 3 |
| Signal transduction mechanism | 0 | 1 |
| Germination receptor | 0 | 2 |
| Phage protein | 1 | 0 |
| Unknown function | 7 | 5 |
| Total | 46 | 24 |

a: Function categorization analysis is based on COG database and literature references.
b: Proteins increased at least 2-fold in germinated versus dormant spore samples.
c: Proteins decreased at least 2-fold in germinated versus dormant spore samples.

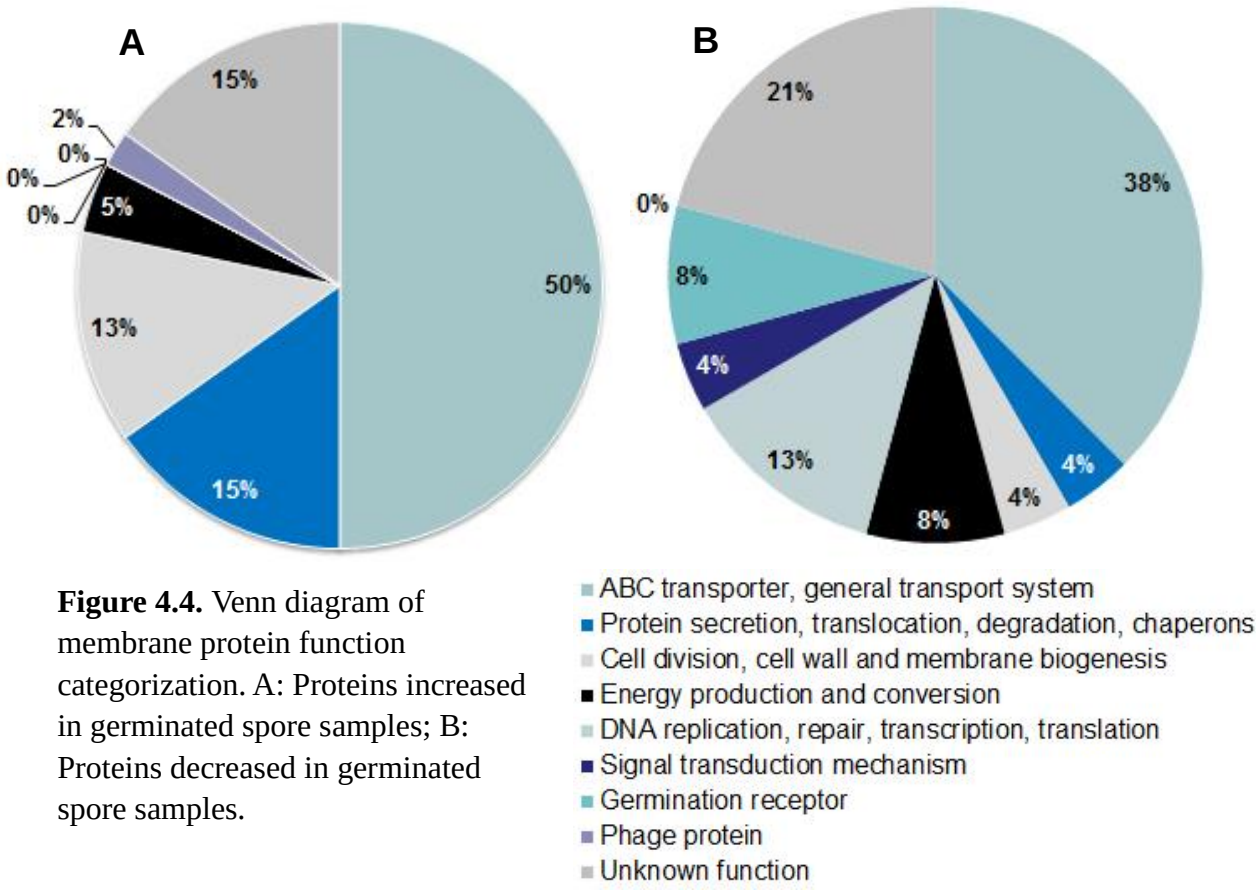


**Figure 4.4.** Venn diagram of membrane protein function categorization. A: Proteins increased in germinated spore samples; B: Proteins decreased in germinated spore samples.

**Table 4.1 Membrane protein identification**

| UniProt ID | gene name (CPR #) | fold change (G/D) [a] | THMs[b] | membrane association[c] | protein function |
|---|---|---|---|---|---|
| Q0SQX6 | 2181 | 0.2 | 0 | lipoprotein | transcription termination factor Rho |
| Q0SVP6 | 0476 | 0.3 | 0 | lipoprotein | ABC transporter, substrate-binding protein |
| Q0SQZ1 | 2166 | 0.3 | 1 | IMP | ATP synthase subunit b, AtpF |
| Q0SPW6 | 2594 | 0.3 | 6 | IMP | putative phage infection protein |
| Q0SR24 | 2124 | 0.3 | 10 | IMP | PTS system, glucose-specific IIBC component ptsG |
| Q0SVC0 | 0603 | 0.5 | 1 | lipoprotein | phosphate ABC transporter, phosphate-binding protein PstS_1 |
| Q0SU32 | 1053 | 0.5 | 4 | IMP | GerA spore germination protein GerAA |
| Q0SUE8 | 0935 | 0.5 | 12 | IMP | PTS system, N-acetylglucosamine-specific IIBC component NagE |
| Q0SWC5 | 0241 | 0.6 | 0 | lipoprotein | uncharacterized protein |
| Q0SS66 | 1726 | 0.6 | 0 | lipoprotein | GTPase Der |
| Q0SRL7 | 1930 | 0.6 | 1 | IMP | penicillin-binding protein 1A, PbpA |
| Q0SRG7 | 1981 | 0.6 | 4 | IMP | putative permease |
| Q0SQB8 | 2427 | 0.6 | 4 | IMP | PIN/TRAM domain protein |
| Q0SRL1 | 1936 | 0.6 | 6 | IMP | spermidine/putrescine ABC transporter, permease protein PotB |
| Q0STU6 | 1139 | 0.7 | 0 | lipoprotein | 3-oxoacyl-[acyl-carrier-protein] synthase 2 FabF |
| Q0SW79 | 0292 | 0.7 | 4 | IMP | cell division protein FtsX |
| Q0SRC9 | 2019 | 0.7 | 4 | IMP | stage V sporulation protein AC, SpoVAC |
| Q0SVP5 | 0477 | 0.7 | 6 | IMP | ABC transporter, permease protein |
| Q0SSH7 | 1614 | 0.7 | 7 | IMP | V-type ATPase, I subunit |
| Q0SSP8 | 1542 | 0.8 | 0 | lipoprotein | phage shock protein A, PspA |
| Q0SQS7 | 2254 | 0.8 | 0 | lipoprotein | oligopeptide/dipeptide ABC transporter, ATP-binding protein |

| | | | | | |
|---|---|---|---|---|---|
| Q0SS79 | 1713 | 0.8 | 4 | IMP | putative neutral zinc metallopeptidase |
| Q0SPQ1 | 2671 | 0.8 | 6 | IMP | membrane protein OxaA |
| Q0SW99 | 0271 | 0.9 | 1 | IMP | putative transcriptional regulator |
| Q0SVF8 | 0565 | 0.9 | 2 | IMP | ATP-dependent zinc metalloprotease FtsH |
| Q0SVA8 | 0615 | 0.9 | 4 | IMP | spore germination protein, GerABKA family GerKA |
| Q0SUM3 | 0859 | 0.9 | 4 | IMP | uncharacterized protein |
| Q0SPW7 | 2593 | 0.9 | 6 | IMP | putative phage infection protein |
| Q0SVC5 | 0598 | 1 | 1 | IMP | cell envelope-related transcriptional attenuator domain family |
| Q0ST94 | 1343 | 1 | 8 | IMP | galactoside ABC transporter, permease protein MglC |
| Q0STF9 | 1276 | 1.1 | 16 | IMP | oligopeptide transporter, OPT family |
| Q0SR43 | 2105 | 1.2 | 0 | lipoprotein | site-determining protein MinD |
| Q0SQZ5 | 2162 | 1.2 | 0 | lipoprotein | ATP synthase subunit beta, AtpD |
| Q0SVU0 | 0431 | 1.2 | 1 | IMP | uncharacterized protein |
| Q0SQ68 | 2492 | 1.2 | 1 | lipoprotein | foldase protein PrsA |
| Q0SRD1 | 2017 | 1.2 | 4 | IMP | stage V sporulation protein AE, SpoVAE |
| Q0SUH9 | 0904 | 1.3 | 0 | lipoprotein | substrate-binding protein MsmE |
| Q0SSC7 | 1665 | 1.3 | 4 | IMP | RIP metalloprotease RseP |
| Q0SQP3 | 2289 | 1.3 | 6 | IMP | zinc-transporting ATPase |
| Q0SV26 | 0698 | 1.4 | 0 | lipoprotein | ABC transporter, ATP-binding protein |
| Q0SW78 | 0293 | 1.4 | 1 | IMP | carboxyl-terminal protease |
| Q0SR23 | 2125 | 1.4 | 1 | lipoprotein | ABC transporter, substrate-binding protein |
| Q0STA8 | 1329 | 1.4 | 5 | IMP | CDP-diacylglycerol--serine O-phosphatidyltransferase PssA |
| Q0SS49 | 1743 | 1.5 | 1 | IMP | uncharacterized protein |
| Q0SUS6 | 0806 | 1.5 | 3 | IMP | PTS system, mannose/fructose/sorbose family, IID component |
| Q0SW07 | 0364 | 1.5 | 4 | IMP | ABC transporter, permease/ATP-binding protein |

| | | | | | |
|---|---|---|---|---|---|
| Q0SRP0 | 1907 | 1.5 | 6 | IMP | protein-export membrane protein SecF |
| Q0SUR3 | 0819 | 1.5 | 12 | IMP | antibiotic ABC transporter, permease protein |
| Q0SU31 | 1054 | 1.5 | 12 | IMP | C4-dicarboxylate anaerobic carrier family protein |
| Q0SS83 | 1709 | 1.6 | 1 | IMP | serine/threonine protein kinase pknB-like protein |
| Q0SRN6 | 1911 | 1.6 | 1 | IMP | preprotein translocase, YajC subunit YajC_2 |
| Q0SUS7 | 0805 | 1.6 | 7 | IMP | PTS system, mannose/fructose/sorbose family, IIC component |
| Q0SRK4 | 1943 | 1.9 | 2 | IMP | D-alanyl-D-alanine carboxypeptidase family protein |
| Q0SWD6 | 0230 | 1.9 | 3 | IMP | uncharacterized protein |
| Q0SWK4 | 0159 | 1.9 | 12 | IMP | arginine/ornithine antiporter ArcD |
| Q0SQG4 | 2379 | 2 | 10 | IMP | protein translocase subunit SecY |
| Q0ST89 | 1348 | 2.2 | 2 | IMP | uncharacterized protein |
| Q0SQ55 | 2505 | 2.2 | 9 | IMP | nucleoside transporter, NupC family |
| Q0SQS2 | 2259 | 2.2 | 12 | IMP | major facilitator family transporter |
| Q0STX0 | 1115 | 2.3 | 1 | lipoprotein | iron compound ABC transporter, iron-binding protein |
| Q0SWI7 | 0176 | 2.3 | 13 | IMP | sodium:solute transporter |
| Q0SVJ4 | 0528 | 2.5 | 1 | IMP | stage V sporulation protein D |
| Q0SUA1 | 0983 | 2.5 | 6 | IMP | cation efflux family protein |
| Q0SSH8 | 1613 | 2.6 | 4 | IMP | V-type ATPase, K subunit |
| Q0SRN9 | 1908 | 2.6 | 6 | IMP | protein translocase subunit SecD |
| Q0SVP4 | 0478 | 2.9 | 6 | IMP | ABC transporter, permease protein |
| Q0SW39 | 0332 | 3.1 | 1 | IMP | putative penicillin-binding protein |
| Q0SQ81 | 2472 | 3.7 | 2 | IMP | ATP-dependent zinc metalloprotease FtsH |
| Q0SQK2 | 2340 | 4.4 | 0 | lipoprotein | ABC transporter, ATP-binding protein |
| Q0SVX2 | 0399 | 4.7 | 3 | IMP | PTS system, mannose/fructose/sorbose family, IID component |
| Q0SU83 | 1001 | 6.4 | 7 | IMP | glycerol uptake facilitator protein GlpE |

| | | | | | |
|---|---|---|---|---|---|
| Q0SWW1 | 0076 | D | 0 | lipoprotein | putative pyruvate, phosphate dikinase regulatory protein |
| Q0SVB6 | 0607 | D | 0 | lipoprotein | phosphate import ATP-binding protein PstB |
| Q0SS48 | 1744 | D | 0 | lipoprotein | GTP-binding protein TypA |
| Q0SRD8 | 2010 | D | 0 | lipoprotein | elongation factor 4 LepA |
| Q0STE2 | 1293 | D | 2 | IMP | preprotein translocase, SecG subunit |
| Q0SRW8 | 1824 | D | 4 | IMP | small basic protein |
| Q0SR25 | 2123 | D | 4 | IMP | MutS domain-containing protein |
| Q0SVV6 | 0415 | D | 5 | IMP | uncharacterized protein |
| Q0SQY9 | 2168 | D | 5 | IMP | ATP synthase subunit a, AtpB |
| Q0SSE6 | 1646 | D | 6 | IMP | Phosphatidylglycerophosphate synthase PgsA |
| Q0SVV3 | 0418 | D | 9 | IMP | PTS system, IIBC component |
| Q0SRL6 | 1931 | D | 9 | IMP | sodium:alanine symporter family protein |
| Q0SVA9 | 0614 | D | 10 | IMP | spore germination protein GerKB |
| Q0SV08 | 0716 | D | 10 | IMP | YeeE/YedE family protein |
| Q0SWR9 | 0093 | D | 12 | IMP | PTS system, N-acetylglucosamine-specific IIBC component NagE |
| Q0SPX4 | 2586 | D | 13 | IMP | xanthine/uracil permease family protein |
| Q0SWT6 | 0033 | G | 0 | lipoprotein | phosphatidylserine decarboxylase proenzyme Psd |
| Q0SWB6 | 0253 | G | 0 | lipoprotein | PPIC-type PPIASE domain protein |
| Q0SW80 | 0291 | G | 0 | lipoprotein | putative cell division ATP-binding protein FtsE |
| Q0SW59 | 0312 | G | 0 | lipoprotein | uncharacterized protein |
| Q0SUH6 | 0907 | G | 0 | lipoprotein | sugar ABC transporter, ATP-binding protein MsmK |
| Q0SU63 | 1021 | G | 0 | lipoprotein | ABC transporter, ATP-binding protein |
| Q0SSA5 | 1687 | G | 0 | lipoprotein | signal recognition particle receptor FtsY |
| Q0SRB4 | 2034 | G | 0 | membrane-associated | MurG transferase |
| Q0SQW9 | 2188 | G | 0 | lipoprotein | cphB, cyanophycinase |

| | | | | | |
|---|---|---|---|---|---|
| Q0SQS6 | 2255 | G | 0 | lipoprotein | oligopeptide/dipeptide ABC transporter, ATP-binding protein |
| Q0SVI2 | 0540 | G | 1 | lipoprotein | ABC transporter, substrate-binding protein |
| Q0SSJ7 | 1594 | G | 1 | lipoprotein | putative lipoprotein |
| Q0SVF9 | 0564 | G | 1 | IMP | signal peptidase I |
| Q0SRW6 | 1826 | G | 1 | IMP | cell division protein FtsQ |
| Q0SR78 | 2070 | G | 1 | IMP | CspC family protein |
| Q0SQT7 | 2244 | G | 1 | IMP | uncharacterized protein |
| Q0SQ36 | 2524 | G | 1 | IMP | uncharacterized protein |
| Q0SWV4 | 0036 | G | 2 | IMP | putative transporter |
| Q0SW05 | 0366 | G | 2 | IMP | toxin secretion/phage lysis holin |
| Q0SVY4 | 0387 | G | 2 | IMP | uncharacterized protein |
| Q0SQ93 | 2452 | G | 2 | IMP | putative cation transporter |
| Q0SUZ4 | 0730 | G | 4 | IMP | uncharacterized protein |
| Q0SR70 | 2078 | G | 4 | IMP | transmembrane protein Vexp3 |
| Q0SW08 | 0363 | G | 6 | IMP | ABC transporter, permease/ATP-binding protein |
| Q0SQS4 | 2257 | G | 6 | IMP | Oligopeptide/dipeptide ABC transporter, permease protein |
| Q0SSP0 | 1550 | G | 8 | IMP | ABC transporter, permease protein |
| Q0SSG1 | 1631 | G | 9 | IMP | ferrous iron transport protein B, FeoB_2 |
| Q0SSS6 | 1513 | G | 10 | IMP | PTS system, sucrose-specific IIBC component |
| Q0SRC2 | 2026 | G | 10 | IMP | cation-transporting ATPase, P-type |
| Q0SU50 | 1034 | G | 12 | IMP | amino acid permease family protein |

[a]: Scaffold version 3.0 was used for relative abundance analysis as described in methods.

[b]: PSORTb 3.0 was used for transmembrane helix (TMHs) analysis.

[c]: PSORTb 3.0 was used for protein localization analysis, PRED-LIPO and LipoP 1.0 were used for lipoprotein prediction.

**Table 4.3. Differentially detected Membrane Protein Function Categorization**

| UniProt ID | gene name (CPR_) | fold change (G/D) | protein function | Function categorization[a] |
|---|---|---|---|---|
| Q0SVP6 | 0476 | 0.3 | ABC transporter, substrate-binding protein | ABC transporter, general transport system |
| Q0SR24 | 2124 | 0.3 | PTS system, glucose-specific IIBC component PtsG | ABC transporter, general transport system |
| Q0SVC0 | 0603 | 0.5 | Phosphate ABC transporter, phosphate-binding protein PstS | ABC transporter, general transport system |
| Q0SUE8 | 0935 | 0.5 | PTS system, N-acetylglucosamine-specific IIBC component NagE | ABC transporter, general transport system |
| Q0SQS2 | 2259 | 2.2 | Major facilitator family transporter | ABC transporter, general transport system |
| Q0SQ55 | 2505 | 2.2 | Nucleoside transporter, NupC family | ABC transporter, general transport system |
| Q0SWI7 | 0176 | 2.3 | Sodium:solute transporter | ABC transporter, general transport system |
| Q0STX0 | 1115 | 2.3 | Iron compound ABC transporter, iron-binding protein | ABC transporter, general transport system |
| Q0SUA1 | 0983 | 2.5 | Cation efflux family protein | ABC transporter, general transport system |
| Q0SVP4 | 0478 | 2.9 | ABC transporter, permease protein | ABC transporter, general transport system |
| Q0SQK2 | 2340 | 4.4 | ABC transporter, ATP-binding protein | ABC transporter, general transport system |
| Q0SVX2 | 0399 | 4.7 | PTS system, mannose/fructose/sorbose family, IID component | ABC transporter, general transport system |
| Q0SU83 | 1001 | 6.4 | Glycerol uptake facilitator protein GlpE | ABC transporter, general transport system |
| Q0SWR9 | 0093 | D | PTS system, N-acetylglucosamine-specific IIBC component NagE | ABC transporter, general transport system |
| Q0SVV3 | 0418 | D | PTS system, IIBC component | ABC transporter, general transport system |
| Q0SVB6 | 0607 | D | Phosphate import ATP-binding protein PstB | ABC transporter, general transport system |
| Q0SRL6 | 1931 | D | Sodium:alanine symporter family protein | ABC transporter, general transport system |
| Q0SPX4 | 2586 | D | Xanthine/uracil permease family protein | ABC transporter, general transport system |
| Q0SWV4 | 0036 | G | Putative transporter | ABC transporter, general transport system |
| Q0SW08 | 0363 | G | multidrug ABC transporter, permease/ATP-binding protein | ABC transporter, general transport system |
| Q0SVI2 | 0540 | G | ABC transporter, substrate-binding protein | ABC transporter, general transport system |

| | | | | |
|---|---|---|---|---|
| Q0SUH6 | 0907 | G | Sugar ABC transporter, ATP-binding protein MsmK | ABC transporter, general transport system |
| Q0SU63 | 1021 | G | ABC transporter, ATP-binding protein | ABC transporter, general transport system |
| Q0SU50 | 1034 | G | Amino acid permease family protein | ABC transporter, general transport system |
| Q0SSS6 | 1513 | G | PTS system, sucrose-specific IIBC component | ABC transporter, general transport system |
| Q0SSP0 | 1550 | G | ABC transporter, permease protein | ABC transporter, general transport system |
| Q0SSG1 | 1631 | G | Ferrous iron transport protein B FeoB | ABC transporter, general transport system |
| Q0SRC2 | 2026 | G | Cation-transporting ATPase, P-type | ABC transporter, general transport system |
| Q0SR70 | 2078 | G | Transmembrane protein Vexp3 | ABC transporter, general transport system |
| Q0SQS6 | 2255 | G | Oligopeptide/dipeptide ABC transporter, ATP-binding protein | ABC transporter, general transport system |
| Q0SQS4 | 2257 | G | Oligopeptide/dipeptide ABC transporter, permease protein | ABC transporter, general transport system |
| Q0SQ93 | 2452 | G | Putative cation transporter | ABC transporter, general transport system |
| Q0SQX6 | 2181 | 0.2 | Transcription termination factor Rho | DNA replication, repair, transcription, translation |
| Q0SR25 | 2123 | 0.5 | MutS domain-containing protein | DNA replication, repair, transcription, translation |
| Q0SRD8 | 2010 | D | Elongation factor 4 LepA | DNA replication, repair, transcription, translation |
| Q0SVJ4 | 0528 | 2.5 | Stage V sporulation protein D | Cell division, Cell wall and membrane biogenesis |
| Q0SW39 | 0332 | 3.1 | Putative penicillin-binding protein | Cell division, Cell wall and membrane biogenesis |
| Q0SSE6 | 1646 | D | Phosphatidylglycerophosphate synthase PgsA | Cell division, Cell wall and membrane biogenesis |
| Q0SWT6 | 0033 | G | Phosphatidylserine decarboxylase proenzyme Psd | Cell division, Cell wall and membrane biogenesis |
| Q0SW80 | 0291 | G | Putative cell division ATP-binding protein FtsE | Cell division, Cell wall and membrane biogenesis |
| Q0SRW6 | 1826 | G | Cell division protein FtsQ | Cell division, Cell wall and membrane biogenesis |
| Q0SRB4 | 2034 | G | MurG transferase | Cell division, Cell wall and membrane biogenesis |
| Q0SQZ1 | 2166 | 0.3 | ATP synthase subunit b AtpF | Energy production and conversion |
| Q0SSH8 | 1613 | 2.6 | V-type ATPase, K subunit | Energy production and conversion |
| Q0SQY9 | 2168 | D | ATP synthase subunit a AtpB | Energy production and conversion |
| Q0SQW9 | 2188 | G | Cyanophycinase CphB | Energy production and conversion |

| | | | | |
|---|---|---|---|---|
| Q0SU32 | 1053 | 0.5 | GerA spore germination protein, GerAA | germination receptor |
| Q0SVA9 | 0614 | D | Spore germination protein, GerKB | germination receptor |
| Q0SW05 | 0366 | G | Toxin secretion/phage lysis holin | phage protein |
| Q0SQG4 | 2379 | 2 | Protein translocase subunit SecY | protein secretion, translocation, turnover |
| Q0SRN9 | 1908 | 2.6 | Protein translocase subunit SecD | protein secretion, translocation, turnover |
| Q0SQ81 | 2472 | 3.7 | ATP-dependent zinc metalloprotease FtsH | protein secretion, translocation, turnover |
| Q0STE2 | 1293 | D | Preprotein translocase, SecG subunit | protein secretion, translocation, turnover |
| Q0SWB6 | 0253 | G | PPIC-type PPIASE domain protein | protein secretion, translocation, turnover |
| Q0SVF9 | 0564 | G | Signal peptidase I | protein secretion, translocation, turnover |
| Q0SSA5 | 1687 | G | Signal recognition particle receptor FtsY | protein secretion, translocation, turnover |
| Q0SR78 | 2070 | G | CspC family protein | protein secretion, translocation, turnover |
| Q0SS48 | 1744 | D | GTP-binding protein TypA | signal transduction mechanism |
| Q0SPW6 | 2594 | 0.3 | Putative phage infection protein | Unknown function |
| Q0ST89 | 1348 | 2.2 | Uncharacterized protein | Unknown function |
| Q0SWW1 | 0076 | D | Putative pyruvate, phosphate dikinase regulatory protein | Unknown function |
| Q0SVV6 | 0415 | D | Uncharacterized protein | Unknown function |
| Q0SV08 | 0716 | D | YeeE/YedE family protein | Unknown function |
| Q0SRW8 | 1824 | D | Small basic protein Sbp | Unknown function |
| Q0SW59 | 0312 | G | Uncharacterized protein | Unknown function |
| Q0SVY4 | 0387 | G | Uncharacterized protein | Unknown function |
| Q0SUZ4 | 0730 | G | Uncharacterized protein | Unknown function |
| Q0SSJ7 | 1594 | G | Uncharacterized protein | Unknown function |
| Q0SQT7 | 2244 | G | Uncharacterized protein | Unknown function |
| Q0SQ36 | 2524 | G | Uncharacterized protein | Unknown function |

[a]: Function categorization analysis was based on COG database and literature references.

# Chapter 5

# Final Discussion

*C. perfringens* can form very spreading colonies on agar surfaces, but were considered to be a non-motile organism. In 2006, the Melville lab first defined this colony translocation in *C. perfringens* strain 13 as gliding motility (16). Unlike the well-studied gliding motility found in *Myxococcus xanthus*, *C. perfringens* can only move as a group with end to end connections along the long axis of the cell. Direction reversal is not possible, and no individual cell movement is observed (16). What are the components of the gliding machinery? To address this question, we used both forward and reverse genetics to uncover the mystery of gliding motility in *C. perfringens*.

In Chapter 2, we described the incorporation of two newly developed genetic tools, the tightly regulated, lactose-inducible promoter system and the CatP/GalK negative selection system, into the classical mariner transposable element, and developed the *Himar 1* mariner transposon-mediated random insertion mutagenesis strategy (22, 59). The genome-wide insertion mutant pool was screened for gliding motility deficiency and more than 20 genes were found to be related to this phenotype. In Chapter 3, instead of looking for gliding motility-deficient mutants, we started with two spontaneous mutants from *C. perfringens* SM101 possessing hypermotility, and the specific mutation causing this hypermotile phenotype was discovered using whole-genome sequencing and complementation studies.

The insertion of the mariner transposon into the peptidoglycan hydrolase homologue encoding gene *sagA* resulted in round-shaped cells without end-to-end connections and also dramatically reduced gliding motility. The mutation in the cell division gene, *ftsI or minE*, resulted in elongated filamentous cell growth and significantly increased gliding motility. Those results lead us to believe that continuous cell growth and maintaining the end-to-end connection are important for *C. perfringens* gliding motility. However, there are still several questions left open. First, what components contribute to the cell end-to-end connection is

still a mystery. Screening of the gliding motility deficient mutant pool didn't reveal any mutants with insertions in any of the 4 pilin subunit homologues nor the two fimbriae coding genes. However, this couldn't rule out the possibility of their involvement. In-frame deletion mutation studies of those genes should provide more insights. Another question would be how cell division and/or the cell wall structure contribute to the gliding motility. Is the peptidoglycan synthesis the driving force? Or is there any protein-peptidoglycan interaction like what was observed in *Flavobacterium johnsoniae* gliding motility (136)? Also, regarding the hypermotility phenotype, will a *minC* or *minD* mutant provide the hypermotility phenotype observed in *minE* mutant? The role of those proteins in gliding motility remains to be determined.

A potential application of the random insertion mutagenesis system, with appropriate modification, to facilitate the study of bacteria sporulation and spore germination mechanisms would be useful. We constructed a *galKT*-deletion strain from SM101. We are going to test whether the mariner transposon is able to insert into the chromosome of this strain randomly and efficiently.

Another focus of the research in this dissertation was to gain new information on the spore germination mechanisms in *C. perfringens* SM101. It's been known that the germination initiation starts with the interaction between the environmental signals, normally low-molecular-weight nutrients, and the germinant receptors located in the spore inner membrane. Though intense studies have been done on those germinant receptors in both *Bacillus* and *C. perfringens* SM101, the molecular mechanism of germination initiation is still an unfinished puzzle. How do the germinant receptors sense and respond to the environment? What is the available nutrient concentration threshold for a spore to commit to germination? How is the signal to exit dormancy transferred from the inner membrane inward

to the spore core and also outward to the spore cortex?

In Chapter 4, we performed SDS-PAGE gel-based mass spectrometry to map the inner membrane proteins from dormant and germinated spores of *C .perfringens* SM101. Due to the hydrophobicity of membrane proteins, we picked 1D-SDS-PAGE to avoid protein precipitation that is commonly found when using 2D-SDS-PAGE, and it also gave us a broad range of proteins with different sizes and isoelectric point (pI) values. We identified over 100 membrane proteins, with almost 40% of them were showing at least two fold abundance increase in germinated spore samples versus dormant, and 20.5% with at least two fold decrease. In dormant spores, the inner membrane is impermeable to many compounds and the majority of lipid in this membrane is immobile (108). During spore germination, the optical density can drop by 50% in the first 10 minutes, which indicates the spore core rehydration (135). Due to the core rehydration and expansion, the inner membrane will expand. It's possible that this membrane surface expansion will release some of the proteins that were originally loosely associated with the membrane, and also expose some of the integral membrane proteins for easier access by later extraction buffer and trypsin digestion. It's even more possible that the reorganization of the spore inner membrane protein composition during spore germination is a quick and necessary physiological adjustment for carrying out all the germination activities accurately and efficiently. This is supported by our observation of the abundance increase with lots of transporter proteins in germinated spores, especially for ion transporters. One direction of our future work would be exploring the role of those proteins during spore germination.

Another interesting finding is the identification of cyanophycinase, CphB, from germinated spore samples. Cyanophycin is a water-insoluble reserve polymer mainly found in cyanobacteria. It is produced from nonribosomal peptide synthesis by the enzyme CphA,

and used as a natural storage substance for nitrogen (137). Former research in our lab showed that *C. perfringens* SM101 produced granules in the mother cells during sporulation, but the properties of those granules were not determined (138). We now speculate that the granules are cyanophycin. In a recent paper, researchers found that the cyanophycin metabolism in heterocyst-forming cyanobacteria cells is compartmentalized. The vegetative cells perform oxygenic photosynthesis to provide reduced carbon, while the heterocysts synthesize the cyanophycin to provide fixed nitrogen resources (139). Since sporulation is a high energy demand process, why would *C. perfringens* synthesize this granule in the mother cell compartment during sporulation? Does it serve as a nitrogen and/or carbon source for germination, out growth, or both? From our proteome data, we detected more cyanophycinase. This enzyme is able to degrade the cyanophycin granules specifically. This observation brought up several questions to us: First, are the cyanophycin granules transported into the forespores or released into the environment after mother cell lysis? A second question is when and where the cyanophycin granules are degraded by the cyanophycinase. A third question is how the cyanophycinase activity is regulated. *C. perfringens* genome sequence data indicates that cyanophycin synthetase and cyanophycinase coding genes in SM101 form an operon. What is the regulatory mechanism for holding the cyanophycinase inactive form when the cyanophycin are made?

It's exciting to know that I am coming to the end of my exploration of *C. perfringens*, but thinking about those potential future work directions from our current data is even more exciting. I think the random mutagenesis system and the proteome data we generated will help future researchers to further unveil more mysteries about this ancient organism to us.

# REFERENCES


1. Rood JI & Cole ST (1991) Molecular Genetics and Pathogenesis of *Clostridium perfringens*. *Microbiol Rev* 55(4):621-648.
2. Schaechter M, Engleberg C, DiRita VJ, & Dermody T (2007) *Schaechter's Mechanisms of Microbial Disease* (Lippincott Williams & Wilkins, Philadelphia) 4th Ed pp xxi, 762 p.
3. Canard B & Cole ST (1989) Genome Organization of the Anaerobic Pathogen *Clostridium perfringens*. *Proceedings of the National Academy of Sciences of the United States of America* 86(17):6676-6680.
4. Lahti P, Heikinheimo A, Johansson T, & Korkeala H (2008) *Clostridium perfringens* Type A Strains Carrying a Plasmid-Borne Enterotoxin Gene (Genotype Is1151-Cpe or Is1470-Like-Cpe) as a Common Cause of Food Poisoning. *J Clin Microbiol* 46(1):371-373.
5. Deguchi A, *et al.* (2009) Genetic Characterization of Type A Enterotoxigenic *Clostridium perfringens* Strains. *PLoS One* 4(5):e5598.
6. Hedberg CW, Palazzi-Churas KL, Radke VJ, Selman CA, & Tauxe RV (2008) The Use of Clinical Profiles in the Investigation of Foodborne Outbreaks in Restaurants: United States, 1982-1997. *Epidemiology and Infection* 136(1):65-72.
7. Wen Q & McClane BA (2004) Detection of Enterotoxigenic *Clostridium perfringens* Type A Isolates in American Retail Foods. *Appl Environ Microbiol* 70(5):2685-2691.
8. Dalton CB, *et al.* (2004) Foodborne Disease Outbreaks in Australia, 1995 to 2000. *Commun Dis Intell* 28(2):211-224.
9. Kohler T, Curty LK, Barja F, van Delden C, & Pechere JC (2000) Swarming of *Pseudomonas aeruginosa* Is Dependent on Cell-to-Cell Signaling and Requires Flagella and Pili. *J Bacteriol* 182(21):5990-5996.
10. Harshey RM & Matsuyama T (1994) Dimorphic Transition in *Escherichia coli* and *Salmonella typhimurium*: Surface-Induced Differentiation into Hyperflagellate Swarmer Cells. *Proc Natl Acad Sci U S A* 91(18):8631-8635.
11. Kearns DB & Losick R (2003) Swarming Motility in Undomesticated *Bacillus subtilis*. *Mol Microbiol* 49(3):581-590.
12. Mattick JS (2002) Type IV Pili and Twitching Motility. *Annu Rev Microbiol* 56:289-314.
13. Burrows LL (2012) *Pseudomonas aeruginosa* Twitching Motility: Type IV Pili in Action. *Annu Rev Microbiol* 66:493-520.
14. Braun TF, Khubbar MK, Saffarini DA, & McBride MJ (2005) *Flavobacterium johnsoniae* Gliding Motility Genes Identified by *Mariner* Mutagenesis. *J Bacteriol* 187(20):6943-6952.
15. Harshey RM (2003) Bacterial Motility on a Surface: Many Ways to a Common Goal. *Annu Rev Microbiol* 57:249-273.
16. Varga JJ, *et al.* (2006) Type IV Pili-Dependent Gliding Motility in the Gram-Positive Pathogen *Clostridium perfringens* and Other *Clostridia*. *Mol Microbiol* 62(3):680-694.
17. Wang J, *et al.* (2013) The Metabolic Regulation of Sporulation and Parasporal Crystal Formation in *Bacillus thuringiensis* Revealed by Transcriptomics and Proteomics. *Mol Cell Proteomics* 12(5):1363-1376.
18. Mendez M, *et al.* (2008) Carbon Catabolite Repression of Type IV Pilus-Dependent Gliding Motility in the Anaerobic Pathogen *Clostridium perfringens*. *J Bacteriol* 190(1):48-60.

19. Melville S & Craig L (2013) Type IV Pili in Gram-Positive Bacteria. *Microbiol Mol Biol Rev* 77(3):323-341.
20. Shimizu T, *et al.* (2002) Complete Genome Sequence of *Clostridium perfringens*, an Anaerobic Flesh-Eater. *Proceedings of the National Academy of Sciences of the United States of America* 99(2):996-1001.
21. Heap JT, Pennington OJ, Cartman ST, Carter GP, & Minton NP (2007) The Clostron: A Universal Gene Knock-out System for the Genus *Clostridium*. *Journal of Microbiological Methods* 70(3):452-464.
22. Nariya H, Miyata S, Suzuki M, Tamai E, & Okabe A (2011) Development and Application of a Method for Counterselectable in-Frame Deletion in *Clostridium perfringens*. *Appl Environ Microbiol* 77(4):1375-1382.
23. Kumar RS, *et al.* (2013) Biochemistry and Physiology of the Beta Class Carbonic Anhydrase (CPB) from *Clostridium perfringens* Strain 13. *J Bacteriol* 195(10):2262-2269.
24. Obana N & Nakamura K (2011) A Novel Toxin Regulator, the CPE1446-CPE1447 Protein Heteromeric Complex, Controls Toxin Genes in *Clostridium perfringens*. *J Bacteriol* 193(17):4417-4424.
25. Obana N, Nakamura K, & Nomura N (2014) A Sporulation Factor Is Involved in the Morphological Change of *Clostridium perfringens* Biofilms in Response to Temperature. *J Bacteriol* 196(8):1540-1550.
26. Cartman ST & Minton NP (2010) A Mariner-Based Transposon System for in Vivo Random Mutagenesis of *Clostridium difficile*. *Applied and Environmental Microbiology* 76(4):1103-1109.
27. Vidal JE, Chen JM, Li JH, & McClane BA (2009) Use of an Ez-Tn5-Based Random Mutagenesis System to Identify a Novel Toxin Regulatory Locus in *Clostridium perfringens* Strain 13. *PLoS One* 4(7):-.
28. Setlow P (2006) Spores of *Bacillus subtilis*: Their Resistance to and Killing by Radiation, Heat and Chemicals. *J Appl Microbiol* 101(3):514-525.
29. Paredes-Sabja D, Torres JA, Setlow P, & Sarker MR (2008) *Clostridium perfringens* Spore Germination: Characterization of Germinants and Their Receptors. *J Bacteriol* 190(4):1190-1201.
30. Paidhungat M & Setlow P (2001) Localization of a Germinant Receptor Protein (Gerba) to the Inner Membrane of *Bacillus subtilis* Spores. *J Bacteriol* 183(13):3982-3990.
31. Mason JM & Setlow P (1986) Essential Role of Small, Acid-Soluble Spore Proteins in Resistance of *Bacillus subtilis* Spores to Uv Light. *J Bacteriol* 167(1):174-178.
32. Voth DE & Ballard JD (2005) *Clostridium difficile* Toxins: Mechanism of Action and Role in Disease. *Clinical Microbiology Reviews* 18(2):247-+.
33. Moir A, Corfe BM, & Behravan J (2002) Spore Germination. *Cell Mol Life Sci* 59(3):403-409.
34. Setlow P (2003) Spore Germination. *Curr Opin Microbiol* 6(6):550-556.
35. Setlow B, Melly E, & Setlow P (2001) Properties of Spores of *Bacillus subtilis* Blocked at an Intermediate Stage in Spore Germination. *Journal of Bacteriology* 183(16):4894-4899.
36. Tani K, Watanabe T, Matsuda H, Nasu M, & Kondo M (1996) Cloning and Sequencing of the Spore Germination Gene of *Bacillus megaterium* Atcc 12872: Similarities to the NaH-Antiporter Gene of *Enterococcus hirae*. *Microbiology and Immunology* 40(2):99-105.
37. Thackray PD, Behravan J, Southworth TW, & Moir A (2001) Gern, an Antiporter Homologue Important in Germination of *Bacillus cereus* Endospores. *Journal of Bacteriology* 183(2):476-482.
38. Behravan J, Chirakkal H, Masson A, & Moir A (2000) Mutations in the GerP Locus of *Bacillus subtilis*

and *Bacillus cereus* Affect Access of Germinants to Their Targets in Spores. *Journal of Bacteriology* 182(7):1987-1994.

39. Moir A (2006) How Do Spores Germinate? *Journal of Applied Microbiology* 101(3):526-530.
40. Heffron JD, Lambert EA, Sherry N, & Popham DL (2010) Contributions of Four Cortex Lytic Enzymes to Germination of *Bacillus anthracis* Spores. *J Bacteriol* 192(3):763-770.
41. Shimamoto S, Moriyama R, Sugimoto K, Miyata S, & Makino S (2001) Partial Characterization of an Enzyme Fraction with Protease Activity Which Converts the Spore Peptidoglycan Hydrolase (SleC) Precursor to an Active Enzyme During Germination of *Clostridium perfringens* S40 Spores and Analysis of a Gene Cluster Involved in the Activity. *Journal of Bacteriology* 183(12):3742-3751.
42. Atluri S, Ragkousi K, Cortezzo DE, & Setlow P (2006) Cooperativity between Different Nutrient Receptors in Germination of Spores of *Bacillus subtilis* and Reduction of This Cooperativity by Alterations in the GerB Receptor. *Journal of Bacteriology* 188(1):28-36.
43. Sorg JA & Sonenshein AL (2008) Bile Salts and Glycine as Cogerminants for *Clostridium difficile* Spores. *Journal of Bacteriology* 190(7):2505-2512.
44. Paidhungat M & Setlow P (2000) Role of Ger Proteins in Nutrient and Nonnutrient Triggering of Spore Germination in *Bacillus subtilis*. *J Bacteriol* 182(9):2513-2519.
45. Moir A & Smith DA (1990) The Genetics of Bacterial Spore Germination. *Annu Rev Microbiol* 44:531-553.
46. Hudson KD, *et al.* (2001) Localization of GerAA and GerAC Germination Proteins in the *Bacillus subtilis* Spore. *J Bacteriol* 183(14):4317-4322.
47. Irie R, Okamoto T, & Fujita Y (1982) A Germination Mutant of *Bacillus subtilis* Deficient in Response to Glucose. *Journal of General and Applied Microbiology* 28(4):345-354.
48. Corfe BM, Sammons RL, Smith DA, & Mauel C (1994) The GerB Region of the *Bacillus subtilis* 168 Chromosome Encodes a Homolog of the GerA Spore Germination Operon. *Microbiology-Uk* 140:471-478.
49. Igarashi T & Setlow P (2005) Interaction between Individual Protein Components of the GerA and GerB Nutrient Receptors That Trigger Germination of *Bacillus subtilis* Spores. *Journal of Bacteriology* 187(7):2513-2518.
50. Sacks LE (1981) Influence of Cations on Lysozyme-Induced Germination of Coatless Spores of *Clostridium perfringens* 86. *Biochim Biophys Acta* 674(1):118-127.
51. Pelczar PL, Igarashi T, Setlow B, & Setlow P (2007) Role of GerD in Germination of *Bacillus subtilis* Spores. *J Bacteriol* 189(3):1090-1098.
52. Shah IM, Laaberki MH, Popham DL, & Dworkin J (2008) A Eukaryotic-Like Ser/Thr Kinase Signals Bacteria to Exit Dormancy in Response to Peptidoglycan Fragments. *Cell* 135(3):486-496.
53. Rood JI (1998) Virulence Genes of *Clostridium perfringens*. *Annu Rev Microbiol* 52:333-360.
54. Awad MM & Rood JI (1997) Isolation of Alpha-Toxin, Theta-Toxin and Kappa-Toxin Mutants of *Clostridium perfringens* by Tn916 Mutagenesis. *Microb Pathog* 22(5):275-284.
55. Briolat V & Reysset G (2002) Identification of the *Clostridium perfringens* Genes Involved in the Adaptive Response to Oxidative Stress. *J Bacteriol* 184(9):2333-2343.
56. Lyristis M, *et al.* (1994) Identification and Molecular Analysis of a Locus That Regulates Extracellular Toxin Production in *Clostridium perfringens*. *Mol Microbiol* 12(5):761-777.
57. Lanckriet A, *et al.* (2009) Generation of Single-Copy Transposon Insertions in *Clostridium perfringens*

by Electroporation of Phage Mu DNA Transposition Complexes. *Appl Environ Microbiol* 75(9):2638-2642.

58. Myers GS, *et al.* (2006) Skewed Genomic Variability in Strains of the Toxigenic Bacterial Pathogen, *Clostridium perfringens*. *Genome Res* 16(8):1031-1040.
59. Hartman AH, Liu H, & Melville SB (2011) Construction and Characterization of a Lactose-Inducible Promoter System for Controlled Gene Expression in *Clostridium perfringens*. *Appl Environ Microbiol* 77(2):471-478.
60. Lampe DJ, Churchill ME, & Robertson HM (1996) A Purified Mariner Transposase Is Sufficient to Mediate Transposition in Vitro. *The EMBO journal* 15(19):5470-5479.
61. Heap JT, Pennington OJ, Cartman ST, & Minton NP (2009) A Modular System for *Clostridium* Shuttle Plasmids. *J Microbiol Methods* 78(1):79-85.
62. Sambrook J, Fritsch EF, & Maniatis T (1989) *Molecular Cloning: A Laboratory Manual, 2nd Ed.* (Cold Spring Harbor Laboratory Press, Cold Spring Habor, NY) 2nd Ed.
63. Sliusarenko O, Heinritz J, Emonet T, & Jacobs-Wagner C (2011) High-Throughput, Subpixel Precision Analysis of Bacterial Morphogenesis and Intracellular Spatio-Temporal Dynamics. *Molecular microbiology* 80(3):612-627.
64. Both D, Schneider G, & Schnell R (2011) Peptidoglycan Remodeling in *Mycobacterium tuberculosis*: Comparison of Structures and Catalytic Activities of RipA and RipB. *Journal of molecular biology* 413(1):247-260.
65. Chia JS, *et al.* (2001) A 60-Kilodalton Immunodominant Glycoprotein Is Essential for Cell Wall Integrity and the Maintenance of Cell Shape in *Streptococcus mutans*. *Infection and immunity* 69(11):6987-6998.
66. Gao LY, Pak M, Kish R, Kajihara K, & Brown EJ (2006) A *Mycobacterial* Operon Essential for Virulence in Vivo and Invasion and Intracellular Persistence in Macrophages. *Infection and immunity* 74(3):1757-1767.
67. Teng F, Kawalec M, Weinstock GM, Hryniewicz W, & Murray BE (2003) An *Enterococcus faecium* Secreted Antigen, SagA, Exhibits Broad-Spectrum Binding to Extracellular Matrix Proteins and Appears Essential for *E. faecium* Growth. *Infection and immunity* 71(9):5033-5041.
68. Zhao Y & Melville SB (1998) Identification and Characterization of Sporulation-Dependent Promoters Upstream of the Enterotoxin Gene (Cpe) of *Clostridium perfringens*. *J Bacteriol* 180(1):136-142.
69. Cameron DE, Urbach JM, & Mekalanos JJ (2008) A Defined Transposon Mutant Library and Its Use in Identifying Motility Genes in *Vibrio cholerae*. *Proceedings of the National Academy of Sciences of the United States of America* 105(25):8736-8741.
70. Sengupta N, *et al.* (2010) Comparative Proteomic Analysis of Extracellular Proteins of *Clostridium perfringens* Type A and Type C Strains. *Infection and immunity* 78(9):3957-3968.
71. Hett EC, Chao MC, Deng LL, & Rubin EJ (2008) A *Mycobacterial* Enzyme Essential for Cell Division Synergizes with Resuscitation-Promoting Factor. *PLoS pathogens* 4(2):e1000001.
72. Liu H, Bouillaut L, Sonenshein AL, & Melville SB (2013) Use of a *Mariner*-Based Transposon Mutagenesis System to Isolate *Clostridium perfringens* Mutants Deficient in Gliding Motility. *J Bacteriol* 195(3):629-636.
73. Cowles KN & Gitai Z (2010) Surface Association and the MreB Cytoskeleton Regulate Pilus Production, Localization and Function in *Pseudomonas aeruginosa*. *Mol Microbiol* 76(6):1411-1426.

74. Varga J (2006) The Role of CcpA in Regulating the Carbon-Starvation Response of *Clostridium perfringens*. Ph.D. (Virginia Tech, UNI Dissertation Service, Ann Arbor, MI).
75. Melville SB, Labbe R, & Sonenshein AL (1994) Expression from the *Clostridium perfringens* CPE Promoter in C. Perfringens and *Bacillus subtilis*. *Infect Immun* 62(12):5550-5558.
76. Pospiech A & Neumann B (1995) A Versatile Quick-Prep of Genomic DNA from Gram-Positive Bacteria. *Trends Genet* 11(6):217-218.
77. Sambrook J & Russel DW (2001) *Molecular Cloning, a Laboratory Manual, 3rd Edition* (Cold Spring Harbor Laboratory Press, Cold Spring Harbor, New York).
78. Orsburn B, Melville SB, & Popham DL (2008) Factors Contributing to Heat Resistance of *Clostridium perfringens* Endospores. *Appl Environ Microbiol* 74(11):3328-3335.
79. González-Castro MJ, López-Hernández J, Simal-Lozano J, & Oruña-Concha MJ (1997) Determination of Amino Acids in Green Beans by Derivitization with Phenylisothiocyanate and High-Performance Liquid Chromatography with Ultraviolet Detection. *J. Chrom. Sci.* 35:181-185.
80. Meador-Parton J & Popham DL (2000) Structural Analysis of *Bacillus subtilis* Spore Peptidoglycan During Sporulation. *J. Bacteriol.* 182:4491-4499.
81. Fu LY, Wang GZ, Ma BG, & Zhang HY (2011) Exploring the Common Molecular Basis for the Universal DNA Mutation Bias: Revival of Lowdin Mutation Model. *Biochem Biophys Res Commun* 409(3):367-371.
82. Eberhardt C, Kuerschner L, & Weiss DS (2003) Probing the Catalytic Activity of a Cell Division-Specific Transpeptidase in Vivo with Beta-Lactams. *J Bacteriol* 185(13):3726-3734.
83. Robinson WB, Mealor AE, Stevens SE, Jr., & Ospeck M (2007) Measuring the Force Production of the Hormogonia of *Mastigocladus laminosus*. *Biophys J* 93(2):699-703.
84. Lutkenhaus J (2007) Assembly Dynamics of the Bacterial MinCDE System and Spatial Regulation of the Z Ring. *Annu Rev Biochem* 76:539-562.
85. Edwards DH & Errington J (1997) The *Bacillus subtilis* DivIVA Protein Targets to the Division Septum and Controls the Site Specificity of Cell Division. *Mol Microbiol* 24(5):905-915.
86. Zhao CR, de Boer PA, & Rothfield LI (1995) Proper Placement of the *Escherichia coli* Division Site Requires Two Functions That Are Associated with Different Domains of the MinE Protein. *Proc Natl Acad Sci U S A* 92(10):4313-4317.
87. Shi J, Blundell TL, & Mizuguchi K (2001) FUGUE: Sequence-Structure Homology Recognition Using Environment-Specific Substitution Tables and Structure-Dependent gap Penalties. *J Mol Biol* 310(1):243-257.
88. Orsburn B, Sucre K, Popham DL, & Melville SB (2009) The SpmA/B and DacF Proteins of *Clostridium perfringens* Play Important Roles in Spore Heat Resistance. *FEMS Microbiol Lett* 291(2):188-194.
89. Abel-Santos E (2012) Bacterial Spores: Current Research and Applications. *Bacterial Spores: Current Research and Applications*:1-281.
90. Paredes-Sabja D, Setlow P, & Sarker MR (2009) GerO, a Putative $Na^+/H^+$-$K^+$ Antiporter, Is Essential for Normal Germination of Spores of the Pathogenic Bacterium *Clostridium perfringens*. *Journal of Bacteriology* 191(12):3822-3831.
91. Vepachedu VR & Setlow P (2007) Role of SpoVA Proteins in Release of Dipicolinic Acid During Germination of *Bacillus subtilis* Spores Triggered by Dodecylamine or Lysozyme. *Journal of*

*Bacteriology* 189(5):1565-1572.

92. Chen Y RW, Helm RF, Melville SB, Popham DL (2014) Levels of Germination Proteins in *Bacillus subtilis* Dormant, Superdormant, and Germinating Spores. *PLoS ONE* 9(4):e95781.
93. Yu NY, *et al.* (2010) PSORTb 3.0: Improved Protein Subcellular Localization Prediction with Refined Localization Subcategories and Predictive Capabilities for All Prokaryotes. *Bioinformatics* 26(13):1608-1615.
94. Bagos PG, Tsirigos KD, Liakopoulos TD, & Hamodrakas SJ (2008) Prediction of Lipoprotein Signal Peptides in Gram-Positive Bacteria with a Hidden Markov Model. *J Proteome Res* 7(12):5082-5093.
95. Juncker AS, *et al.* (2003) Prediction of Lipoprotein Signal Peptides in Gram-Negative Bacteria. *Protein Sci* 12(8):1652-1662.
96. Michaelis AM & Gitai Z (2010) Dynamic Polar Sequestration of Excess MurG May Regulate Enzymatic Function. *J Bacteriol* 192(18):4597-4605.
97. Tatusov RL, Galperin MY, Natale DA, & Koonin EV (2000) The COG Database: A Tool for Genome-Scale Analysis of Protein Functions and Evolution. *Nucleic Acids Res* 28(1):33-36.
98. Setlow P (2013) Summer Meeting 2011 When the Sleepers Wake: The Germination of Spores of *Bacillus* Species. *J Appl Microbiol* 115(6):1251-1268.
99. Raeymaekers L, Wuytack E, Willems I, Michiels CW, & Wuytack F (2002) Expression of a P-Type $Ca^{(2+)}$-Transport ATPase in *Bacillus subtilis* During Sporulation. *Cell Calcium* 32(2):93.
100. Higgins CF (2001) Abc Transporters: Physiology, Structure and Mechanism -an Overview. *Res Microbiol* 152(3-4):205-210.
101. Luyten K, *et al.* (1995) Fps1, a Yeast Member of the MIP Family of Channel Proteins, Is a Facilitator for Glycerol Uptake and Efflux and Is Inactive under Osmotic Stress. *EMBO J* 14(7):1360-1371.
102. Echevarria M, Windhager EE, Tate SS, & Frindt G (1994) Cloning and Expression of AQP3, a Water Channel from the Medullary Collecting Duct of Rat Kidney. *Proc Natl Acad Sci U S A* 91(23):10997-11001.
103. Beijer L, Nilsson RP, Holmberg C, & Rutberg L (1993) The GlpP and GlpF Genes of the Glycerol Regulon in *Bacillus subtilis*. *J Gen Microbiol* 139(2):349-359.
104. Zardoya R (2005) Phylogeny and Evolution of the Major Intrinsic Protein Family. *Biol Cell* 97(6):397-414.
105. Rodriguez MC, *et al.* (2000) A Functional Water Channel Protein in the Pathogenic Bacterium *Brucella abortus*. *Microbiology* 146 Pt 12:3251-3257.
106. Gupta AB, *et al.* (2012) MIPModDB: A Central Resource for the Superfamily of Major Intrinsic Proteins. *Nucleic Acids Res* 40(Database issue):D362-369.
107. Dembek M, Stabler RA, Witney AA, Wren BW, & Fairweather NF (2013) Transcriptional Analysis of Temporal Gene Expression in Germinating *Clostridium difficile* 630 Endospores. *PLoS One* 8(5):e64011.
108. Cowan AE, *et al.* (2004) Lipids in the Inner Membrane of Dormant Spores of *Bacillus* Species Are Largely Immobile. *Proc Natl Acad Sci U S A* 101(20):7733-7738.
109. Vepachedu VR & Setlow P (2005) Localization of SpoVAD to the Inner Membrane of Spores of *Bacillus subtilis*. *J Bacteriol* 187(16):5677-5682.
110. Sainsbury S, *et al.* (2011) Crystal Structures of Penicillin-Binding Protein 3 from *Pseudomonas aeruginosa*: Comparison of Native and Antibiotic-Bound Forms. *J Mol Biol* 405(1):173-184.

111. Paradis-Bleau C, *et al.* (2010) Lipoprotein Cofactors Located in the Outer Membrane Activate Bacterial Cell Wall Polymerases. *Cell* 143(7):1110-1120.
112. Lycklama ANJA & Driessen AJ (2012) The Bacterial Sec-Translocase: Structure and Mechanism. *Philos Trans R Soc Lond B Biol Sci* 367(1592):1016-1028.
113. Angelini S, Deitermann S, & Koch HG (2005) FtsY, the Bacterial Signal-Recognition Particle Receptor, Interacts Functionally and Physically with the SecYEG Translocon. *EMBO Rep* 6(5):476-481.
114. Paetzel M, Dalbey RE, & Strynadka NC (2000) The Structure and Mechanism of Bacterial Type I Signal Peptidases. A Novel Antibiotic Target. *Pharmacol Ther* 87(1):27-49.
115. Zellmeier S, Zuber U, Schumann W, & Wiegert T (2003) The Absence of FtsH Metalloprotease Activity Causes Overexpression of the SigmaW-Controlled PbpE Gene, Resulting in Filamentous Growth of *Bacillus subtilis*. *J Bacteriol* 185(3):973-982.
116. Ito K & Akiyama Y (2005) Cellular Functions, Mechanism of Action, and Regulation of FtsH Protease. *Annu Rev Microbiol* 59:211-231.
117. Dartigalongue C & Raina S (1998) A New Heat-Shock Gene, PpiD, Encodes a Peptidyl-Prolyl Isomerase Required for Folding of Outer Membrane Proteins in *Escherichia coli*. *EMBO J* 17(14):3968-3980.
118. Banasavadi-Siddegowda YK, *et al.* (2011) FKBP38 Peptidylprolyl Isomerase Promotes the Folding of Cystic Fibrosis Transmembrane Conductance Regulator in the Endoplasmic Reticulum. *J Biol Chem* 286(50):43071-43080.
119. Watts KM & Hunstad DA (2008) Components of SurA Required for Outer Membrane Biogenesis in Uropathogenic *Escherichia coli*. *PLoS One* 3(10):e3359.
120. Phadtare S & Inouye M (2001) Role of CspC and CspE in Regulation of Expression of RpoS and UspA, the Stress Response Proteins in *Escherichia coli*. *J Bacteriol* 183(4):1205-1214.
121. Korza G & Setlow P (2013) Topology and Accessibility of Germination Proteins in the *Bacillus subtilis* Spore Inner Membrane. *J Bacteriol* 195(7):1484-1491.
122. Urakami K, Miyata S, Moriyama R, Sugimoto K, & Makino S (1999) Germination-Specific Cortex-Lytic Enzymes from *Clostridium perfringens* S40 Spores: Time of Synthesis, Precursor Structure and Regulation of Enzymatic Activity. *FEMS Microbiol Lett* 173(2):467-473.
123. Qin Y, *et al.* (2006) The Highly Conserved LepA Is a Ribosomal Elongation Factor That Back-Translocates the Ribosome. *Cell* 127(4):721-733.
124. Pech M, *et al.* (2011) Elongation Factor 4 (EF4/LepA) Accelerates Protein Synthesis at Increased $Mg^{2+}$ Concentrations. *Proc Natl Acad Sci U S A* 108(8):3199-3203.
125. Banawas S, *et al.* (2013) The *Clostridium perfringens* Germinant Receptor Protein GerKC Is Located in the Spore Inner Membrane and Is Crucial for Spore Germination. *J Bacteriol* 195(22):5084-5091.
126. Yi X & Setlow P (2010) Studies of the Commitment Step in the Germination of Spores of *Bacillus* Species. *J Bacteriol* 192(13):3424-3433.
127. Igarashi T & Setlow P (2006) Transcription of the *Bacillus subtilis* GerK Operon, Which Encodes a Spore Germinant Receptor, and Comparison with That of Operons Encoding Other Germinant Receptors. *J Bacteriol* 188(11):4131-4136.
128. Corfe BM, Moir A, Popham D, & Setlow P (1994) Analysis of the Expression and Regulation of the GerB Spore Germination Operon of *Bacillus subtilis* 168. *Microbiology* 140 ( Pt 11):3079-3083.

129. Feavers IM, *et al.* (1990) The Regulation of Transcription of the GerA Spore Germination Operon of *Bacillus subtilis*. *Mol Microbiol* 4(2):275-282.
130. Paredes-Sabja D, Setlow B, Setlow P, & Sarker MR (2008) Characterization of *Clostridium perfringens* Spores That Lack SpoVA Proteins and Dipicolinic Acid. *J Bacteriol* 190(13):4648-4659.
131. Huang CM, *et al.* (2004) Identification of *Bacillus anthracis* Proteins Associated with Germination and Early Outgrowth by Proteomic Profiling of Anthrax Spores. *Proteomics* 4(9):2653-2661.
132. Kuwana R, *et al.* (2002) Proteomics Characterization of Novel Spore Proteins of *Bacillus subtilis*. *Microbiology* 148(Pt 12):3971-3982.
133. Lai EM, *et al.* (2003) Proteomic Analysis of the Spore Coats of *Bacillus subtilis* and *Bacillus anthracis*. *J Bacteriol* 185(4):1443-1454.
134. Jagtap P, *et al.* (2006) Early Events of *Bacillus anthracis* Germination Identified by Time-Course Quantitative Proteomics. *Proteomics* 6(19):5199-5211.
135. Keijser BJ, *et al.* (2007) Analysis of Temporal Gene Expression During *Bacillus subtilis* Spore Germination and Outgrowth. *J Bacteriol* 189(9):3624-3634.
136. McBride MJ (2001) Bacterial Gliding Motility: Multiple Mechanisms for Cell Movement over Surfaces. *Annu Rev Microbiol* 55:49-75.
137. Ziegler K, *et al.* (1998) Molecular Characterization of Cyanophycin Synthetase, the Enzyme Catalyzing the Biosynthesis of the Cyanobacterial Reserve Material Multi-L-Arginyl-Poly-L-Aspartate (Cyanophycin). *European Journal of Biochemistry* 254(1):154-159.
138. Harry KH, Zhou R, Kroos L, & Melville SB (2009) Sporulation and Enterotoxin (CPE) Synthesis Are Controlled by the Sporulation-Specific Sigma Factors SigE and SigK in *Clostridium perfringens*. *Journal of Bacteriology* 191(8):2728-2742.
139. Burnat M, Herrero A, & Flores E (2014) Compartmentalized Cyanophycin Metabolism in the Diazotrophic Filaments of a Heterocyst-Forming Cyanobacterium. *Proc Natl Acad Sci U S A* 111(10):3823-3828.

# APPENDIX

Table S4.1

Table S4.2

**Table S4.1. Total proteins detected in dormant spore inner membrane samples**

| UniProt ID | gene name (CPR_) | protein localization[a] | protein function |
|---|---|---|---|
| tr\|Q0SQS3\|Q0SQS3_CLOPS | 2258 | cell wall | Oligopeptide/dipeptide ABC transporter, oligopeptide/dipeptide-binding protein |
| tr\|Q0SWX9\|Q0SWX9_CLOPS | 0006 | Cytoplasmic | DNA gyrase subunit B, GyrB |
| tr\|Q0SWX8\|Q0SWX8_CLOPS | 0007 | Cytoplasmic | DNA gyrase subunit A, GyrA |
| sp\|Q0SWW9\|SYS_CLOPS | 0014 | Cytoplasmic | Serine--tRNA ligase, SerS |
| tr\|Q0SWX5\|Q0SWX5_CLOPS | 0015 | Cytoplasmic | Uncharacterized protein |
| sp\|Q0SWT9\|PEPT_CLOPS | 0029 | Cytoplasmic | Peptidase T, PepT |
| tr\|Q0SWT7\|Q0SWT7_CLOPS | 0032 | Cytoplasmic | Uncharacterized |
| tr\|Q0SWZ0\|Q0SWZ0_CLOPS | 0082 | Cytoplasmic | Glycogen synthase, GlgA |
| tr\|Q0SWY9\|Q0SWY9_CLOPS | 0083 | Cytoplasmic | Phosphorylase |
| sp\|Q0SWS5\|GLGC_CLOPS | 0086 | Cytoplasmic | Glucose-1-phosphate adenylyltransferase, GlgC |
| tr\|Q0SWS4\|Q0SWS4_CLOPS | 0087 | Cytoplasmic | Glucose-1-phosphate adenylyltransferase, GlgD subunit |
| tr\|Q0SWS0\|Q0SWS0_CLOPS | 0092 | Cytoplasmic | Putative PTS system, N-acetylglucosamine-specific IIA component |
| tr\|Q0SWR5\|Q0SWR5_CLOPS | 0098 | Cytoplasmic | Putative glucokinase |
| tr\|Q0SWR4\|Q0SWR4_CLOPS | 0099 | Cytoplasmic | Rubredoxin/rubrerythrin |
| sp\|Q0SWR1\|LDH_CLOPS | 0102 | Cytoplasmic | L-lactate dehydrogenase, LDH |
| tr\|Q0SWN1\|Q0SWN1_CLOPS | 0132 | Cytoplasmic | Rubrerythrin, Rbr_1 |
| tr\|Q0SWK7\|Q0SWK7_CLOPS | 0156 | cytoplasmic | Beta-galactosidase |
| sp\|Q0SWK6\|ARCA_CLOPS | 0157 | Cytoplasmic | Arginine deiminase, ArcA |
| sp\|Q0SWK5\|OTC_CLOPS | 0158 | Cytoplasmic | Ornithine carbamoyltransferase, ArcB |
| tr\|Q0SWJ0\|Q0SWJ0_CLOPS | 0173 | Cytoplasmic | Nitroreductase family protein |
| tr\|Q0SWG2\|Q0SWG2_CLOPS | 0203 | Cytoplasmic | Heme oxygenase |
| tr\|Q0SWB3\|Q0SWB3_CLOPS | 0256 | Cytoplasmic | Glycosyl transferase, group 1 family protein |

| | | | |
|---|---|---|---|
| tr\|Q0SWA8\|Q0SWA8_CLOPS | 0261 | Cytoplasmic | [Fe] hydrogenase |
| tr\|Q0SW95\|Q0SW95_CLOPS | 0275 | Cytoplasmic | Metallo-beta-lactamase family/flavodoxin |
| tr\|Q0SW87\|Q0SW87_CLOPS | 0284 | Cytoplasmic | Uncharacterized protein |
| tr\|Q0SW84\|Q0SW84_CLOPS | 0287 | Cytoplasmic | Putative transketolase, N-terminal subunit |
| tr\|Q0SW83\|Q0SW83_CLOPS | 0288 | Cytoplasmic | Putative transketolase, C-terminal subunit |
| tr\|Q0SW42\|Q0SW42_CLOPS | 0329 | Cytoplasmic | UvrABC system protein, UvrA |
| sp\|Q0SW37\|MURB_CLOPS | 0334 | Cytoplasmic | UDP-N-acetylenolpyruvoylglucosamine reductase, MurB |
| tr\|Q0SW30\|Q0SW30_CLOPS | 0341 | Cytoplasmic | 6-phosphofructokinase, PfkA |
| tr\|Q0SW29\|Q0SW29_CLOPS | 0342 | Cytoplasmic | Pyruvate kinase, Pyk_1 |
| tr\|Q0SW01\|Q0SW01_CLOPS | 0370 | Cytoplasmic | Uridine phosphorylase, Udp |
| sp\|Q0SW00\|DEOB_CLOPS | 0371 | Cytoplasmic | Phosphopentomutase, DeoB |
| tr\|Q0SVZ8\|Q0SVZ8_CLOPS | 0373 | Cytoplasmic | Histidine decarboxylase, pyruvoyl type |
| tr\|Q0SVT9\|Q0SVT9_CLOPS | 0432 | Cytoplasmic | Uncharacterized protein |
| tr\|Q0SVR5\|Q0SVR5_CLOPS | 0456 | Cytoplasmic | UDP-glucose/GDP-mannose dehydrogenase family |
| tr\|Q0SVQ3\|Q0SVQ3_CLOPS | 0468 | Cytoplasmic | UDP-glucose 4-epimerase, GalE_2 |
| tr\|Q0SVP7\|Q0SVP7_CLOPS | 0475 | Cytoplasmic | Alpha-galactosidase, Aga |
| tr\|Q0SVL0\|Q0SVL0_CLOPS | 0512 | Cytoplasmic | Nitrite/sulfite reductase homolog |
| tr\|Q0SVK3\|Q0SVK3_CLOPS | 0519 | Cytoplasmic | FMN-dependent NADH-azoreductase, AzoR |
| tr\|Q0SVF7\|Q0SVF7_CLOPS | 0566 | Cytoplasmic | Uncharacterized protein |
| tr\|Q0SVE6\|Q0SVE6_CLOPS | 0577 | Cytoplasmic | M18 family aminopeptidase |
| tr\|Q0SVE2\|Q0SVE2_CLOPS | 0581 | Cytoplasmic | Peptide chain release factor 3, PrfC |
| sp\|Q0SVB1\|SYQ_CLOPS | 0612 | Cytoplasmic | Glutamine--tRNA ligase, GlnS |
| tr\|Q0SVA5\|Q0SVA5_CLOPS | 0618 | Cytoplasmic | Uncharacterized protein |
| sp\|Q0SVA4\|SYY_CLOPS | 0619 | Cytoplasmic | Tyrosine--tRNA ligase, TyrS |
| tr\|Q0SV42\|Q0SV42_CLOPS | 0682 | Cytoplasmic | Rubredoxin/rubrerythrin |

| | | | |
|---|---|---|---|
| sp\|Q0SV41\|TAL_CLOPS | 0683 | Cytoplasmic | Probable transaldolase, Tal |
| tr\|Q0SV09\|Q0SV09_CLOPS | 0715 | Cytoplasmic | Pyridine nucleotide-disulphide oxidoreductase family protein |
| sp\|Q0SUV5\|AZOR_CLOPS | 0777 | Cytoplasmic | FMN-dependent NADH-azoreductase, AzoR |
| tr\|Q0SUS8\|Q0SUS8_CLOPS | 0804 | Cytoplasmic | PTS system, mannose/fructose/sorbose family, IIAB |
| tr\|Q0SUR7\|Q0SUR7_CLOPS | 0815 | cytoplasmic | Glycosyl hydrolase, family 2 |
| tr\|Q0SUP2\|Q0SUP2_CLOPS | 0840 | Cytoplasmic | Rubrerythrin, Rbr_2 |
| tr\|Q0SUP0\|Q0SUP0_CLOPS | 0842 | Cytoplasmic | Nadh-dependent butanol dehydrogenase a |
| tr\|Q0SUH5\|Q0SUH5_CLOPS | 0908 | Cytoplasmic | Sucrose-6-phosphate hydrolase |
| tr\|Q0SUE9\|Q0SUE9_CLOPS | 0934 | Cytoplasmic | Spore coat peptide assembly protein CotJC |
| tr\|Q0SUC5\|Q0SUC5_CLOPS | 0959 | Cytoplasmic | Glycosyl hydrolase, family 20 |
| tr\|Q0SUB0\|Q0SUB0_CLOPS | 0974 | Cytoplasmic | Hydroxylamine reductase, Hcp |
| tr\|Q0SU99\|Q0SU99_CLOPS | 0985 | Cytoplasmic | Uncharacterized protein |
| tr\|Q0SU73\|Q0SU73_CLOPS | 1011 | Cytoplasmic | 1,3-propanediol dehydrogenase, DhaT |
| tr\|Q0SU57\|Q0SU57_CLOPS | 1027 | Cytoplasmic | Collagen triple helix repeat protein |
| tr\|Q0SU24\|Q0SU24_CLOPS | 1061 | cytoplasmic | Oxidoreductase, 2-nitropropane dioxygenase family |
| sp\|Q0SU18\|SYE_CLOPS | 1067 | Cytoplasmic | Glutamate--tRNA ligase, GltX |
| tr\|Q0SU09\|Q0SU09_CLOPS | 1076 | Cytoplasmic | M18 family aminopeptidase |
| tr\|Q0SU05\|Q0SU05_CLOPS | 1080 | Cytoplasmic | Uncharacterized protein |
| tr\|Q0STZ4\|Q0STZ4_CLOPS | 1091 | Cytoplasmic | Rubredoxin/flavodoxin/oxidoreductase |
| tr\|Q0STY1\|Q0STY1_CLOPS | 1104 | Cytoplasmic | Uncharacterized protein |
| tr\|Q0STW2\|Q0STW2_CLOPS | 1123 | Cytoplasmic | Cyclopropane-fatty-acyl-phospholipid synthase, Cfa |
| tr\|Q0STV6\|Q0STV6_CLOPS | 1129 | Cytoplasmic | Tetratricopeptide repeat protein |
| tr\|Q0STV5\|Q0STV5_CLOPS | 1130 | Cytoplasmic | Glutamine-dependent NAD(+) synthetase, NadE |
| tr\|Q0STV3\|Q0STV3_CLOPS | 1132 | Cytoplasmic | SPFH domain protein/band 7 family protein |
| sp\|Q0STU9\|FABH_CLOPS | 1136 | Cytoplasmic | 3-oxoacyl-[acyl-carrier-protein] synthase 3, FabH |

| | | | |
|---|---|---|---|
| tr\|Q0STU8\|Q0STU8_CLOPS | 1137 | Cytoplasmic | Malonyl CoA-acyl carrier protein transacylase, FabD |
| tr\|Q0STU7\|Q0STU7_CLOPS | 1138 | Cytoplasmic | 3-oxoacyl-[acyl-carrier-protein] reductase, FabG |
| sp\|Q0STU4\|FABZ_CLOPS | 1141 | Cytoplasmic | 3-hydroxyacyl-[acyl-carrier-protein] dehydratase FabZ |
| tr\|Q0STU3\|Q0STU3_CLOPS | 1142 | Cytoplasmic | Acetyl-CoA carboxylase, biotin carboxylase subunit, AccC |
| sp\|Q0STS8\|CAPPA_CLOPS | 1157 | Cytoplasmic | Phosphoenolpyruvate carboxylase, PpcA |
| tr\|Q0STR6\|Q0STR6_CLOPS | 1169 | Cytoplasmic | Formate acetyltransferase, Pfl |
| tr\|Q0STQ4\|Q0STQ4_CLOPS | 1181 | Cytoplasmic | Threonine dehydratase, catabolic, TdcB |
| tr\|Q0STP7\|Q0STP7_CLOPS | 1188 | Cytoplasmic | Haloacid dehalogenase, IB family protein |
| tr\|Q0STN2\|Q0STN2_CLOPS | 1203 | Cytoplasmic | 6-phosphofructokinase, PfkA |
| tr\|Q0STM9\|Q0STM9_CLOPS | 1206 | Cytoplasmic | UDP-N-acetylmuramyl tripeptide synthetase MurC homolog |
| tr\|Q0STL0\|Q0STL0_CLOPS | 1225 | Cytoplasmic | Amidohydrolase family protein |
| tr\|Q0STI9\|Q0STI9_CLOPS | 1246 | Cytoplasmic | Uncharacterized protein |
| tr\|Q0STI8\|Q0STI8_CLOPS | 1247 | Cytoplasmic | Uncharacterized protein |
| sp\|Q0STE8\|XPT2_CLOPS | 1287 | Cytoplasmic | Xanthine phosphoribosyltransferase 2, Xpt2 |
| tr\|Q0STE7\|Q0STE7_CLOPS | 1288 | Cytoplasmic | Tetratricopeptide repeat protein |
| tr\|Q0STE3\|Q0STE3_CLOPS | 1292 | cytoplasmic | Ribonuclease R, Rnr |
| sp\|Q0STE0\|ENO_CLOPS | 1295 | Cytoplasmic | Enolase, Eno |
| sp\|Q0STD7\|GPMI_CLOPS | 1298 | Cytoplasmic | 2,3-bisphosphoglycerate-independent phosphoglycerate mutase, GpmI |
| sp\|Q0STD6\|TPIS_CLOPS | 1299 | Cytoplasmic | Triosephosphate isomerase, TpiA |
| sp\|Q0STD5\|PGK_CLOPS | 1300 | Cytoplasmic | Phosphoglycerate kinase, Pgk |
| tr\|Q0STD4\|Q0STD4_CLOPS | 1301 | Cytoplasmic | Glyceraldehyde-3-phosphate dehydrogenase, type I , Gap |
| tr\|Q0STB4\|Q0STB4_CLOPS | 1323 | Cytoplasmic | CBS domain/MgtE intracellular domain protein |
| tr\|Q0STA6\|Q0STA6_CLOPS | 1331 | Cytoplasmic | Rubrerythrin |
| sp\|Q0STA4\|Y1333_CLOPS | 1333 | Cytoplasmic | UPF0229 protein |
| tr\|Q0STA3\|Q0STA3_CLOPS | 1334 | Cytoplasmic | Non-specific serine/threonine protein kinase, PrkA |

| | | | |
|---|---|---|---|
| sp\|Q0ST92\|GAL1_CLOPS | 1345 | Cytoplasmic | Galactokinase, GalK |
| tr\|Q0ST87\|Q0ST87_CLOPS | 1350 | Cytoplasmic | Fructose-1,6-bisphosphate aldolase, class II, Fba |
| tr\|Q0ST63\|Q0ST63_CLOPS | 1375 | Cytoplasmic | Methionine aminopeptidase, Map_1 |
| sp\|Q0ST54\|CLPX_CLOPS | 1384 | Cytoplasmic | ATP-dependent Clp protease ATP-binding subunit ClpX |
| sp\|Q0ST53\|CLPP_CLOPS | 1385 | Cytoplasmic | ATP-dependent Clp protease proteolytic subunit, ClpP |
| tr\|Q0ST49\|Q0ST49_CLOPS | 1389 | Cytoplasmic | ATP-dependent RNA helicase, DEAD/DEAH box family |
| sp\|Q0ST47\|DEOD_CLOPS | 1391 | cytoplasmic | Purine nucleoside phosphorylase DeoD-type, DeoD |
| tr\|Q0ST43\|Q0ST43_CLOPS | 1395 | Cytoplasmic | Putative peptidase |
| sp\|Q0ST36\|THII_CLOPS | 1402 | Cytoplasmic | Probable tRNA sulfurtransferase, ThiI |
| tr\|Q0ST22\|Q0ST22_CLOPS | 1416 | cytoplasmic | ClpB protein |
| tr\|Q0SSY7\|Q0SSY7_CLOPS | 1451 | Cytoplasmic | Uncharacterized protein |
| tr\|Q0SST9\|Q0SST9_CLOPS | 1499 | Cytoplasmic | Glutamate dehydrogenase, GdhA |
| tr\|Q0SSS2\|Q0SSS2_CLOPS | 1517 | Cytoplasmic | SpoVK domain protein |
| tr\|Q0SSR9\|Q0SSR9_CLOPS | 1520 | Cytoplasmic | Uncharacterized protein |
| tr\|Q0SSQ1\|Q0SSQ1_CLOPS | 1539 | Cytoplasmic | Peptidyl-prolyl cis-trans isomerase, cyclophilin-type |
| tr\|Q0SSM8\|Q0SSM8_CLOPS | 1563 | Cytoplasmic | Uncharacterized protein |
| tr\|Q0SSI4\|Q0SSI4_CLOPS | 1607 | Cytoplasmic | V-type ATP synthase subunit D, AtpD |
| sp\|Q0SSI3\|VATB_CLOPS | 1608 | Cytoplasmic | V-type ATP synthase beta chain, AtpB |
| sp\|Q0SSI2\|VATA_CLOPS | 1609 | Cytoplasmic | V-type ATP synthase alpha chain, AtpA |
| sp\|Q0SSH9\|VATE_CLOPS | 1612 | Cytoplasmic | V-type ATP synthase subunit E, AtpE |
| tr\|Q0SSF9\|Q0SSF9_CLOPS | 1633 | Cytoplasmic | Arginine--tRNA ligase, ArgS |
| tr\|Q0SSF4\|Q0SSF4_CLOPS | 1638 | Cytoplasmic | Putative DNA polymerase III, epsilon subunit |
| sp\|Q0SSE8\|RNY_CLOPS | 1644 | Cytoplasmic | Ribonuclease Y, Rny |
| sp\|Q0SSE7\|RECA_CLOPS | 1645 | Cytoplasmic | Protein RecA |
| sp\|Q0SSE5\|RIMO_CLOPS | 1647 | Cytoplasmic | Ribosomal protein S12 methylthiotransferase RimO |

| | | | |
|---|---|---|---|
| tr\|Q0SSE3\|Q0SSE3_CLOPS | 1649 | Cytoplasmic | Putative endopeptidase, ClpP |
| sp\|Q0SSE0\|PNP_CLOPS | 1652 | Cytoplasmic | Polyribonucleotide nucleotidyltransferase, Pnp |
| sp\|Q0SSD4\|IF2_CLOPS | 1658 | Cytoplasmic | Translation initiation factor IF-2, InfB |
| tr\|Q0SSC8\|Q0SSC8_CLOPS | 1664 | Cytoplasmic | 4-hydroxy-3-methylbut-2-en-1-yl diphosphate synthase, IspG |
| sp\|Q0SSC2\|PYRH_CLOPS | 1670 | cytoplasmic | Uridylate kinase, PyrH |
| sp\|Q0SSC1\|EFTS_CLOPS | 1671 | Cytoplasmic | Elongation factor Ts, Tsf |
| sp\|Q0SSC0\|RS2_CLOPS | 1672 | Cytoplasmic | 30S ribosomal protein S2, RpsB |
| tr\|Q0SSB2\|Q0SSB2_CLOPS | 1680 | Cytoplasmic | 50S ribosomal protein L19, RplS |
| tr\|Q0SS97\|Q0SS97_CLOPS | 1695 | Cytoplasmic | Acetate kinase, AckA_2 |
| tr\|Q0SS89\|Q0SS89_CLOPS | 1703 | Cytoplasmic | DAK2 domain protein |
| sp\|Q0SS87\|RL28_CLOPS | 1705 | Cytoplasmic | 50S ribosomal protein L28, RpmB |
| tr\|Q0SS68\|Q0SS68_CLOPS | 1724 | Cytoplasmic | Stage IV sporulation protein A, SpoIVA |
| tr\|Q0SS60\|Q0SS60_CLOPS | 1732 | Cytoplasmic | RNA polymerase sigma factor, SigG |
| tr\|Q0SS51\|Q0SS51_CLOPS | 1741 | Cytoplasmic | Peptidase, U32 family |
| tr\|Q0SS47\|Q0SS47_CLOPS | 1745 | Cytoplasmic | RNA-metabolizing metallo-beta-lactamase family protein |
| sp\|Q0SS42\|SYA_CLOPS | 1750 | Cytoplasmic | Alanine--tRNA ligase, AlaS |
| tr\|Q0SS37\|Q0SS37_CLOPS | 1755 | Cytoplasmic | Cysteine desulfurase, IscS |
| tr\|Q0SS25\|Q0SS25_CLOPS | 1767 | Cytoplasmic | Nitrate reductase, catalytic subunit, NarA |
| sp\|Q0SRY9\|EFP_CLOPS | 1803 | Cytoplasmic | Elongation factor P, Efp |
| tr\|Q0SRV2\|Q0SRV2_CLOPS | 1841 | Cytoplasmic | Phosphoglucomutase/phosphomannomutase family protein |
| tr\|Q0SRU2\|Q0SRU2_CLOPS | 1851 | Cytoplasmic | Phenylalanine--tRNA ligase beta subunit, PheT |
| sp\|Q0SRT7\|RL20_CLOPS | 1856 | Cytoplasmic | 50S ribosomal protein L20, RplT |
| sp\|Q0SRT6\|RL35_CLOPS | 1857 | Cytoplasmic | 50S ribosomal protein L35, RpmI |
| tr\|Q0SRS6\|Q0SRS6_CLOPS | 1871 | cytoplasmic | Aspartate-semialdehyde dehydrogenase, Asd |
| tr\|Q0SRS2\|Q0SRS2_CLOPS | 1875 | cytoplasmic | Putative cob(I)alamin adenosyltransferase |

| | | | |
|---|---|---|---|
| tr\|Q0SRR1\|Q0SRR1_CLOPS | 1886 | Cytoplasmic | Valine--tRNA ligase, ValS |
| sp\|Q0SRP8\|SYD_CLOPS | 1899 | cytoplasmic | Aspartate--tRNA ligase, AspS |
| tr\|Q0SRM0\|Q0SRM0_CLOPS | 1927 | Cytoplasmic | GTPase HflX |
| tr\|Q0SRL9\|Q0SRL9_CLOPS | 1928 | Cytoplasmic | Hypoxanthine phosphoribosyltransferase, Hpt_1 |
| tr\|Q0SRI7\|Q0SRI7_CLOPS | 1961 | Cytoplasmic | Dephospho-CoA kinase, CoaE |
| tr\|Q0SRI3\|Q0SRI3_CLOPS | 1965 | Cytoplasmic | Aminopeptidase |
| tr\|Q0SRG5\|Q0SRG5_CLOPS | 1983 | Cytoplasmic | Pyruvate, phosphate dikinase, PpdK |
| sp\|Q0SRF3\|RS21_CLOPS | 1995 | Cytoplasmic | 30S ribosomal protein, RpsU |
| tr\|Q0SRE4\|Q0SRE4_CLOPS | 2004 | Cytoplasmic | Chaperone protein DnaJ |
| sp\|Q0SRE3\|DNAK_CLOPS | 2005 | Cytoplasmic | Chaperone protein DnaK |
| tr\|Q0SRD0\|Q0SRD0_CLOPS | 2018 | Cytoplasmic | Stage V sporulation protein AD, SpoVAD |
| sp\|Q0SRC7\|SP2AB_CLOPS | 2021 | Cytoplasmic | Anti-sigma F factor, SpoIIAB |
| tr\|Q0SRC1\|Q0SRC1_CLOPS | 2027 | Cytoplasmic | Putative manganese-dependent inorganic pyrophosphatase |
| tr\|Q0SRB9\|Q0SRB9_CLOPS | 2029 | Cytoplasmic | Glutamate decarboxylase |
| tr\|Q0SRA9\|Q0SRA9_CLOPS | 2039 | Cytoplasmic | DNA gyrase/topoisomerase IV, A subunit family protein |
| tr\|Q0SR89\|Q0SR89_CLOPS | 2059 | cytoplasmic | FemAB family protein |
| sp\|Q0SR54\|OBG_CLOPS | 2094 | Cytoplasmic | GTPase obg |
| sp\|Q0SR51\|RL21_CLOPS | 2097 | Cytoplasmic | 50S ribosomal protein L21, RplU |
| tr\|Q0SR48\|Q0SR48_CLOPS | 2100 | Cytoplasmic | Radical SAM domain protein |
| tr\|Q0SR38\|Q0SR38_CLOPS | 2110 | Cytoplasmic | Rod shape-determining protein MreB |
| tr\|Q0SR33\|Q0SR33_CLOPS | 2115 | Cytoplasmic | Aminoacyl-histidine dipeptidase, PepD_1 |
| tr\|Q0SR32\|Q0SR32_CLOPS | 2116 | Cytoplasmic | Pyruvate kinase, Pyk |
| sp\|Q0SR11\|SECA_CLOPS | 2139 | Cytoplasmic | Protein translocase subunit SecA |
| sp\|Q0SR05\|METK_CLOPS | 2145 | Cytoplasmic | S-adenosylmethionine synthase, MetK |
| sp\|Q0SQZ4\|ATPG_CLOPS | 2163 | Cytoplasmic | ATP synthase gamma chain, AtpG |

| | | | |
|---|---|---|---|
| sp\|Q0SQZ3\|ATPA_CLOPS | 2164 | Cytoplasmic | ATP synthase subunit alpha, AtpA |
| tr\|Q0SQY7\|Q0SQY7_CLOPS | 2170 | Cytoplasmic | Acetyl-CoA acetyltransferase |
| tr\|Q0SQY6\|Q0SQY6_CLOPS | 2171 | Cytoplasmic | UDP-N-acetylglucosamine 2-epimerase, MnaA |
| sp\|Q0SQY5\|UPP_CLOPS | 2172 | Cytoplasmic | Uracil phosphoribosyltransferase, Upp |
| sp\|Q0SQY1\|RF1_CLOPS | 2176 | Cytoplasmic | Peptide chain release factor 1, PrfA |
| sp\|Q0SQX5\|PYRG_CLOPS | 2182 | Cytoplasmic | CTP synthase, PyrG |
| tr\|Q0SQW8\|Q0SQW8_CLOPS | 2189 | cytoplasmic | LysM domain protein |
| sp\|Q0SQS9\|G6PI_CLOPS | 2252 | cytoplasmic | Glucose-6-phosphate isomerase, Pgi |
| tr\|Q0SQS0\|Q0SQS0_CLOPS | 2261 | Cytoplasmic | Inosine-5'-monophosphate dehydrogenase, GuaB |
| tr\|C6UAS4\|C6UAS4_CLOPS | 2275 | Cytoplasmic | 60 kDa chaperonin, GroEL |
| tr\|Q0SQP9\|Q0SQP9_CLOPS | 2283 | Cytoplasmic | 3-hydroxybutyryl-CoA dehydrogenase, Hbd |
| tr\|Q0SQP8\|Q0SQP8_CLOPS | 2284 | Cytoplasmic | Electron transfer flavoprotein, alpha subunit/FixB family protein, fixB |
| tr\|Q0SQP6\|Q0SQP6_CLOPS | 2286 | Cytoplasmic | Butyryl-CoA dehydrogenase, Bcd |
| tr\|Q0SQP5\|Q0SQP5_CLOPS | 2287 | Cytoplasmic | 3-hydroxybutyryl-CoA dehydratase ,Crt |
| sp\|Q0SQP4\|REX_CLOPS | 2288 | Cytoplasmic | Redox-sensing transcriptional repressor Rex |
| tr\|Q0SQN8\|Q0SQN8_CLOPS | 2294 | Cytoplasmic | Mannose-1-phosphate guanylyltransferase |
| sp\|Q0SQM4\|SYT_CLOPS | 2317 | Cytoplasmic | Threonine--tRNA ligase, ThrS |
| tr\|Q0SQL9\|Q0SQL9_CLOPS | 2322 | Cytoplasmic | Glutamine--fructose-6-phosphate aminotransferase [isomerizing], GlmS1 |
| tr\|Q0SQL8\|Q0SQL8_CLOPS | 2323 | Cytoplasmic | Rubrerythrin family protein |
| sp\|Q0SQL7\|GLMM_CLOPS | 2324 | Cytoplasmic | Phosphoglucosamine mutase, GlmM |
| tr\|Q0SQL0\|Q0SQL0_CLOPS | 2332 | Cytoplasmic | Phosphorylase, GlgP |
| tr\|Q0SQK1\|Q0SQK1_CLOPS | 2341 | Cytoplasmic | Iron hydrogenase, HydA |
| sp\|Q0SQK0\|BUK_CLOPS | 2342 | cytoplasmic | Probable butyrate kinase, Buk |
| tr\|Q0SQJ9\|Q0SQJ9_CLOPS | 2343 | cytoplasmic | Phosphate butyryltransferase, Ptb |
| tr\|Q0SQJ2\|Q0SQJ2_CLOPS | 2350 | Cytoplasmic | Thioredoxin, Trx |

| | | | |
|---|---|---|---|
| tr\|Q0SQJ1\|Q0SQJ1_CLOPS | 2351 | cytoplasmic | Isoaspartyl dipeptidase , IadA |
| tr\|Q0SQJ0\|Q0SQJ0_CLOPS | 2352 | Cytoplasmic | Phosphoenolpyruvate-protein phosphotransferase, PtsI |
| sp\|Q0SQH9\|RS9_CLOPS | 2363 | Cytoplasmic | 30S ribosomal protein S9, RpsI |
| sp\|Q0SQH8\|RL13_CLOPS | 2364 | Cytoplasmic | 50S ribosomal protein L13, RplM |
| sp\|Q0SQH4\|RL17_CLOPS | 2369 | Cytoplasmic | 50S ribosomal protein L17, RplQ |
| sp\|Q0SQH3\|RPOA_CLOPS | 2370 | Cytoplasmic | DNA-directed RNA polymerase subunit alpha, RpoA |
| sp\|Q0SQH2\|RS4A_CLOPS | 2371 | Cytoplasmic | 30S ribosomal protein S4 A, RpsD |
| sp\|Q0SQH1\|RS11_CLOPS | 2372 | Cytoplasmic | 30S ribosomal protein S11, RpsK |
| sp\|Q0SQH0\|RS13_CLOPS | 2373 | Cytoplasmic | 30S ribosomal protein S13, RpsM |
| sp\|Q0SQG1\|RS5_CLOPS | 2382 | Cytoplasmic | 30S ribosomal protein S5, RpsE |
| sp\|Q0SQG0\|RL18_CLOPS | 2383 | Cytoplasmic | 50S ribosomal protein L18, RplR |
| sp\|Q0SQF9\|RL6_CLOPS | 2384 | Cytoplasmic | 50S ribosomal protein L6, RplF |
| sp\|Q0SQF8\|RS8_CLOPS | 2385 | Cytoplasmic | 30S ribosomal protein S8, RpsH |
| sp\|Q0SQF6\|RL5_CLOPS | 2387 | Cytoplasmic | 50S ribosomal protein L5, RplE |
| sp\|Q0SQF5\|RL24_CLOPS | 2388 | Cytoplasmic | 50S ribosomal protein L24, RplX |
| sp\|Q0SQF4\|RL14_CLOPS | 2389 | Cytoplasmic | 50S ribosomal protein L14, RplN |
| sp\|Q0SQF3\|RS17_CLOPS | 2390 | Cytoplasmic | 30S ribosomal protein S17, RpsQ |
| sp\|Q0SQF1\|RL16_CLOPS | 2392 | Cytoplasmic | 50S ribosomal protein L16, RplP |
| sp\|Q0SQF0\|RS3_CLOPS | 2393 | Cytoplasmic | 30S ribosomal protein S3, RpsC |
| sp\|Q0SQE9\|RL22_CLOPS | 2394 | Cytoplasmic | 50S ribosomal protein L22, RplV |
| sp\|Q0SQE8\|RS19_CLOPS | 2395 | Cytoplasmic | 30S ribosomal protein S19, RpsS |
| sp\|Q0SQE4\|RL3_CLOPS | 2399 | cytoplasmic | 50S ribosomal protein L3, RplC |
| sp\|Q0SQC8\|EFTU_CLOPS | 2402 | cytoplasmic | Elongation factor Tu, Tuf1 |
| sp\|Q0SQE1\|EFG_CLOPS | 2403 | Cytoplasmic | Elongation factor G, FusA |
| sp\|Q0SQD9\|RS12_CLOPS | 2405 | Cytoplasmic | 30S ribosomal protein S12, RpsL |

| | | | |
|---|---|---|---|
| sp\|Q0SQD7\|RPOC_CLOPS | 2407 | Cytoplasmic | DNA-directed RNA polymerase subunit beta, RpoC |
| sp\|Q0SQD6\|RPOB_CLOPS | 2408 | Cytoplasmic | DNA-directed RNA polymerase subunit beta, RpoB |
| tr\|Q0SQD4\|Q0SQD4_CLOPS | 2410 | Cytoplasmic | 50S ribosomal protein L10, RplJ |
| sp\|Q0SQD3\|RL1_CLOPS | 2411 | Cytoplasmic | 50S ribosomal protein L1, RplA |
| sp\|Q0SQD2\|RL11_CLOPS | 2412 | Cytoplasmic | 50S ribosomal protein L11, RplK |
| tr\|Q0SQC4\|Q0SQC4_CLOPS | 2421 | Cytoplasmic | Thymidylate synthase ThyX |
| sp\|Q0SQC1\|SYC_CLOPS | 2424 | Cytoplasmic | Cysteine--tRNA ligase, CysS |
| sp\|Q0SQC0\|SYP_CLOPS | 2425 | Cytoplasmic | Proline--tRNA ligase, ProS |
| tr\|Q0SQB1\|Q0SQB1_CLOPS | 2434 | Cytoplasmic | Glyceraldehyde-3-phosphate dehydrogenase, NADP-dependent, GapN |
| tr\|Q0SQ95\|Q0SQ95_CLOPS | 2450 | Cytoplasmic | Amidohydrolase homolog |
| tr\|Q0SQ87\|Q0SQ87_CLOPS | 2465 | Cytoplasmic | Glycine--tRNA ligase, GlyS |
| sp\|Q0SQ86\|SYK_CLOPS | 2467 | Cytoplasmic | Lysine--tRNA ligase, LysS |
| tr\|Q0SQ69\|Q0SQ69_CLOPS | 2491 | Cytoplasmic | Stage V sprulation protein T, SpoVT |
| tr\|Q0SQ67\|Q0SQ67_CLOPS | 2493 | Cytoplasmic | Transcription-repair coupling factor, Mfd |
| tr\|Q0SQ62\|Q0SQ62_CLOPS | 2498 | Cytoplasmic | Ribose-phosphate pyrophosphokinase, PrsA |
| sp\|Q0SQ51\|SYN_CLOPS | 2509 | cytoplasmic | Asparagine--tRNA ligase, AsnS |
| sp\|Q0SQ50\|AMPA_CLOPS | 2510 | cytoplasmic | Probable cytosol aminopeptidase, PepA |
| tr\|Q0SQ42\|Q0SQ42_CLOPS | 2518 | Cytoplasmic | DegV family protein |
| tr\|Q0SQ35\|Q0SQ35_CLOPS | 2525 | Cytoplasmic | Uncharacterized protein |
| tr\|Q0SQ27\|Q0SQ27_CLOPS | 2533 | Cytoplasmic | Methionine--tRNA ligase, MetG_2 |
| tr\|Q0SQ21\|Q0SQ21_CLOPS | 2539 | Cytoplasmic | Xaa-pro aminopeptidase, PepP |
| tr\|Q0SQ20\|Q0SQ20_CLOPS | 2540 | Cytoplasmic | Aldehyde-alcohol dehydrogenase, AdhE |
| tr\|Q0SQ10\|Q0SQ10_CLOPS | 2550 | Cytoplasmic | Isoleucine--tRNA ligase, IleS |
| sp\|Q0SQ01\|GLPK_CLOPS | 2559 | Cytoplasmic | Glycerol kinase, GlpK |
| tr\|Q0SPZ6\|Q0SPZ6_CLOPS | 2564 | Cytoplasmic | Putative lipoprotein |

| | | | |
|---|---|---|---|
| tr\|Q0SPY7\|Q0SPY7_CLOPS | 2573 | Cytoplasmic | Putative glutamine synthetase |
| sp\|Q0SPX8\|PROA_CLOPS | 2582 | Cytoplasmic | Gamma-glutamyl phosphate reductase, ProA |
| tr\|Q0SPX6\|Q0SPX6_CLOPS | 2584 | Cytoplasmic | Oxidoreductase, short chain dehydrogenase/reductase family |
| tr\|Q0SPU4\|Q0SPU4_CLOPS | 2616 | Cytoplasmic | UDP-N-acetylglucosamine 1-carboxyvinyltransferase, MurA_2 |
| tr\|Q0SPT1\|Q0SPT1_CLOPS | 2641 | Cytoplasmic | Adenylosuccinate synthetase, PurA |
| tr\|Q0SPS1\|Q0SPS1_CLOPS | 2651 | Cytoplasmic | DHH family protein |
| sp\|Q0SPR8\|RS18_CLOPS | 2654 | Cytoplasmic | 30S ribosomal protein S18 ,RpsR |
| tr\|Q0SPQ8\|Q0SPQ8_CLOPS | 2664 | Cytoplasmic | Uncharacterized protein |
| sp\|Q0SPP8\|RL34_CLOPS | 2674 | Cytoplasmic | 50S ribosomal protein L34, RpmH |
| sp\|Q0SWW1\|PDRP_CLOPS | 0076 | Cytoplasmic membrane | Putative pyruvate, phosphate dikinase regulatory protein |
| tr\|Q0SWR9\|Q0SWR9_CLOPS | 0093 | Cytoplasmic Membrane | PTS system, N-acetylglucosamine-specific IIBC component, NagE |
| tr\|Q0SWK4\|Q0SWK4_CLOPS | 0159 | Cytoplasmic Membrane | Arginine/ornithine antiporter, ArcD |
| tr\|Q0SWI7\|Q0SWI7_CLOPS | 0176 | Cytoplasmic Membrane | Sodium:solute transporter |
| tr\|Q0SWD6\|Q0SWD6_CLOPS | 0230 | Cytoplasmic Membrane | Uncharacterized protein |
| tr\|Q0SWC5\|Q0SWC5_CLOPS | 0241 | Cytoplasmic Membrane | Uncharacterized protein |
| tr\|Q0SW99\|Q0SW99_CLOPS | 0271 | Cytoplasmic Membrane | Putative transcriptional regulator |
| tr\|Q0SW79\|Q0SW79_CLOPS | 0292 | Cytoplasmic Membrane | Cell division protein FtsX |
| tr\|Q0SW78\|Q0SW78_CLOPS | 0293 | Cytoplasmic Membrane | Carboxyl-terminal protease |
| tr\|Q0SW39\|Q0SW39_CLOPS | 0332 | Cytoplasmic Membrane | Putative penicillin-binding protein |
| tr\|Q0SW08\|Q0SW08_CLOPS | 0363 | Cytoplasmic Membrane | ABC transporter, permease/ATP-binding protein |
| tr\|Q0SW07\|Q0SW07_CLOPS | 0364 | Cytoplasmic Membrane | ABC transporter, permease/ATP-binding protein |
| tr\|Q0SVX2\|Q0SVX2_CLOPS | 0399 | Cytoplasmic Membrane | PTS system, mannose/fructose/sorbose family, IID component |
| tr\|Q0SVV6\|Q0SVV6_CLOPS | 0415 | Cytoplasmic Membrane | Uncharacterized protein |
| tr\|Q0SVV3\|Q0SVV3_CLOPS | 0418 | Cytoplasmic Membrane | PTS system, IIBC component |
| tr\|Q0SVU0\|Q0SVU0_CLOPS | 0431 | Cytoplasmic Membrane | Uncharacterized protein |

| | | | |
|---|---|---|---|
| tr\|Q0SVP6\|Q0SVP6_CLOPS | 0476 | Cytoplasmic Membrane | ABC transporter, substrate-binding protein |
| tr\|Q0SVP5\|Q0SVP5_CLOPS | 0477 | Cytoplasmic Membrane | ABC transporter, permease protein |
| tr\|Q0SVP4\|Q0SVP4_CLOPS | 0478 | Cytoplasmic Membrane | ABC transporter, permease protein |
| tr\|Q0SVJ4\|Q0SVJ4_CLOPS | 0528 | Cytoplasmic Membrane | Stage V sporulation protein D |
| tr\|Q0SVF9\|Q0SVF9_CLOPS | 0564 | Cytoplasmic Membrane | Signal peptidase I |
| tr\|Q0SVF8\|Q0SVF8_CLOPS | 0565 | Cytoplasmic Membrane | ATP-dependent zinc metalloprotease FtsH |
| tr\|Q0SVC5\|Q0SVC5_CLOPS | 0598 | Cytoplasmic Membrane | Cell envelope-related transcriptional attenuator domain family |
| tr\|Q0SVC0\|Q0SVC0_CLOPS | 0603 | Cytoplasmic Membrane | Phosphate ABC transporter, phosphate-binding protein, PstS_1 |
| sp\|Q0SVB6\|PSTB_CLOPS | 0607 | Cytoplasmic Membrane | Phosphate import ATP-binding protein PstB |
| tr\|Q0SVA9\|Q0SVA9_CLOPS | 0614 | Cytoplasmic Membrane | Spore germination protein |
| tr\|Q0SVA8\|Q0SVA8_CLOPS | *0615* | Cytoplasmic Membrane | Spore germination protein, GerABKA family |
| tr\|Q0SV26\|Q0SV26_CLOPS | 0698 | Cytoplasmic Membrane | ABC transporter, ATP-binding protein |
| tr\|Q0SV08\|Q0SV08_CLOPS | 0716 | Cytoplasmic Membrane | YeeE/YedE family protein |
| tr\|Q0SUS7\|Q0SUS7_CLOPS | 0805 | Cytoplasmic Membrane | PTS system, mannose/fructose/sorbose family, IIC component |
| tr\|Q0SUS6\|Q0SUS6_CLOPS | 0806 | Cytoplasmic Membrane | PTS system, mannose/fructose/sorbose family, IID component |
| tr\|Q0SUR3\|Q0SUR3_CLOPS | 0819 | Cytoplasmic Membrane | Antibiotic ABC transporter, permease protein |
| tr\|Q0SUM3\|Q0SUM3_CLOPS | 0859 | Cytoplasmic Membrane | Uncharacterized protein |
| tr\|Q0SUH9\|Q0SUH9_CLOPS | 0904 | Cytoplasmic Membrane | Substrate-binding protein MsmE |
| tr\|Q0SUE8\|Q0SUE8_CLOPS | 0935 | Cytoplasmic Membrane | PTS system, N-acetylglucosamine-specific IIBC component, NagE |
| tr\|Q0SUA1\|Q0SUA1_CLOPS | 0983 | Cytoplasmic Membrane | Cation efflux family protein |
| tr\|Q0SU83\|Q0SU83_CLOPS | 1001 | Cytoplasmic Membrane | Glycerol uptake facilitator protein, GlpE |
| tr\|Q0SU32\|Q0SU32_CLOPS | *1053* | Cytoplasmic Membrane | GerA spore germination protein |
| tr\|Q0SU31\|Q0SU31_CLOPS | 1054 | Cytoplasmic Membrane | C4-dicarboxylate anaerobic carrier family protein |
| tr\|Q0STX0\|Q0STX0_CLOPS | 1115 | Cytoplasmic Membrane | Iron compound ABC transporter, iron-binding protein |
| tr\|Q0STU6\|Q0STU6_CLOPS | 1139 | Cytoplasmic Membrane | 3-oxoacyl-[acyl-carrier-protein] synthase 2, FabF |

| | | | |
|---|---|---|---|
| tr\|Q0STF9\|Q0STF9_CLOPS | 1276 | Cytoplasmic Membrane | Oligopeptide transporter, OPT family |
| tr\|Q0STE2\|Q0STE2_CLOPS | 1293 | Cytoplasmic Membrane | Preprotein translocase, SecG subunit |
| tr\|Q0STA8\|Q0STA8_CLOPS | 1329 | Cytoplasmic Membrane | CDP-diacylglycerol--serine O-phosphatidyltransferase, PssA |
| tr\|Q0ST94\|Q0ST94_CLOPS | 1343 | Cytoplasmic Membrane | Galactoside ABC transporter, permease protein, MglC |
| tr\|Q0ST89\|Q0ST89_CLOPS | 1348 | Cytoplasmic Membrane | Uncharacterized protein |
| tr\|Q0SSP8\|Q0SSP8_CLOPS | 1542 | Cytoplasmic Membrane | Phage shock protein A, PspA |
| tr\|Q0SSH8\|Q0SSH8_CLOPS | 1613 | Cytoplasmic Membrane | V-type ATPase, K subunit |
| tr\|Q0SSH7\|Q0SSH7_CLOPS | 1614 | Cytoplasmic Membrane | V-type ATPase, I subunit |
| tr\|Q0SSE6\|Q0SSE6_CLOPS | 1646 | Cytoplasmic Membrane | CDP-diacylglycerol--glycerol-3-phosphate 3-phosphatidyltransferase, PgsA |
| tr\|Q0SSC7\|Q0SSC7_CLOPS | 1665 | Cytoplasmic Membrane | RIP metalloprotease RseP |
| tr\|Q0SS83\|Q0SS83_CLOPS | 1709 | Cytoplasmic Membrane | Serine/threonine protein kinase BH2504 |
| tr\|Q0SS79\|Q0SS79_CLOPS | 1713 | Cytoplasmic Membrane | Putative neutral zinc metallopeptidase |
| sp\|Q0SS66\|DER_CLOPS | 1726 | Cytoplasmic Membrane | GTPase Der |
| tr\|Q0SS49\|Q0SS49_CLOPS | 1743 | Cytoplasmic Membrane | Uncharacterized protein |
| tr\|Q0SS48\|Q0SS48_CLOPS | 1744 | Cytoplasmic Membrane | GTP-binding protein TypA |
| tr\|Q0SRW8\|Q0SRW8_CLOPS | 1824 | Cytoplasmic Membrane | Small basic protein, Sbp |
| tr\|Q0SRP0\|Q0SRP0_CLOPS | 1907 | Cytoplasmic Membrane | Protein-export membrane protein SecF |
| tr\|Q0SRN9\|Q0SRN9_CLOPS | 1908 | Cytoplasmic Membrane | Protein translocase subunit SecD |
| tr\|Q0SRN6\|Q0SRN6_CLOPS | 1911 | Cytoplasmic Membrane | Preprotein translocase, YajC_2 |
| sp\|Q0SRL7\|PBPA_CLOPS | 1930 | Cytoplasmic Membrane | Penicillin-binding protein 1A, PbpA |
| tr\|Q0SRL6\|Q0SRL6_CLOPS | 1931 | Cytoplasmic membrane | Sodium:alanine symporter family protein |
| tr\|Q0SRL1\|Q0SRL1_CLOPS | 1936 | Cytoplasmic Membrane | Spermidine/putrescine ABC transporter, permease protein PotB |
| tr\|Q0SRK4\|Q0SRK4_CLOPS | 1943 | Cytoplasmic Membrane | D-alanyl-D-alanine carboxypeptidase family protein |
| tr\|Q0SRG7\|Q0SRG7_CLOPS | 1981 | Cytoplasmic Membrane | Putative permease |
| sp\|Q0SRD8\|LEPA_CLOPS | 2010 | Cytoplasmic Membrane | Elongation factor 4, LepA |

| | | | |
|---|---|---|---|
| tr\|Q0SRD1\|Q0SRD1_CLOPS | 2017 | Cytoplasmic Membrane | Stage V sporulation protein AE, SpoVAE |
| tr\|Q0SRC9\|Q0SRC9_CLOPS | 2019 | Cytoplasmic Membrane | Stage V sporulation protein AC, SpoVAC |
| sp\|Q0SRB4\|MURG_CLOPS | 2034 | Cytoplasmic Membrane | MUrG transferasetransferase |
| tr\|Q0SR43\|Q0SR43_CLOPS | 2105 | Cytoplasmic Membrane | Site-determining protein, MinD |
| tr\|Q0SR25\|Q0SR25_CLOPS | 2123 | Cytoplasmic Membrane | MutS domain protein |
| tr\|Q0SR24\|Q0SR24_CLOPS | 2124 | Cytoplasmic Membrane | PTS system, glucose-specific IIBC component, PtsG |
| tr\|Q0SR23\|Q0SR23_CLOPS | 2125 | Cytoplasmic Membrane | ABC transporter, substrate-binding protein |
| sp\|Q0SQZ5\|ATPB_CLOPS | 2162 | Cytoplasmic Membrane | ATP synthase subunit beta, AtpD |
| sp\|Q0SQZ1\|ATPF_CLOPS | 2166 | Cytoplasmic Membrane | ATP synthase subunit b, AtpF |
| tr\|Q0SQY9\|Q0SQY9_CLOPS | 2168 | Cytoplasmic Membrane | ATP synthase subunit a, AtpB |
| tr\|Q0SQX6\|Q0SQX6_CLOPS | 2181 | Cytoplasmic Membrane | Transcription termination factor Rho |
| tr\|Q0SQW9\|Q0SQW9_CLOPS | 2188 | Cytoplasmic Membrane | Cyanophycinase, CphB |
| tr\|Q0SQS7\|Q0SQS7_CLOPS | 2254 | Cytoplasmic Membrane | Oligopeptide/dipeptide ABC transporter, ATP-binding protein |
| tr\|Q0SQS2\|Q0SQS2_CLOPS | 2259 | Cytoplasmic Membrane | Major facilitator family transporter |
| tr\|Q0SQP3\|Q0SQP3_CLOPS | 2289 | Cytoplasmic Membrane | Zinc-transporting atpase |
| tr\|Q0SQK2\|Q0SQK2_CLOPS | 2340 | Cytoplasmic Membrane | ABC transporter, ATP-binding protein |
| tr\|Q0SQG4\|Q0SQG4_CLOPS | 2379 | Cytoplasmic Membrane | Protein translocase subunit SecY |
| tr\|Q0SQB8\|Q0SQB8_CLOPS | 2427 | Cytoplasmic Membrane | PIN/TRAM domain protein |
| tr\|Q0SQ81\|Q0SQ81_CLOPS | 2472 | Cytoplasmic Membrane | ATP-dependent zinc metalloprotease FtsH |
| sp\|Q0SQ68\|PRSA_CLOPS | 2492 | Cytoplasmic Membrane | Foldase protein PrsA |
| tr\|Q0SQ55\|Q0SQ55_CLOPS | 2505 | Cytoplasmic Membrane | Nucleoside transporter, NupC family |
| tr\|Q0SPX4\|Q0SPX4_CLOPS | 2586 | Cytoplasmic Membrane | Xanthine/uracil permease family protein |
| tr\|Q0SPW7\|Q0SPW7_CLOPS | 2593 | Cytoplasmic Membrane | Putative phage infection protein |
| tr\|Q0SPW6\|Q0SPW6_CLOPS | 2594 | Cytoplasmic Membrane | Putative phage infection protein |
| tr\|Q0SPQ1\|Q0SPQ1_CLOPS | 2671 | Cytoplasmic Membrane | Membrane protein OxaA |

| | | | |
|---|---|---|---|
| tr\|Q0STI4\|Q0STI4_CLOPS | 1251 | extracellular | Superoxide dismutase, SodF |
| tr\|Q0STC4\|Q0STC4_CLOPS | 1311 | extracellular | Glycosyl hydrolase, family 25 |
| tr\|Q0SWT8\|Q0SWT8_CLOPS | 0030 | unknown | DegV family protein |
| sp\|Q0SWN5\|CINA_CLOPS | 0128 | unknown | Putative competence-damage inducible protein, CinA |
| tr\|Q0SWH6\|Q0SWH6_CLOPS | 0188 | unknown | 5'-nucleotidase, lipoprotein e(P4) family |
| tr\|Q0SW97\|Q0SW97_CLOPS | 0273 | unknown | UDP-glucose 4-epimerase, GalE_1 |
| tr\|Q0SW33\|Q0SW33_CLOPS | 0338 | unknown | Putative lioprotein |
| tr\|Q0SVR9\|Q0SVR9_CLOPS | 0452 | unknown | Capsule chain length determinant protein |
| tr\|Q0SVM0\|Q0SVM0_CLOPS | 0502 | unknown | Putative lipoprotein |
| tr\|Q0SUS5\|Q0SUS5_CLOPS | 0807 | unknown | Uncharacterized protein |
| tr\|Q0SU80\|Q0SU80_CLOPS | 1004 | unknown | Glycerol dehydratase, large subunit, DhaB |
| tr\|Q0STY5\|Q0STY5_CLOPS | 1100 | unknown | Putative lipoprotein |
| tr\|Q0STM6\|Q0STM6_CLOPS | 1209 | unknown | VanW-related protein |
| tr\|Q0STC9\|Q0STC9_CLOPS | 1306 | unknown | Lipoprotein, BMP family |
| tr\|Q0STC5\|Q0STC5_CLOPS | 1310 | unknown | VanW-like family protein |
| tr\|Q0STB8\|Q0STB8_CLOPS | 1319 | unknown | 1-acyl-sn-glycerol-3-phosphate acyltransferase family protein |
| tr\|Q0ST96\|Q0ST96_CLOPS | 1341 | unknown | Putative galactoside ABC transporter, galactoside-binding protein |
| tr\|Q0ST88\|Q0ST88_CLOPS | 1349 | unknown | Uncharacterized protein |
| tr\|Q0ST82\|Q0ST82_CLOPS | 1355 | unknown | Uncharacterized protein |
| tr\|Q0SSX2\|Q0SSX2_CLOPS | 1466 | unknown | Uncharacterized protein |
| tr\|Q0SST6\|Q0SST6_CLOPS | 1502 | unknown | Uncharacterized protein |
| tr\|Q0SSN8\|Q0SSN8_CLOPS | 1552 | unknown | Lipoprotein, BMP family |
| tr\|Q0SSE2\|Q0SSE2_CLOPS | 1650 | unknown | Aspartokinase |
| tr\|Q0SS80\|Q0SS80_CLOPS | 1712 | unknown | Ribosomal RNA small subunit methyltransferase B, Sun |
| tr\|Q0SS20\|Q0SS20_CLOPS | 1772 | unknown | Uncharacterized protein |

| | | | |
|---|---|---|---|
| tr\|Q0SRV7\|Q0SRV7_CLOPS | 1836 | unknown | Delta-lactam-biosynthetic de-N-acetylase, PdaA |
| tr\|Q0SRI6\|Q0SRI6_CLOPS | 1962 | unknown | DNA polymerase, PolA |
| tr\|Q0SRG6\|Q0SRG6_CLOPS | 1982 | unknown | Uncharacterized protein |
| tr\|Q0SRC3\|Q0SRC3_CLOPS | 2025 | unknown | Uncharacterized protein |
| tr\|Q0SRB6\|Q0SRB6_CLOPS | 2032 | unknown | Pyruvate-flavodoxin oxidoreductase, NifJ |
| tr\|Q0SR94\|Q0SR94_CLOPS | 2054 | unknown | Molybdate ABC transporter, molybdate-binding protein, ModA |
| tr\|Q0SR41\|Q0SR41_CLOPS | 2107 | unknown | Putative penicillin-binding protein |
| tr\|Q0SQV7\|Q0SQV7_CLOPS | 2200 | unknown | Serine protease |
| tr\|Q0SQR1\|Q0SQR1_CLOPS | 2270 | unknown | Prepilin-type N-terminal cleavage/methylation domain protein |
| tr\|Q0SQP7\|Q0SQP7_CLOPS | 2285 | unknown | Electron transfer flavoprotein, beta subunit/FixA family protein |
| tr\|Q0SQK4\|Q0SQK4_CLOPS | 2338 | unknown | Putative maltose/maltodextrin ABC transporter, maltose/maltodextrin-binding protein |
| tr\|Q0SQJ7\|Q0SQJ7_CLOPS | 2345 | unknown | Uncharacterized protein |
| sp\|Q0SQG3\|RL15_CLOPS | 2380 | unknown | 50S ribosomal protein L15, RplO |
| sp\|Q0SQE7\|RL2_CLOPS | 2396 | unknown | 50S ribosomal protein L2, RplB |
| sp\|Q0SQE5\|RL4_CLOPS | 2398 | unknown | 50S ribosomal protein L4, RplD |
| sp\|Q0SQ58\|MURC_CLOPS | 2502 | unknown | UDP-N-acetylmuramate--L-alanine ligase, MurC |
| tr\|Q0SQ56\|Q0SQ56_CLOPS | 2504 | unknown | Purine nucleoside phosphorylase, PunA |
| tr\|Q0SQ30\|Q0SQ30_CLOPS | 2530 | unknown | Uncharacterized protein |
| tr\|Q0SPZ4\|Q0SPZ4_CLOPS | 2566 | unknown | Spore cortex-lytic enzyme SleC |
| tr\|Q0SPY2\|Q0SPY2_CLOPS | 2578 | unknown | Conserved domain protein |
| tr\|Q0SPX1\|Q0SPX1_CLOPS | 2589 | unknown | Conserved domain protein |

a: PSORTb 3.0 was used for protein localization analysis.

**Table S4.2. Total proteins detected in germinated spore inner membrane samples**

| UniProt ID | gene name (CPR_) | protein localization[a] | protein function |
|---|---|---|---|
| tr\|Q0SQS3\|Q0SQS3_CLOPS | 2258 | cell wall | Oligopeptide/dipeptide ABC transporter, oligopeptide/dipeptide-binding protein |
| tr\|Q0SWX7\|Q0SWX7_CLOPS | 0002 | Cytoplasmic | DNA polymerase III subunit beta, DnaN |
| sp\|Q0SWW9\|SYS_CLOPS | 0014 | Cytoplasmic | Serine--tRNA ligase, SerS |
| tr\|Q0SWX5\|Q0SWX5_CLOPS | 0015 | Cytoplasmic | Uncharacterized protein |
| tr\|Q0SWZ0\|Q0SWZ0_CLOPS | 0082 | Cytoplasmic | Glycogen synthase, GlgA |
| tr\|Q0SWY9\|Q0SWY9_CLOPS | 0083 | Cytoplasmic | Phosphorylase |
| sp\|Q0SWS5\|GLGC_CLOPS | 0086 | Cytoplasmic | Glucose-1-phosphate adenylyltransferase, GlgC |
| tr\|Q0SWS4\|Q0SWS4_CLOPS | 0087 | Cytoplasmic | Glucose-1-phosphate adenylyltransferase, GlgD |
| tr\|Q0SWS0\|Q0SWS0_CLOPS | 0092 | Cytoplasmic | Putative PTS system, N-acetylglucosamine-specific IIA component |
| tr\|Q0SWR5\|Q0SWR5_CLOPS | 0098 | Cytoplasmic | Putative glucokinase |
| tr\|Q0SWR4\|Q0SWR4_CLOPS | 0099 | Cytoplasmic | Rubredoxin/rubrerythrin |
| tr\|Q0SWN1\|Q0SWN1_CLOPS | 0132 | Cytoplasmic | Rubrerythrin, Rbr_1 |
| sp\|Q0SWK5\|OTC_CLOPS | 0158 | Cytoplasmic | Ornithine carbamoyltransferase, ArcB |
| tr\|Q0SWJ0\|Q0SWJ0_CLOPS | 0173 | Cytoplasmic | Nitroreductase family protein |
| tr\|Q0SWG2\|Q0SWG2_CLOPS | 0203 | Cytoplasmic | Heme oxygenase |
| tr\|Q0SWB7\|Q0SWB7_CLOPS | 0251 | Cytoplasmic | AhpC/TSA family protein |
| tr\|Q0SWB3\|Q0SWB3_CLOPS | 0256 | Cytoplasmic | Glycosyl transferase, group 1 family protein |
| tr\|Q0SWA8\|Q0SWA8_CLOPS | 0261 | Cytoplasmic | [Fe] hydrogenase |
| tr\|Q0SW95\|Q0SW95_CLOPS | 0275 | Cytoplasmic | Metallo-beta-lactamase family/flavodoxin |
| tr\|Q0SW87\|Q0SW87_CLOPS | 0284 | Cytoplasmic | Uncharacterized protein |
| tr\|Q0SW84\|Q0SW84_CLOPS | 0287 | Cytoplasmic | Putative transketolase, N-terminal subunit |

| | | | |
|---|---|---|---|
| tr\|Q0SW83\|Q0SW83_CLOPS | 0288 | Cytoplasmic | Putative transketolase, C-terminal subunit |
| tr\|Q0SW42\|Q0SW42_CLOPS | 0329 | Cytoplasmic | UvrABC system protein A, UvrA |
| tr\|Q0SW30\|Q0SW30_CLOPS | 0341 | Cytoplasmic | 6-phosphofructokinase, PfkA |
| tr\|Q0SW29\|Q0SW29_CLOPS | 0342 | Cytoplasmic | Pyruvate kinase, Pyk_1 |
| sp\|Q0SW00\|DEOB_CLOPS | 0371 | Cytoplasmic | Phosphopentomutase, DeoB |
| tr\|Q0SVV7\|Q0SVV7_CLOPS | 0414 | Cytoplasmic | Uncharacterized protein |
| tr\|Q0SVT9\|Q0SVT9_CLOPS | 0432 | Cytoplasmic | Uncharacterized protein |
| tr\|Q0SVQ3\|Q0SVQ3_CLOPS | 0468 | Cytoplasmic | UDP-glucose 4-epimerase, GalE_2 |
| tr\|Q0SVL0\|Q0SVL0_CLOPS | 0512 | Cytoplasmic | Nitrite/sulfite reductase homolog |
| tr\|Q0SVK3\|Q0SVK3_CLOPS | 0519 | Cytoplasmic | FMN-dependent NADH-azoreductase, AzoR |
| tr\|Q0SVH4\|Q0SVH4_CLOPS | 0548 | Cytoplasmic | Uncharacterized protein |
| tr\|Q0SVE6\|Q0SVE6_CLOPS | 0577 | Cytoplasmic | M18 family aminopeptidase |
| tr\|Q0SVA5\|Q0SVA5_CLOPS | 0618 | Cytoplasmic | Uncharacterized protein |
| sp\|Q0SVA4\|SYY_CLOPS | 0619 | Cytoplasmic | Tyrosine--tRNA ligase, TyrS |
| tr\|Q0SV42\|Q0SV42_CLOPS | 0682 | Cytoplasmic | Rubredoxin/rubrerythrin |
| sp\|Q0SV41\|TAL_CLOPS | 0683 | Cytoplasmic | Probable transaldolase, Tal |
| tr\|Q0SUZ0\|Q0SUZ0_CLOPS | 0734 | Cytoplasmic | Uncharacterized protein |
| sp\|Q0SUV5\|AZOR_CLOPS | 0777 | Cytoplasmic | FMN-dependent NADH-azoreductase, AzoR |
| tr\|Q0SUS8\|Q0SUS8_CLOPS | 0804 | Cytoplasmic | PTS system, mannose/fructose/sorbose family, IIAB component |
| tr\|Q0SUP2\|Q0SUP2_CLOPS | 0840 | Cytoplasmic | Rubrerythrin, Rbr_2 |
| tr\|Q0SUP0\|Q0SUP0_CLOPS | 0842 | Cytoplasmic | Nadh-dependent butanol dehydrogenase a |
| tr\|Q0SUM4\|Q0SUM4_CLOPS | 0858 | Cytoplasmic | Acetyltransferase, GNAT family |
| tr\|Q0SUH5\|Q0SUH5_CLOPS | 0908 | Cytoplasmic | Sucrose-6-phosphate hydrolase |
| tr\|Q0SUE9\|Q0SUE9_CLOPS | 0934 | Cytoplasmic | Spore coat peptide assembly protein CotJC |
| tr\|Q0SUB0\|Q0SUB0_CLOPS | 0974 | Cytoplasmic | Hydroxylamine reductase, Hcp |

| | | | |
|---|---|---|---|
| tr\|Q0SU99\|Q0SU99_CLOPS | 0985 | Cytoplasmic | Uncharacterized protein |
| tr\|Q0SU73\|Q0SU73_CLOPS | 1011 | Cytoplasmic | 1,3-propanediol dehydrogenase, DhaT |
| tr\|Q0SU58\|Q0SU58_CLOPS | 1026 | Cytoplasmic | Glutathione peroxidase |
| tr\|Q0SU57\|Q0SU57_CLOPS | 1027 | Cytoplasmic | Collagen triple helix repeat protein |
| tr\|Q0SU38\|Q0SU38_CLOPS | 1047 | Cytoplasmic | Ferritin family protein |
| tr\|Q0SU24\|Q0SU24_CLOPS | 1061 | cytoplasmic | Oxidoreductase, 2-nitropropane dioxygenase family |
| sp\|Q0SU11\|HPRK_CLOPS | 1074 | Cytoplasmic | HPr kinase/phosphorylase, HprK |
| tr\|Q0SU06\|Q0SU06_CLOPS | 1079 | Cytoplasmic | Uncharacterized protein |
| tr\|Q0SU05\|Q0SU05_CLOPS | 1080 | Cytoplasmic | Uncharacterized protein |
| tr\|Q0STY1\|Q0STY1_CLOPS | 1104 | Cytoplasmic | Uncharacterized protein |
| tr\|Q0STV6\|Q0STV6_CLOPS | 1129 | Cytoplasmic | Tetratricopeptide repeat protein |
| tr\|Q0STV5\|Q0STV5_CLOPS | 1130 | Cytoplasmic | Glutamine-dependent NAD(+) synthetase, NadE |
| tr\|Q0STV3\|Q0STV3_CLOPS | 1132 | Cytoplasmic | SPFH domain protein/band 7 family protein |
| sp\|Q0STU9\|FABH_CLOPS | 1136 | Cytoplasmic | 3-oxoacyl-[acyl-carrier-protein] synthase 3, FabH |
| tr\|Q0STU8\|Q0STU8_CLOPS | 1137 | Cytoplasmic | Malonyl CoA-acyl carrier protein transacylase, FabD |
| tr\|Q0STU7\|Q0STU7_CLOPS | 1138 | Cytoplasmic | 3-oxoacyl-[acyl-carrier-protein] reductase, FabG |
| sp\|Q0STU4\|FABZ_CLOPS | 1141 | Cytoplasmic | 3-hydroxyacyl-[acyl-carrier-protein] dehydratase FabZ |
| tr\|Q0STU3\|Q0STU3_CLOPS | 1142 | Cytoplasmic | Acetyl-CoA carboxylase, biotin carboxylase subunit, AccC |
| tr\|Q0STR6\|Q0STR6_CLOPS | 1169 | Cytoplasmic | Formate acetyltransferase, Pfl |
| tr\|Q0STQ4\|Q0STQ4_CLOPS | 1181 | Cytoplasmic | Threonine dehydratase, catabolic, TdcB |
| tr\|Q0STN2\|Q0STN2_CLOPS | 1203 | Cytoplasmic | 6-phosphofructokinase, PfkA |
| tr\|Q0STM9\|Q0STM9_CLOPS | 1206 | Cytoplasmic | UDP-N-acetylmuramyl tripeptide synthetase MurC homolog |
| tr\|Q0STM0\|Q0STM0_CLOPS | 1215 | Cytoplasmic | Putative CoA-substrate-specific enzyme activase |
| tr\|Q0STL0\|Q0STL0_CLOPS | 1225 | Cytoplasmic | Amidohydrolase family protein |
| tr\|Q0STK4\|Q0STK4_CLOPS | 1231 | Cytoplasmic | Putative dipeptidase |

| | | | |
|---|---|---|---|
| tr\|Q0STI9\|Q0STI9_CLOPS | 1246 | Cytoplasmic | Uncharacterized protein |
| tr\|Q0STI8\|Q0STI8_CLOPS | 1247 | Cytoplasmic | Uncharacterized protein |
| tr\|Q0STH0\|Q0STH0_CLOPS | 1265 | Cytoplasmic | NADPH-dependent butanol dehydrogenase, Adh1 |
| tr\|Q0STE7\|Q0STE7_CLOPS | 1288 | Cytoplasmic | Tetratricopeptide repeat protein |
| tr\|Q0STE3\|Q0STE3_CLOPS | 1292 | cytoplasmic | Ribonuclease R, Rnr |
| sp\|Q0STE0\|ENO_CLOPS | 1295 | Cytoplasmic | Enolase, Eno |
| sp\|Q0STD7\|GPMI_CLOPS | 1298 | Cytoplasmic | 2,3-bisphosphoglycerate-independent phosphoglycerate mutase, GpmI |
| sp\|Q0STD6\|TPIS_CLOPS | 1299 | Cytoplasmic | Triosephosphate isomerase, TpiA |
| sp\|Q0STD5\|PGK_CLOPS | 1300 | Cytoplasmic | Phosphoglycerate kinase, Pgk |
| tr\|Q0STD4\|Q0STD4_CLOPS | 1301 | Cytoplasmic | Glyceraldehyde-3-phosphate dehydrogenase, type I, Gap |
| tr\|Q0STC8\|Q0STC8_CLOPS | 1307 | Cytoplasmic | DegV family protein |
| tr\|Q0STB6\|Q0STB6_CLOPS | 1321 | Cytoplasmic | Serine acetyltransferase, CysE |
| tr\|Q0STA9\|Q0STA9_CLOPS | 1328 | Cytoplasmic | Diacylglycerol kinase catalytic domain protein |
| tr\|Q0STA6\|Q0STA6_CLOPS | 1331 | Cytoplasmic | Rubrerythrin |
| sp\|Q0STA4\|Y1333_CLOPS | 1333 | Cytoplasmic | UPF0229 protein |
| tr\|Q0STA3\|Q0STA3_CLOPS | 1334 | Cytoplasmic | Non-specific serine/threonine protein kinase, PrkA |
| sp\|Q0ST92\|GAL1_CLOPS | 1345 | Cytoplasmic | Galactokinase, GalK |
| tr\|Q0ST87\|Q0ST87_CLOPS | 1350 | Cytoplasmic | Fructose-1,6-bisphosphate aldolase, class II, Fba |
| sp\|Q0ST54\|CLPX_CLOPS | 1384 | Cytoplasmic | ATP-dependent Clp protease ATP-binding subunit ClpX |
| sp\|Q0ST53\|CLPP_CLOPS | 1385 | Cytoplasmic | ATP-dependent Clp protease proteolytic subunit, ClpP |
| sp\|Q0ST52\|TIG_CLOPS | 1386 | Cytoplasmic | Trigger factor, Tig |
| sp\|Q0ST47\|DEOD_CLOPS | 1391 | cytoplasmic | Purine nucleoside phosphorylase DeoD-type, DeoD |
| tr\|Q0ST22\|Q0ST22_CLOPS | 1416 | cytoplasmic | ClpB protein |
| tr\|Q0SSZ0\|Q0SSZ0_CLOPS | 1448 | Cytoplasmic | Aminotransferase, class V |
| tr\|Q0SSS9\|Q0SSS9_CLOPS | 1510 | Cytoplasmic | Fructokinase |

| | | | |
|---|---|---|---|
| tr\|Q0SSR9\|Q0SSR9_CLOPS | 1520 | Cytoplasmic | Uncharacterized protein |
| tr\|Q0SSQ1\|Q0SSQ1_CLOPS | 1539 | Cytoplasmic | Peptidyl-prolyl cis-trans isomerase, cyclophilin-type |
| tr\|Q0SSM8\|Q0SSM8_CLOPS | 1563 | Cytoplasmic | Uncharacterized protein |
| tr\|Q0SSI4\|Q0SSI4_CLOPS | 1607 | Cytoplasmic | V-type ATP synthase subunit D, AtpD |
| sp\|Q0SSI3\|VATB_CLOPS | 1608 | Cytoplasmic | V-type ATP synthase beta chain, AtpB |
| sp\|Q0SSI2\|VATA_CLOPS | 1609 | Cytoplasmic | V-type ATP synthase alpha chain, AtpA |
| sp\|Q0SSH9\|VATE_CLOPS | 1612 | Cytoplasmic | V-type ATP synthase subunit E, AtpE |
| tr\|Q0SSG4\|Q0SSG4_CLOPS | 1627 | Cytoplasmic | Conserved domain protein |
| tr\|Q0SSF9\|Q0SSF9_CLOPS | 1633 | Cytoplasmic | Arginine--tRNA ligase, ArgS |
| tr\|Q0SSF5\|Q0SSF5_CLOPS | 1637 | Cytoplasmic | PhoH family protein |
| tr\|Q0SSF4\|Q0SSF4_CLOPS | 1638 | Cytoplasmic | Putative DNA polymerase III, epsilon subunit |
| tr\|Q0SSF1\|Q0SSF1_CLOPS | 1641 | Cytoplasmic | Phosphocarrier, HPr family |
| tr\|Q0SSF0\|Q0SSF0_CLOPS | 1642 | Cytoplasmic | Aspartate aminotransferase, AspB |
| sp\|Q0SSE8\|RNY_CLOPS | 1644 | Cytoplasmic | Ribonuclease Y, Rny |
| sp\|Q0SSE7\|RECA_CLOPS | 1645 | Cytoplasmic | Protein RecA |
| sp\|Q0SSE5\|RIMO_CLOPS | 1647 | Cytoplasmic | Ribosomal protein S12 methylthiotransferase RimO |
| tr\|Q0SSE3\|Q0SSE3_CLOPS | 1649 | Cytoplasmic | Putative endopeptidase, ClpP |
| sp\|Q0SSE0\|PNP_CLOPS | 1652 | Cytoplasmic | Polyribonucleotide nucleotidyltransferase, Pnp |
| sp\|Q0SSD9\|RS15_CLOPS | 1653 | Cytoplasmic | 30S ribosomal protein S15, RpsO |
| tr\|Q0SSD1\|Q0SSD1_CLOPS | 1661 | Cytoplasmic | N utilization substance protein A, NusA |
| tr\|Q0SSC8\|Q0SSC8_CLOPS | 1664 | Cytoplasmic | 4-hydroxy-3-methylbut-2-en-1-yl diphosphate synthase, IspG |
| sp\|Q0SSC2\|PYRH_CLOPS | 1670 | cytoplasmic | Uridylate kinase, PyrH |
| sp\|Q0SSC1\|EFTS_CLOPS | 1671 | Cytoplasmic | Elongation factor Ts, Tsf |
| sp\|Q0SSC0\|RS2_CLOPS | 1672 | Cytoplasmic | 30S ribosomal protein S2, RpsB |
| tr\|Q0SSB2\|Q0SSB2_CLOPS | 1680 | Cytoplasmic | 50S ribosomal protein L19, RplS |

| | | | |
|---|---|---|---|
| sp\|Q0SSA8\|RS16_CLOPS | 1684 | Cytoplasmic | 30S ribosomal protein S16, RpsP |
| tr\|Q0SS97\|Q0SS97_CLOPS | 1695 | Cytoplasmic | Acetate kinase, AckA_2 |
| tr\|Q0SS89\|Q0SS89_CLOPS | 1703 | Cytoplasmic | DAK2 domain protein |
| sp\|Q0SS87\|RL28_CLOPS | 1705 | Cytoplasmic | 50S ribosomal protein L28, RpmB |
| tr\|Q0SS75\|Q0SS75_CLOPS | 1717 | Cytoplasmic | Phosphopantothenoylcysteine decarboxylase/phosphopantothenate--cysteine ligase, CoaBC |
| tr\|Q0SS68\|Q0SS68_CLOPS | 1724 | Cytoplasmic | Stage IV sporulation protein A, SpoIVA |
| tr\|Q0SS60\|Q0SS60_CLOPS | 1732 | Cytoplasmic | RNA polymerase sigma factor, SigG |
| tr\|Q0SS51\|Q0SS51_CLOPS | 1741 | Cytoplasmic | Peptidase, U32 family |
| tr\|Q0SS47\|Q0SS47_CLOPS | 1745 | Cytoplasmic | RNA-metabolizing metallo-beta-lactamase family protein |
| tr\|Q0SS37\|Q0SS37_CLOPS | 1755 | Cytoplasmic | Cysteine desulfurase, IscS |
| sp\|Q0SRY9\|EFP_CLOPS | 1803 | Cytoplasmic | Elongation factor P, Efp |
| tr\|Q0SRV8\|Q0SRV8_CLOPS | 1835 | Cytoplasmic | GTP-binding protein YchF |
| tr\|Q0SRV2\|Q0SRV2_CLOPS | 1841 | Cytoplasmic | Phosphoglucomutase/phosphomannomutase family protein |
| sp\|Q0SRT7\|RL20_CLOPS | 1856 | Cytoplasmic | 50S ribosomal protein L20, RplT |
| sp\|Q0SRT6\|RL35_CLOPS | 1857 | Cytoplasmic | 50S ribosomal protein L35, RpmI |
| tr\|Q0SRS6\|Q0SRS6_CLOPS | 1871 | cytoplasmic | Aspartate-semialdehyde dehydrogenase, Asd |
| tr\|Q0SRS2\|Q0SRS2_CLOPS | 1875 | cytoplasmic | Putative cob(I)alamin adenosyltransferase |
| sp\|Q0SRS1\|DAPH_CLOPS | 1876 | Cytoplasmic | 2,3,4,5-tetrahydropyridine-2,6-dicarboxylate N-acetyltransferase, DapH |
| sp\|Q0SRP8\|SYD_CLOPS | 1899 | cytoplasmic | Aspartate--tRNA ligase, AspS |
| tr\|Q0SRM0\|Q0SRM0_CLOPS | 1927 | Cytoplasmic | GTPase HflX |
| tr\|Q0SRI8\|Q0SRI8_CLOPS | 1960 | Cytoplasmic | Transglycosylase, SLT family |
| tr\|Q0SRI3\|Q0SRI3_CLOPS | 1965 | Cytoplasmic | Aminopeptidase |
| tr\|Q0SRH3\|Q0SRH3_CLOPS | 1975 | Cytoplasmic | RNA polymerase sigma factor, RpoD |
| tr\|Q0SRG5\|Q0SRG5_CLOPS | 1983 | Cytoplasmic | Pyruvate, phosphate dikinase, PpdK |
| sp\|Q0SRF3\|RS21_CLOPS | 1995 | Cytoplasmic | 30S ribosomal protein S21, RpsU |

| | | | |
|---|---|---|---|
| tr\|Q0SRE4\|Q0SRE4_CLOPS | 2004 | Cytoplasmic | Chaperone protein DnaJ |
| sp\|Q0SRE3\|DNAK_CLOPS | 2005 | Cytoplasmic | Chaperone protein DnaK |
| sp\|Q0SRD5\|GPR_CLOPS | 2013 | Cytoplasmic | Germination protease, Gpr |
| tr\|Q0SRD0\|Q0SRD0_CLOPS | 2018 | Cytoplasmic | Stage V sporulation protein AD, SpoVAD |
| sp\|Q0SRC7\|SP2AB_CLOPS | 2021 | Cytoplasmic | Anti-sigma F factor, SpoIIAB |
| tr\|Q0SRC6\|Q0SRC6_CLOPS | 2022 | Cytoplasmic | Anti-sigma F factor antagonist, SpoIIAA |
| sp\|Q0SRC4\|DEOC_CLOPS | 2024 | Cytoplasmic | Deoxyribose-phosphate aldolase, DeoC |
| tr\|Q0SRC1\|Q0SRC1_CLOPS | 2027 | Cytoplasmic | Putative manganese-dependent inorganic pyrophosphatase |
| tr\|Q0SRB9\|Q0SRB9_CLOPS | 2029 | Cytoplasmic | Glutamate decarboxylase |
| tr\|Q0SR89\|Q0SR89_CLOPS | 2059 | cytoplasmic | FemAB family protein |
| tr\|Q0SR77\|Q0SR77_CLOPS | 2071 | Cytoplasmic | CspA family protein |
| sp\|Q0SR54\|OBG_CLOPS | 2094 | Cytoplasmic | GTPase obg |
| sp\|Q0SR51\|RL21_CLOPS | 2097 | Cytoplasmic | 50S ribosomal protein L21, RplU |
| tr\|Q0SR48\|Q0SR48_CLOPS | 2100 | Cytoplasmic | Radical SAM domain protein |
| tr\|Q0SR38\|Q0SR38_CLOPS | 2110 | Cytoplasmic | Rod shape-determining protein MreB |
| tr\|Q0SR33\|Q0SR33_CLOPS | 2115 | Cytoplasmic | Aminoacyl-histidine dipeptidase, PepD_1 |
| tr\|Q0SR32\|Q0SR32_CLOPS | 2116 | Cytoplasmic | Pyruvate kinase, Pyk |
| tr\|Q0SR19\|Q0SR19_CLOPS | 2131 | Cytoplasmic | CBS domain protein |
| sp\|Q0SR11\|SECA_CLOPS | 2139 | Cytoplasmic | Protein translocase subunit SecA |
| sp\|Q0SR05\|METK_CLOPS | 2145 | Cytoplasmic | S-adenosylmethionine synthase, MetK |
| sp\|Q0SQZ4\|ATPG_CLOPS | 2163 | Cytoplasmic | ATP synthase gamma chain, AtpG |
| sp\|Q0SQZ3\|ATPA_CLOPS | 2164 | Cytoplasmic | ATP synthase subunit alpha, AtpA |
| tr\|Q0SQY7\|Q0SQY7_CLOPS | 2170 | Cytoplasmic | Acetyl-CoA acetyltransferase |
| tr\|Q0SQY6\|Q0SQY6_CLOPS | 2171 | Cytoplasmic | UDP-N-acetylglucosamine 2-epimerase, MnaA |
| sp\|Q0SQY5\|UPP_CLOPS | 2172 | Cytoplasmic | Uracil phosphoribosyltransferase, Upp |

| | | | |
|---|---|---|---|
| sp\|Q0SQX5\|PYRG_CLOPS | 2182 | Cytoplasmic | CTP synthase, PyrG |
| tr\|Q0SQW8\|Q0SQW8_CLOPS | 2189 | cytoplasmic | LysM domain protein |
| sp\|Q0SQS9\|G6PI_CLOPS | 2252 | cytoplasmic | Glucose-6-phosphate isomerase, Pgi |
| tr\|C6UAS4\|C6UAS4_CLOPS | 2275 | Cytoplasmic | 60 kDa chaperonin, GroEL |
| tr\|Q0SQP9\|Q0SQP9_CLOPS | 2283 | Cytoplasmic | 3-hydroxybutyryl-CoA dehydrogenase, Hbd |
| tr\|Q0SQP8\|Q0SQP8_CLOPS | 2284 | Cytoplasmic | Electron transfer flavoprotein, alpha subunit/FixB family protein, FixB |
| tr\|Q0SQP6\|Q0SQP6_CLOPS | 2286 | Cytoplasmic | Butyryl-CoA dehydrogenase, Bcd |
| tr\|Q0SQP5\|Q0SQP5_CLOPS | 2287 | Cytoplasmic | 3-hydroxybutyryl-CoA dehydratase, Crt |
| sp\|Q0SQP4\|REX_CLOPS | 2288 | Cytoplasmic | Redox-sensing transcriptional repressor rex |
| tr\|Q0SQN8\|Q0SQN8_CLOPS | 2294 | Cytoplasmic | Mannose-1-phosphate guanylyltransferase |
| sp\|Q0SQM4\|SYT_CLOPS | 2317 | Cytoplasmic | Threonine--tRNA ligase, ThrS |
| tr\|Q0SQL9\|Q0SQL9_CLOPS | 2322 | Cytoplasmic | Glutamine--fructose-6-phosphate aminotransferase [isomerizing], GlmS |
| tr\|Q0SQL8\|Q0SQL8_CLOPS | 2323 | Cytoplasmic | Rubrerythrin family protein |
| sp\|Q0SQL7\|GLMM_CLOPS | 2324 | Cytoplasmic | Phosphoglucosamine mutase, GlmM |
| sp\|Q0SQK0\|BUK_CLOPS | 2342 | cytoplasmic | Probable butyrate kinase buk |
| tr\|Q0SQJ9\|Q0SQJ9_CLOPS | 2343 | cytoplasmic | Phosphate butyryltransferase ptb |
| tr\|Q0SQJ1\|Q0SQJ1_CLOPS | 2351 | cytoplasmic | Isoaspartyl dipeptidase, IadA |
| tr\|Q0SQJ0\|Q0SQJ0_CLOPS | 2352 | Cytoplasmic | Phosphoenolpyruvate-protein phosphotransferase, PtsI |
| sp\|Q0SQI8\|RS4B_CLOPS | 2354 | Cytoplasmic | 30S ribosomal protein S4 B, RpsD2 |
| sp\|Q0SQH9\|RS9_CLOPS | 2363 | Cytoplasmic | 30S ribosomal protein S9, RpsI |
| sp\|Q0SQH8\|RL13_CLOPS | 2364 | Cytoplasmic | 50S ribosomal protein L13, RplM |
| sp\|Q0SQH4\|RL17_CLOPS | 2369 | Cytoplasmic | 50S ribosomal protein L17, RplQ |
| sp\|Q0SQH3\|RPOA_CLOPS | 2370 | Cytoplasmic | DNA-directed RNA polymerase subunit alpha, RpoA |
| sp\|Q0SQH2\|RS4A_CLOPS | 2371 | Cytoplasmic | 30S ribosomal protein S4 AR, psD1 |
| sp\|Q0SQH1\|RS11_CLOPS | 2372 | Cytoplasmic | 30S ribosomal protein S11, RpsK |

| | | | |
|---|---|---|---|
| sp\|Q0SQH0\|RS13_CLOPS | 2373 | Cytoplasmic | 30S ribosomal protein S13, RpsM |
| sp\|Q0SQG1\|RS5_CLOPS | 2382 | Cytoplasmic | 30S ribosomal protein S5, RpsE |
| sp\|Q0SQG0\|RL18_CLOPS | 2383 | Cytoplasmic | 50S ribosomal protein L18, RplR |
| sp\|Q0SQF9\|RL6_CLOPS | 2384 | Cytoplasmic | 50S ribosomal protein L6, RplF |
| sp\|Q0SQF8\|RS8_CLOPS | 2385 | Cytoplasmic | 30S ribosomal protein S8, RpsH |
| sp\|Q0SQF6\|RL5_CLOPS | 2387 | Cytoplasmic | 50S ribosomal protein L5, RplE |
| sp\|Q0SQF4\|RL14_CLOPS | 2389 | Cytoplasmic | 50S ribosomal protein L14, RplN |
| sp\|Q0SQF3\|RS17_CLOPS | 2390 | Cytoplasmic | 30S ribosomal protein S17, RpsQ |
| sp\|Q0SQF1\|RL16_CLOPS | 2392 | Cytoplasmic | 50S ribosomal protein L16, RplP |
| sp\|Q0SQF0\|RS3_CLOPS | 2393 | Cytoplasmic | 30S ribosomal protein S3, RpsC |
| sp\|Q0SQE9\|RL22_CLOPS | 2394 | Cytoplasmic | 50S ribosomal protein L22, RplV |
| sp\|Q0SQE8\|RS19_CLOPS | 2395 | Cytoplasmic | 30S ribosomal protein S19, RpsS |
| sp\|Q0SQE6\|RL23_CLOPS | 2397 | Cytoplasmic | 50S ribosomal protein L23, RplW |
| sp\|Q0SQE4\|RL3_CLOPS | 2399 | cytoplasmic | 50S ribosomal protein L3, RplC |
| sp\|Q0SQE3\|RS10_CLOPS | 2400 | Cytoplasmic | 30S ribosomal protein S10, RpsJ |
| sp\|Q0SQC8\|EFTU_CLOPS | 2402 | cytoplasmic | Elongation factor Tu, Tuf1 |
| sp\|Q0SQE1\|EFG_CLOPS | 2403 | Cytoplasmic | Elongation factor G, FusA |
| sp\|Q0SQE0\|RS7_CLOPS | 2404 | Cytoplasmic | 30S ribosomal protein S7, RpsG |
| sp\|Q0SQD9\|RS12_CLOPS | 2405 | Cytoplasmic | 30S ribosomal protein S12, RpsL |
| sp\|Q0SQD7\|RPOC_CLOPS | 2407 | Cytoplasmic | DNA-directed RNA polymerase subunit beta, RpoC |
| sp\|Q0SQD6\|RPOB_CLOPS | 2408 | Cytoplasmic | DNA-directed RNA polymerase subunit beta, RpoB |
| sp\|Q0SQD5\|RL7_CLOPS | 2409 | Cytoplasmic | 50S ribosomal protein L7/L12, RplL |
| tr\|Q0SQD4\|Q0SQD4_CLOPS | 2410 | Cytoplasmic | 50S ribosomal protein L10, RplJ |
| sp\|Q0SQD3\|RL1_CLOPS | 2411 | Cytoplasmic | 50S ribosomal protein L1, RplA |
| sp\|Q0SQD2\|RL11_CLOPS | 2412 | Cytoplasmic | 50S ribosomal protein L11, RplK |

| | | | |
|---|---|---|---|
| tr\|Q0SQC4\|Q0SQC4_CLOPS | 2421 | Cytoplasmic | Thymidylate synthase ThyX |
| sp\|Q0SQC1\|SYC_CLOPS | 2424 | Cytoplasmic | Cysteine--tRNA ligase, CysS |
| sp\|Q0SQC0\|SYP_CLOPS | 2425 | Cytoplasmic | Proline--tRNA ligase, ProS |
| tr\|Q0SQB7\|Q0SQB7_CLOPS | 2428 | Cytoplasmic | Uncharacterized protein |
| tr\|Q0SQB1\|Q0SQB1_CLOPS | 2434 | Cytoplasmic | Glyceraldehyde-3-phosphate dehydrogenase, NADP-dependent, GapN |
| tr\|Q0SQ95\|Q0SQ95_CLOPS | 2450 | Cytoplasmic | Amidohydrolase homolog |
| tr\|Q0SQ87\|Q0SQ87_CLOPS | 2465 | Cytoplasmic | Glycine--tRNA ligase, GlyS |
| sp\|Q0SQ86\|SYK_CLOPS | 2467 | Cytoplasmic | Lysine--tRNA ligase, LysS |
| tr\|Q0SQ69\|Q0SQ69_CLOPS | 2491 | Cytoplasmic | Stage V sprulation protein T, SpoVT |
| tr\|Q0SQ62\|Q0SQ62_CLOPS | 2498 | Cytoplasmic | Ribose-phosphate pyrophosphokinase, PrsA |
| sp\|Q0SQ51\|SYN_CLOPS | 2509 | cytoplasmic | Asparagine--tRNA ligase, AsnS |
| sp\|Q0SQ50\|AMPA_CLOPS | 2510 | cytoplasmic | Probable cytosol aminopeptidase, PepA |
| tr\|Q0SQ35\|Q0SQ35_CLOPS | 2525 | Cytoplasmic | Uncharacterized protein |
| tr\|Q0SQ27\|Q0SQ27_CLOPS | 2533 | Cytoplasmic | Methionine--tRNA ligase, MetG_2 |
| tr\|Q0SQ20\|Q0SQ20_CLOPS | 2540 | Cytoplasmic | Aldehyde-alcohol dehydrogenase, AdhE |
| tr\|Q0SQ12\|Q0SQ12_CLOPS | 2548 | Cytoplasmic | Putative catabolite control protein A |
| sp\|Q0SQ01\|GLPK_CLOPS | 2559 | Cytoplasmic | Glycerol kinase, GlpK |
| tr\|Q0SPZ6\|Q0SPZ6_CLOPS | 2564 | Cytoplasmic | Putative lipoprotein |
| tr\|Q0SPZ0\|Q0SPZ0_CLOPS | 2570 | Cytoplasmic | Peptidyl-prolyl cis-trans isomerase |
| sp\|Q0SPX8\|PROA_CLOPS | 2582 | Cytoplasmic | Gamma-glutamyl phosphate reductase, ProA |
| tr\|Q0SPX6\|Q0SPX6_CLOPS | 2584 | Cytoplasmic | Oxidoreductase, short chain dehydrogenase/reductase family |
| tr\|Q0SPS1\|Q0SPS1_CLOPS | 2651 | Cytoplasmic | DHH family protein |
| sp\|Q0SPR8\|RS18_CLOPS | 2654 | Cytoplasmic | 30S ribosomal protein S18, RpsR |
| sp\|Q0SPP8\|RL34_CLOPS | 2674 | Cytoplasmic | 50S ribosomal protein L34, RpmH |
| sp\|Q0SWT6\|PSD_CLOPS | 0033 | Cytoplasmic Membrane | Phosphatidylserine decarboxylase proenzyme psd |

| | | | |
|---|---|---|---|
| tr\|Q0SWV4\|Q0SWV4_CLOPS | 0036 | Cytoplasmic Membrane | Putative transporter |
| tr\|Q0SWK4\|Q0SWK4_CLOPS | 0159 | Cytoplasmic Membrane | Arginine/ornithine antiporter, ArcD |
| tr\|Q0SWI7\|Q0SWI7_CLOPS | 0176 | Cytoplasmic Membrane | Sodium:solute transporter |
| tr\|Q0SWD6\|Q0SWD6_CLOPS | 0230 | Cytoplasmic Membrane | Uncharacterized protein |
| tr\|Q0SWC5\|Q0SWC5_CLOPS | 0241 | Cytoplasmic Membrane | Uncharacterized protein |
| tr\|Q0SWB6\|Q0SWB6_CLOPS | 0253 | Cytoplasmic Membrane | PPIC-type PPIASE domain protein |
| tr\|Q0SW99\|Q0SW99_CLOPS | 0271 | Cytoplasmic Membrane | Putative transcriptional regulator |
| tr\|Q0SW80\|Q0SW80_CLOPS | 0291 | Cytoplasmic Membrane | Putative cell division ATP-binding protein FtsE |
| tr\|Q0SW79\|Q0SW79_CLOPS | 0292 | Cytoplasmic Membrane | Cell division protein FtsX |
| tr\|Q0SW78\|Q0SW78_CLOPS | 0293 | Cytoplasmic Membrane | Carboxyl-terminal protease |
| tr\|Q0SW59\|Q0SW59_CLOPS | 0312 | Cytoplasmic Membrane | Uncharacterized protein |
| tr\|Q0SW39\|Q0SW39_CLOPS | 0332 | Cytoplasmic Membrane | Putative penicillin-binding protein |
| tr\|Q0SW08\|Q0SW08_CLOPS | 0363 | Cytoplasmic Membrane | ABC transporter, permease/ATP-binding protein |
| tr\|Q0SW07\|Q0SW07_CLOPS | 0364 | Cytoplasmic Membrane | ABC transporter, permease/ATP-binding protein |
| tr\|Q0SW05\|Q0SW05_CLOPS | 0366 | Cytoplasmic Membrane | Toxin secretion/phage lysis holin |
| tr\|Q0SVY4\|Q0SVY4_CLOPS | 0387 | Cytoplasmic Membrane | Uncharacterized protein |
| tr\|Q0SVX2\|Q0SVX2_CLOPS | 0399 | Cytoplasmic Membrane | PTS system, mannose/fructose/sorbose family, IID component |
| tr\|Q0SVU0\|Q0SVU0_CLOPS | 0431 | Cytoplasmic Membrane | Uncharacterized protein |
| tr\|Q0SVP6\|Q0SVP6_CLOPS | 0476 | Cytoplasmic Membrane | ABC transporter, substrate-binding protein |
| tr\|Q0SVP5\|Q0SVP5_CLOPS | 0477 | Cytoplasmic Membrane | ABC transporter, permease protein |
| tr\|Q0SVP4\|Q0SVP4_CLOPS | 0478 | Cytoplasmic Membrane | ABC transporter, permease protein |
| tr\|Q0SVJ4\|Q0SVJ4_CLOPS | 0528 | Cytoplasmic Membrane | Stage V sporulation protein D |
| tr\|Q0SVI2\|Q0SVI2_CLOPS | 0540 | Cytoplasmic Membrane | ABC transporter, substrate-binding protei |
| tr\|Q0SVF9\|Q0SVF9_CLOPS | 0564 | Cytoplasmic Membrane | Signal peptidase I |
| tr\|Q0SVF8\|Q0SVF8_CLOPS | 0565 | Cytoplasmic Membrane | ATP-dependent zinc metalloprotease FtsH |

| | | | |
|---|---|---|---|
| tr\|Q0SVC5\|Q0SVC5_CLOPS | 0598 | Cytoplasmic Membrane | Cell envelope-related transcriptional attenuator domain family |
| tr\|Q0SVC0\|Q0SVC0_CLOPS | 0603 | Cytoplasmic Membrane | Phosphate ABC transporter, phosphate-binding protein, PstS_1 |
| tr\|Q0SVA8\|Q0SVA8_CLOPS | 0615 | Cytoplasmic Membrane | Spore germination protein, GerABKA family |
| tr\|Q0SV26\|Q0SV26_CLOPS | 0698 | Cytoplasmic Membrane | ABC transporter, ATP-binding protein |
| tr\|Q0SUZ4\|Q0SUZ4_CLOPS | 0730 | Cytoplasmic Membrane | Uncharacterized protein |
| tr\|Q0SUS7\|Q0SUS7_CLOPS | 0805 | Cytoplasmic Membrane | PTS system, mannose/fructose/sorbose family, IIC component |
| tr\|Q0SUS6\|Q0SUS6_CLOPS | 0806 | Cytoplasmic Membrane | PTS system, mannose/fructose/sorbose family, IID component |
| tr\|Q0SUR3\|Q0SUR3_CLOPS | 0819 | Cytoplasmic Membrane | Antibiotic ABC transporter, permease protein |
| tr\|Q0SUM3\|Q0SUM3_CLOPS | 0859 | Cytoplasmic Membrane | Uncharacterized protein |
| tr\|Q0SUH9\|Q0SUH9_CLOPS | 0904 | Cytoplasmic Membrane | Substrate-binding protein MsmE |
| tr\|Q0SUH6\|Q0SUH6_CLOPS | 0907 | Cytoplasmic Membrane | Sugar ABC transporter, ATP-binding protein , MsmK |
| tr\|Q0SUE8\|Q0SUE8_CLOPS | 0935 | Cytoplasmic Membrane | PTS system, N-acetylglucosamine-specific IIBC component, NagE |
| tr\|Q0SUA1\|Q0SUA1_CLOPS | 0983 | Cytoplasmic Membrane | Cation efflux family protein |
| tr\|Q0SU83\|Q0SU83_CLOPS | 1001 | Cytoplasmic Membrane | Glycerol uptake facilitator protein, GlpE |
| tr\|Q0SU63\|Q0SU63_CLOPS | 1021 | Cytoplasmic Membrane | ABC transporter, ATP-binding protein |
| tr\|Q0SU50\|Q0SU50_CLOPS | 1034 | Cytoplasmic Membrane | Amino acid permease family protein |
| tr\|Q0SU32\|Q0SU32_CLOPS | 1053 | Cytoplasmic Membrane | GerA spore germination protein |
| tr\|Q0SU31\|Q0SU31_CLOPS | 1054 | Cytoplasmic Membrane | C4-dicarboxylate anaerobic carrier family protein |
| tr\|Q0STX0\|Q0STX0_CLOPS | 1115 | Cytoplasmic Membrane | Iron compound ABC transporter, iron-binding protein |
| tr\|Q0STU6\|Q0STU6_CLOPS | 1139 | Cytoplasmic Membrane | 3-oxoacyl-[acyl-carrier-protein] synthase 2, FabF |
| tr\|Q0STF9\|Q0STF9_CLOPS | 1276 | Cytoplasmic Membrane | Oligopeptide transporter, OPT family |
| tr\|Q0STA8\|Q0STA8_CLOPS | 1329 | Cytoplasmic Membrane | CDP-diacylglycerol--serine O-phosphatidyltransferase, PssA |
| tr\|Q0ST94\|Q0ST94_CLOPS | 1343 | Cytoplasmic Membrane | Galactoside ABC transporter, permease protein, MglC |
| tr\|Q0ST89\|Q0ST89_CLOPS | 1348 | Cytoplasmic Membrane | Uncharacterized protein |
| tr\|Q0SSS6\|Q0SSS6_CLOPS | 1513 | Cytoplasmic Membrane | PTS system, sucrose-specific IIBC component |

| | | | |
|---|---|---|---|
| tr\|Q0SSP8\|Q0SSP8_CLOPS | 1542 | Cytoplasmic Membrane | Phage shock protein A, PspA |
| tr\|Q0SSP0\|Q0SSP0_CLOPS | 1550 | Cytoplasmic Membrane | ABC transporter, permease protein |
| tr\|Q0SSJ7\|Q0SSJ7_CLOPS | 1594 | Cytoplasmic Membrane | Putative lipoprotein |
| tr\|Q0SSH8\|Q0SSH8_CLOPS | 1613 | Cytoplasmic Membrane | V-type ATPase, K subunit |
| tr\|Q0SSH7\|Q0SSH7_CLOPS | 1614 | Cytoplasmic Membrane | V-type ATPase, I subunit |
| tr\|Q0SSG1\|Q0SSG1_CLOPS | 1631 | Cytoplasmic Membrane | Ferrous iron transport protein B, FeoB_2 |
| tr\|Q0SSC7\|Q0SSC7_CLOPS | 1665 | Cytoplasmic Membrane | RIP metalloprotease RseP |
| tr\|Q0SSA5\|Q0SSA5_CLOPS | 1687 | Cytoplasmic Membrane | Signal recognition particle receptor FtsY |
| tr\|Q0SS83\|Q0SS83_CLOPS | 1709 | Cytoplasmic Membrane | Serine/threonine protein kinase BH2504 |
| tr\|Q0SS79\|Q0SS79_CLOPS | 1713 | Cytoplasmic Membrane | Putative neutral zinc metallopeptidase |
| sp\|Q0SS66\|DER_CLOPS | 1726 | Cytoplasmic Membrane | GTPase Der |
| tr\|Q0SS49\|Q0SS49_CLOPS | 1743 | Cytoplasmic Membrane | Uncharacterized protein |
| tr\|Q0SRW6\|Q0SRW6_CLOPS | 1826 | Cytoplasmic Membrane | Cell division protein FtsQ |
| tr\|Q0SRP0\|Q0SRP0_CLOPS | 1907 | Cytoplasmic Membrane | Protein-export membrane protein SecF |
| tr\|Q0SRN9\|Q0SRN9_CLOPS | 1908 | Cytoplasmic Membrane | Protein translocase subunit SecD |
| tr\|Q0SRN6\|Q0SRN6_CLOPS | 1911 | Cytoplasmic Membrane | Preprotein translocase, YajC subunit, YajC_2 |
| sp\|Q0SRL7\|PBPA_CLOPS | 1930 | Cytoplasmic Membrane | Penicillin-binding protein 1A, PbpA |
| tr\|Q0SRL1\|Q0SRL1_CLOPS | 1936 | Cytoplasmic Membrane | Spermidine/putrescine ABC transporter, permease protein PotB |
| tr\|Q0SRK4\|Q0SRK4_CLOPS | 1943 | Cytoplasmic Membrane | D-alanyl-D-alanine carboxypeptidase family protein |
| tr\|Q0SRG7\|Q0SRG7_CLOPS | 1981 | Cytoplasmic Membrane | Putative permease |
| tr\|Q0SRD1\|Q0SRD1_CLOPS | 2017 | Cytoplasmic Membrane | Stage V sporulation protein AE, SpoVAE |
| tr\|Q0SRC9\|Q0SRC9_CLOPS | 2019 | Cytoplasmic Membrane | Stage V sporulation protein AC, SpoVAC |
| tr\|Q0SRC2\|Q0SRC2_CLOPS | 2026 | Cytoplasmic Membrane | Cation-transporting ATPase, P-type |
| sp\|Q0SRB4\|MURG_CLOPS | 2034 | Cytoplasmic Membrane | MurG transferasetransferase |
| tr\|Q0SR78\|Q0SR78_CLOPS | 2070 | Cytoplasmic Membrane | CspC family protein |

| | | | |
|---|---|---|---|
| tr\|Q0SR70\|Q0SR70_CLOPS | 2078 | Cytoplasmic Membrane | Transmembrane protein Vexp3 |
| tr\|Q0SR43\|Q0SR43_CLOPS | 2105 | Cytoplasmic Membrane | Site-determining protein, MinD |
| tr\|Q0SR24\|Q0SR24_CLOPS | 2124 | Cytoplasmic Membrane | PTS system, glucose-specific IIBC component, PtsG |
| tr\|Q0SR23\|Q0SR23_CLOPS | 2125 | Cytoplasmic Membrane | ABC transporter, substrate-binding protein |
| sp\|Q0SQZ5\|ATPB_CLOPS | 2162 | Cytoplasmic Membrane | ATP synthase subunit beta, AtpD |
| sp\|Q0SQZ1\|ATPF_CLOPS | 2166 | Cytoplasmic Membrane | ATP synthase subunit b, AtpF |
| tr\|Q0SQX6\|Q0SQX6_CLOPS | 2181 | Cytoplasmic Membrane | Transcription termination factor Rho |
| tr\|Q0SQW9\|Q0SQW9_CLOPS | 2188 | Cytoplasmic Membrane | Cyanophycinase, CphB |
| tr\|Q0SQT7\|Q0SQT7_CLOPS | 2244 | Cytoplasmic Membrane | Uncharacterized protein |
| tr\|Q0SQS7\|Q0SQS7_CLOPS | 2254 | Cytoplasmic Membrane | Oligopeptide/dipeptide ABC transporter, ATP-binding protein |
| tr\|Q0SQS6\|Q0SQS6_CLOPS | 2255 | Cytoplasmic Membrane | Oligopeptide/dipeptide ABC transporter, ATP-binding protein |
| tr\|Q0SQS4\|Q0SQS4_CLOPS | 2257 | Cytoplasmic Membrane | Oligopeptide/dipeptide ABC transporter, permease protein |
| tr\|Q0SQS2\|Q0SQS2_CLOPS | 2259 | Cytoplasmic Membrane | Major facilitator family transporter |
| tr\|Q0SQP3\|Q0SQP3_CLOPS | 2289 | Cytoplasmic Membrane | Zinc-transporting atpase |
| tr\|Q0SQK2\|Q0SQK2_CLOPS | 2340 | Cytoplasmic Membrane | ABC transporter, ATP-binding protein |
| tr\|Q0SQG4\|Q0SQG4_CLOPS | 2379 | Cytoplasmic Membrane | Protein translocase subunit SecY |
| tr\|Q0SQB8\|Q0SQB8_CLOPS | 2427 | Cytoplasmic Membrane | PIN/TRAM domain protein |
| tr\|Q0SQ93\|Q0SQ93_CLOPS | 2452 | Cytoplasmic Membrane | Putative cation transporter2 PE=4 SV=1 |
| tr\|Q0SQ81\|Q0SQ81_CLOPS | 2472 | Cytoplasmic Membrane | ATP-dependent zinc metalloprotease FtsH |
| sp\|Q0SQ68\|PRSA_CLOPS | 2492 | Cytoplasmic Membrane | Foldase protein PrsA |
| tr\|Q0SQ55\|Q0SQ55_CLOPS | 2505 | Cytoplasmic Membrane | Nucleoside transporter, NupC family |
| tr\|Q0SQ36\|Q0SQ36_CLOPS | 2524 | Cytoplasmic Membrane | Uncharacterized protein |
| tr\|Q0SPW7\|Q0SPW7_CLOPS | 2593 | Cytoplasmic Membrane | Putative phage infection protein |
| tr\|Q0SPW6\|Q0SPW6_CLOPS | 2594 | Cytoplasmic Membrane | Putative phage infection protein |
| tr\|Q0SPQ1\|Q0SPQ1_CLOPS | 2671 | Cytoplasmic Membrane | Membrane protein OxaA |

| | | | |
|---|---|---|---|
| tr\|Q0STI4\|Q0STI4_CLOPS | 1251 | extracellular | Superoxide dismutase, SodF |
| tr\|Q0STC4\|Q0STC4_CLOPS | 1311 | extracellular | Glycosyl hydrolase, family 25 |
| tr\|Q0SPZ3\|Q0SPZ3_CLOPS | 2567 | Extracellular | Protease CspB |
| tr\|Q0SWP9\|Q0SWP9_CLOPS | 0114 | unknown | Uncharacterized protein |
| sp\|Q0SWN5\|CINA_CLOPS | 0128 | unknown | Putative competence-damage inducible protein, CinA1 |
| tr\|Q0SWM3\|Q0SWM3_CLOPS | 0140 | unknown | Nad-dependent malic enzyme |
| tr\|Q0SWH6\|Q0SWH6_CLOPS | 0188 | unknown | 5'-nucleotidase, lipoprotein e(P4) family |
| tr\|Q0SW97\|Q0SW97_CLOPS | 0273 | unknown | UDP-glucose 4-epimerase, GalE_1 |
| tr\|Q0SW33\|Q0SW33_CLOPS | 0338 | unknown | Putative lioprotein |
| tr\|Q0SVR9\|Q0SVR9_CLOPS | 0452 | unknown | Capsule chain length determinant protein |
| tr\|Q0SVQ8\|Q0SVQ8_CLOPS | 0463 | unknown | Uncharacterized protein |
| tr\|Q0SVP3\|Q0SVP3_CLOPS | 0479 | unknown | Sortase family protein |
| tr\|Q0SVM0\|Q0SVM0_CLOPS | 0502 | unknown | Putative lipoprotein |
| tr\|Q0SVF6\|Q0SVF6_CLOPS | 0567 | unknown | Amino acid ABC transporter, amino acid-binding protein |
| tr\|Q0SUS5\|Q0SUS5_CLOPS | 0807 | unknown | Uncharacterized protein |
| tr\|Q0SU89\|Q0SU89_CLOPS | 0995 | unknown | Conserved domain protein |
| tr\|Q0STY5\|Q0STY5_CLOPS | 1100 | unknown | Putative lipoprotein |
| tr\|Q0STM6\|Q0STM6_CLOPS | 1209 | unknown | VanW-related protein |
| tr\|Q0STC9\|Q0STC9_CLOPS | 1306 | unknown | Lipoprotein, BMP family |
| tr\|Q0STC5\|Q0STC5_CLOPS | 1310 | unknown | VanW-like family protein |
| tr\|Q0STB8\|Q0STB8_CLOPS | 1319 | unknown | 1-acyl-sn-glycerol-3-phosphate acyltransferase family protein |
| tr\|Q0ST96\|Q0ST96_CLOPS | 1341 | unknown | Putative galactoside ABC transporter, galactoside-binding protein |
| tr\|Q0ST88\|Q0ST88_CLOPS | 1349 | unknown | Uncharacterized protein |
| tr\|Q0ST82\|Q0ST82_CLOPS | 1355 | unknown | Uncharacterized protein |
| tr\|Q0ST46\|Q0ST46_CLOPS | 1392 | unknown | Uncharacterized protein |

| | | | |
|---|---|---|---|
| tr\|Q0SSX2\|Q0SSX2_CLOPS | 1466 | unknown | Uncharacterized protein |
| tr\|Q0SSV8\|Q0SSV8_CLOPS | 1480 | unknown | Metallo-beta-lactamase family protein |
| tr\|Q0SST6\|Q0SST6_CLOPS | 1502 | unknown | Uncharacterized protein |
| tr\|Q0SSN8\|Q0SSN8_CLOPS | 1552 | unknown | Lipoprotein, BMP family |
| tr\|Q0SSJ9\|Q0SSJ9_CLOPS | 1592 | unknown | Uncharacterized protein |
| tr\|Q0SSE2\|Q0SSE2_CLOPS | 1650 | unknown | Aspartokinase |
| tr\|Q0SS88\|Q0SS88_CLOPS | 1704 | unknown | Uncharacterized protein |
| tr\|Q0SS80\|Q0SS80_CLOPS | 1712 | unknown | Ribosomal RNA small subunit methyltransferase B, Sun |
| tr\|Q0SS20\|Q0SS20_CLOPS | 1772 | unknown | Uncharacterized protein |
| tr\|Q0SRV7\|Q0SRV7_CLOPS | 1836 | unknown | Delta-lactam-biosynthetic de-N-acetylase, PdaA |
| tr\|Q0SRG6\|Q0SRG6_CLOPS | 1982 | unknown | Uncharacterized protein |
| tr\|Q0SRC3\|Q0SRC3_CLOPS | 2025 | unknown | Uncharacterized protein |
| tr\|Q0SRB6\|Q0SRB6_CLOPS | 2032 | unknown | Pyruvate-flavodoxin oxidoreductase, NifJ |
| tr\|Q0SR94\|Q0SR94_CLOPS | 2054 | unknown | Molybdate ABC transporter, molybdate-binding protein, ModA |
| tr\|Q0SR35\|Q0SR35_CLOPS | 2113 | unknown | Uncharacterized protein |
| tr\|Q0SQW4\|Q0SQW4_CLOPS | 2193 | unknown | Mannosyltransferase B, MtfB |
| tr\|Q0SQV7\|Q0SQV7_CLOPS | 2200 | unknown | Serine protease |
| tr\|Q0SQR1\|Q0SQR1_CLOPS | 2270 | unknown | Prepilin-type N-terminal cleavage/methylation domain protein |
| tr\|Q0SQP7\|Q0SQP7_CLOPS | 2285 | unknown | Electron transfer flavoprotein, beta subunit/FixA family protein |
| tr\|Q0SQK4\|Q0SQK4_CLOPS | 2338 | unknown | Putative maltose/maltodextrin ABC transporter, maltose/maltodextrin-binding protein |
| tr\|Q0SQJ7\|Q0SQJ7_CLOPS | 2345 | unknown | Uncharacterized protein |
| sp\|Q0SQG3\|RL15_CLOPS | 2380 | unknown | 50S ribosomal protein L15, RplO |
| sp\|Q0SQE7\|RL2_CLOPS | 2396 | unknown | 50S ribosomal protein L2, RplB |
| sp\|Q0SQE5\|RL4_CLOPS | 2398 | unknown | 50S ribosomal protein L4, RplD |
| sp\|Q0SQ58\|MURC_CLOPS | 2502 | unknown | UDP-N-acetylmuramate--L-alanine ligase, MurC |

| | | | |
|---|---|---|---|
| tr\|Q0SQ56\|Q0SQ56_CLOPS | 2504 | unknown | Purine nucleoside phosphorylase, PunA |
| tr\|Q0SQ38\|Q0SQ38_CLOPS | 2522 | unknown | Putative lipoprotein |
| tr\|Q0SQ30\|Q0SQ30_CLOPS | 2530 | unknown | Uncharacterized protein |
| tr\|Q0SPZ4\|Q0SPZ4_CLOPS | 2566 | unknown | Spore cortex-lytic enzyme SleC |
| tr\|Q0SPY2\|Q0SPY2_CLOPS | 2578 | unknown | Conserved domain protein |
| tr\|Q0SPX1\|Q0SPX1_CLOPS | 2589 | unknown | Conserved domain protein |

a: PSORTb 3.0 was used for protein localization analysis.